Universidade de Lisboa

Faculdade de Medicina de Lisboa

Using Genomics for Drug Discovery in Medulloblastoma

Cláudia Maria Coelho de Faria

Orientadores
Prof. Doutor James T. Rutka
Prof. Doutor João Lobo Antunes

Doutoramento em Medicina

Especialidade de Neurocirurgia

A impressão desta dissertação foi aprovada pelo Conselho Científico da Faculdade de Medicina da Universidade de Lisboa em reunião de 22 de Abril de 2014.

To my family

for their love and support every day of my life

Preface

I have always wanted to be a neurosurgeon but the decision to pursue a career in science came later in my life. I did my residency in Neurosurgery at Hospital de Santa Maria from 2004 to 2010 and I devoted the last years of training to Pediatric Neurosurgery. My interest in brain tumor research arose from my patients, particularly from those difficult cases where, despite a successful operation, the tumor recurred thus emphasizing the importance of understanding the tumor biology for patient management.

Having this in mind, and with the invaluable support of Professor João Lobo Antunes, I applied to the Programme for Advanced Medical Education in 2009, a PhD program for medical doctors, sponsored by Fundação Calouste Gulbenkian, Fundação Champalimaud, Ministério da Saúde e Fundação para a Ciência e Tecnologia. The initial six months of the program included classes and seminars on various topics, from basic science to translational research and epidemiology. The goal of this educational period was to provide the students with solid scientific basis to develop research projects oriented for specific clinical questions.

When I joined the program I had the naïve assumption that I couldn't stay away from my natural environment, the operating room without loosing the skills acquired during six years of intense surgical training. The switch from a purely clinical thinking to an integrated clinical and scientific thinking was hard but it became a milestone in my medical career. Having a clear clinical question in mind I have decided to develop my research project in a renowned international brain tumor research centre, The Arthur and Sonia Labatt Brain Tumour Research Centre, at the Hospital for Sick Children in Toronto, Canada.

The choice to move to Toronto was simple. During my residency I had visited for a period the Divison of Neurosurgery at the Hospital for Sick Children in Toronto and I met Dr. James Rutka, pediatric neurosurgeon, senior scientist and Director of The Arthur and Sonia Labatt Brain Tumour Research Centre. Knowing my interest in brain tumor research, he invited me to visit the Centre, showed me the facilities, explained the main research areas and ongoing projects, and introduced me to some of the researchers. When, two years later, I had to choose a research institute to develop my project, I had no doubt that the Labatt Brain Tumour Research Centre was the right place and, therefore, I was extremely grateful for being accepted in Dr. Rutka's laboratory.

I have decided to focus on medulloblastoma, the most common malignant brain tumor in the pediatric population. I was puzzled with the heterogeneous clinical outcome of patients with medulloblastoma treated with standard protocols and I felt that better therapeutic options were urgently needed. The "boom" of genomic data emerging from the study of large cohorts of medulloblastoma samples had recently started. I was fortunate to work at the Labatt Brain Tumour Research Centre when major discoveries on medulloblastoma took place and also to give my contribution to some of those projects. The results from my own research project opened new avenues for targeted therapies and I hope they can translate into clinical trials for children with medulloblastoma in a near future.

My overall experience in Toronto exceeded my best expectations. During my "research residency", as I like to refer to my training in the laboratory, I have learned a wide variety of techniques, I became familiar with the latest technologies in the field and, most importantly, I met extraordinary people from around the globe and created a network of collaborations that will certainly be of great value for my future projects. The exceptional environment at the Labatt Brain Tumour Research Centre have been truly inspiring and, now that I am back to my home institution, I hope to pursue a career as a clinician-scientist to better help my patients both in the operating room and in the laboratory.

Acknowledgments

I would like to express my deepest gratitude to Dr. James Rutka, my PhD supervisor, who welcomed me to his laboratory and guided me in my training as a surgeon-scientist. I am forever grateful for the opportunities he gave me throughout my stay in Toronto. It was a privilege to be part of the Rutka lab and a member of the Labatt Brain Tumour Research Centre.

I wish to express my profound gratitude to Professor João Lobo Antunes, the Director of my Department and Co-supervisor of my PhD, for his mentorship and guidance for over 10 years. He has been an example of a dedicated surgeon, a compassionate physician and an excellent teacher. He recognized and stimulated my scientific curiosity long before I had realized its importance in my career. I am thankful for his encouragement and support of my research, and also for his vision for the future.

I am forever thankful to Dr. José Miguéns, my mentor in Pediatric Neurosurgery, for his support of my research and for his generosity taking care of all the pediatric patients in our Department while I was in Toronto. His exceptional dedication to his patients and clinical thoroughness, have been an inspiration and an example to follow.

I am thankful to the Programme for Advanced Medical Education and particularly to Professor Leonor Parreira for her generous support and advice. The outstanding scientific training provided by the Programme was crucial for my research work in Toronto. I wish to acknowledge the sponsors of the Programme, Fundação Calouste Gulbenkian, Fundação Champalimaud, Ministério da Saúde e Fundação para a Ciência e Tecnologia, for their institutional and financial support.

I am grateful to Dr. Michael Taylor for his guidance and mentorship in my research projects. He always gave me insightful comments and suggestions.

I am thankful to Professor José Pimentel, Head of the Laboratory of Neuropathology at Hospital de Santa Maria, for supporting my research and for helping me establishing fruitful national and international collaborations.

I wish to thank the current and past members of the Rutka lab who contributed their time and advice in helping me achieve my research goals including Dr. Christian Smith, Dr. Roberto Diaz, Dr. Sameer Agnihotri, Dr. Arnold Etame, Dr. Adrienne Weeks, Dr. Yuzo Terakawa, Dr. Jong Hee Chang, Mr. Brian Golbourn, Ms. Amanda Luck, Ms. Nesrin Sahba and Mr. Jim Loukides. I wish to express my gratitude in particular to Dr. Christian Smith for his mentorship and support.

I would like to acknowledge my wonderful collaborators from Dr. Michael Taylor's lab Dr. Adrien Dubuc, Dr. Marc Remke, Dr. Vijay Ramaswamy, Dr. Stephen Mack, Dr. Xiaochong Wu, Dr. Livia Garzia, Dr. Paul Northcott and Mr. Xin Wang, and from the German Cancer Research Centre (DKFZ) in Heidelberg Dr. Stefan Pfister, Dr. Marcel Kool and Dr. Andrey Korshunov, who contributed with many insightful comments and technical expertise in this work.

Table of Contents

Abbreviations

°C	degrees Celsius
µl	microliter
µm	micrometer
µM	micromolar
ADAM	a desintegrin and metalloprotease
ALK	anaplastic lymphoma kinase
ALP	alsterpaullone
ANOVA	analysis of variance
APC	adenomatous polyposis coli
BAD	BCL-2 antagonist of cell death
BLI	bioluminescence imaging
CBL	casitas B-lineage lymphoma
CBP	crebs binding protein
CCND1/2	cyclin dependent kinase 1/2
CCNU	lomustine
CDK	cyclin-dependent kinase
CDK6	cyclin-dependent kinase 6
CDKN2A	cyclin-dependent kinase inhibitor 2A gene
CDKN2B	cyclin-dependent kinase inhibitor 2B gene
CGNP	cerebellar granule neuron precursor
C-MAP	Connectivity Map
CNA	copy-number aberrations
COX-2	cyclooxygenase-2
cm	centimeter
cm^2	square centimeter
cMET	hepatocyte growth factor receptor
CNA	copy number alterations
CSI	craniospinal irradiation
CTNNB1	catenin (cadherin-associated protein) beta 1
DAPI	4',6-diamidino-2-phenylindole
DDX3X	DEAD-box RNA helicase
DHB	2,5-dihydroxybenzoic acid

DKK1/2	Dickkopf 1 and 2
DMEM	Dulbecco's modified Eagle's medium
DMSO	dimethyl sulfoxide
DNA	deoxyribonucleic acid
DR4/5	death receptors 4 and 5
EDTA	ethylenediaminetetraacetic acid
EFS	event-free survival
EGFR	epidermal growth factor receptor
EGL	external granule layer
ERBB2	v-erb-b2 avian erythroblastic leukemia viral oncogene homolog 2
ERK1/2	extracellular signal-regulated kinases 1 and 2
FAK	focal adhesion kinase
FBS	fetal bovine serum
FDA	Food and Drug Administration
FDR	false discovery rate
FFPE	formalin-fixed paraffin-embedded tissue
Flt-3	FMS-like tyrosine kinase 3
FSTL5	follistatin-related protein 5
FZ	flunarizine
GAB 1	GRB2-associated adaptor protein
g	gram
G-CSF	granulocyte colony stimulating factor
GFP	green fluorescent protein
GLI 1/2	glioma-associated oncogene homolog 1 and 2
GO	gene ontology
GRB2	growth factor receptor-bound protein 2
GSEA	gene set enrichment analysis
Gy	gray
HART	hyperfractionated accelerated radiotherapy
HDAC	histone deacetylase inhibitors
H&E	hematoxylin and eosin
HFRT	hyperfractionated radiotherapy
HGF	hepatocyte growth factor
HGFA	hepatocyte growth factor activator

HOX	homeobox protein
hr	hours
HZ	hertz
IGF1R	insulin-like growth factor 1 receptor
IGL	internal granule layer
IHC	immunohistochemistry
IPT	immunoglobulin-like also found in plexins and transcriptional factors
ITO	indium tin oxide
JNK1/2/3	jun amino-terminal kinases 1, 2 and 3
LEF1	lymphoid enhancer-binding factor 1
KEGG	Kyoto encyclopedia of genes and genomes
Kg	kilogram
Ki-67	antigen identified by monoclonal antibody Ki-67
Kit	stem cell factor receptor
LC/MS/MS	liquid chromatography-tandem mass spectrometry
LLOQ	lower limit of quantitation
MACC1	metastasis-associated in colon cancer-1
MAGIC	Medulloblastoma Advanced Genomics International Consortium
MALDI	matrix-assisted laser desorption/ionization
MALDI-TOF	matrix-assisted laser desorption/ionization with time of flight mass spectrometer
MAPK	mitogen activated protein kinase
MGMT	O6-methylguanine-DNA methyltransferase
MTS	(3-(4,5-dimethylthiazol-2-yl)-5-(3-carboxymethoxyphenyl)-2-(4-sulfophenyl)-2H-tetrazolium)
MYC	v-myc myelocytomatosis viral oncogene homolog (avian)
MYCN	v-myc myelocytomatosis viral related oncogene, neuroblastoma derived (avian)
mM	millimolar
mg	milligram
MHC	major histocompatibility complex
mL	milliliter
mm	millimeter
m/z	mass-to-charge

mRNA	messenger ribonucleic acid
mTOR	mammalian target of rapamycin
NCI	National Cancer Institute
NF-κB	nuclear factor kappa-light-chain-enhancer of activated B cells
ng	nanogram
nm	nanometer
ns	nanosecond
OCT	optimal cutting temperature
OS	overall survival
P	p-value
PAGE	polyacrylamide gel electrophoresis
PAI-1	plasminogen activator inhibitor type 1
PARP	poly (ADP-ribose) polymerase
PCR	polymerase chain reaction
PDGF-BB	platelet derived growth factor receptor beta ligand
PDGFR	platelet derived growth factor receptor
PDGFRß	platelet derived growth factor receptor beta
PFAM	protein families
PFS	progression-free survival
PI3K	phosphoinositide 3-kinase
PKCε	protein kinase Cε
PL	piperlongumine
PLC	phospholipase C
PSI	present in the plexins, semaphorins and integrins
p-MET	phosphorylated MET
PTCH1	human homolog of *Drosophila* patched
PTEN	phosphatase and tensin homolog
PVDF	plyvinylidene fluoride
PVT1	Pvt1 ongogene (non-protein coding)
Ret	rearranged during transfection
RIPA	radioimmunoprecipitation assay
RNA	ribonucleic acid
Ron	recepteur d'origine nantais
RTL	rottlerin

SAM	significance analysis of microarrays
SB	sleeping beauty
SCR	stem cell rescue
SDS	sodium dodecyl sulfate
SEM	standard error of the mean
SFRP1	secreted frizzled-related protein 1
SHH	sonic hedgehog
SHP2	SRC homology protein tyrosine phosphatase 3
SMO	smoothened, frizzled family receptor
SNCAIP	synuclein, alpha interacting protein
SNP	single nucleotide polymorphism
SOS	son of sevenless
SPH	serine protease homology
SPINT1/2	serine protease inhibitor Kunitz-type 1 and 2
STAT3	signal transducer and activator of transcription 3
STRT	standard fractionated radiotherapy
SUFU	suppressor of fused
TF	tissue factor
TGF-β	transforming growth factor beta
Tie-2	angiopoietin receptor 2
TMA	tissue microarray
TNF	tumor necrosis factor
TP53	tumour suppressor protein p53
TRAIL	tumor necrosis factor-related apoptosis–inducing ligand
TSP-1	thrombospondin 1
VCP	vincristine, CCNU and prednisone
VEGF	vascular endothelial growth factor
WHO	World Health Organization
WIF	WNT inhibitory factor 1
WNT	wingless-type MMTV integration site family

List of Figures

Chapter 1

Chapter 2

Chapter 3

List of Tables

Chapter 1

Chapter 2

Chapter 3

Abstract

Medulloblastoma is the most common malignant brain tumor in childhood. The standard of care to treat patients with medulloblastoma includes surgical resection, craniospinal irradiaton (in children older than 3 years of age) and high dose chemotherapy. Overall survival rates for patients submitted to conventional treatment protocols have reached 70-80% but the majority of survivors suffer from severe long-term side effects, including developmental, cognitive, neurological and neuroendocrine deficits.

For many years medulloblastoma was considered a single entity, a small, round blue-cell tumor on histology, originating in the cerebellum. Recently, integrative genomic studies have identified at least four distinct molecular subgroups – WNT, sonic hedgehog (SHH), Group 3 and Group 4 – which display disparate transcriptional profiles, genetic abnormalities, patient demographics and clinical outcome. Patients with WNT medulloblastomas have a very good outcome. Patients with SHH and Group 4 tumors have an intermediate prognosis. Group 3 medulloblastomas are characterized by frequent amplifications or aberrant expression of the oncogene *MYC*, a high percentage of metastasis at diagnosis and a very poor prognosis despite aggressive therapy. Although disseminated disease at diagnosis is a known factor of poor survival, the mechanisms of dissemination are not fully understood and metastatic lesions are highly genetically divergent from their matched primary tumor. Therefore, we asked whether we could use genomics to discover novel and less toxic small molecule inhibitors to target medulloblastoma in a subgroup-specific manner.

To answer our research question we used two approaches: 1) targeting the hepatocyte growth factor (HGF)/cMET pathway, known to be important in medulloblastoma pathogenesis, with the cMET inhibitor, foretinib and 2) performing a gene expression-based *in silico* drug screen to identify small molecule inhibitors with selective antitumor effect in Group 3 medulloblastomas.

Aberrant signaling through the (HGF)/cMET pathway is involved in tumor progression and metastasis in several human cancers. cMET is a transmembrane receptor which becomes activated through phosphorylation of tyrosine residues upon binding of its ligand HGF. The recruiment of cytoplasmic effector proteins upon cMET activation triggers multiple downstream effector pathways including mitogen activated protein kinase (MAPK) and phosphoinositide 3-kinase (PI3K). In medulloblastoma, cMET activation has been associated with tumor growth and invasion. To determine the subgroup-specific role of cMET

in medulloblastoma, we analyzed the mRNA expression of three large non-overlapping cohorts of patients with primary medulloblastomas (discovery cohort from Boston, n = 199; validation cohort 1, a multicentre cohort obtained from Heidelberg, n = 439; validation cohort 2, a multicentre cohort obtained from the Medulloblastoma Advanced Genomics International Consortium - MAGIC, n = 285) and demonstrated that *cMET* is a marker of SHH medulloblastoma. Immunohistochemical analysis of activated cMET (phosphorylated cMET) in another independent patient cohort (n = 385) validated these findings and revealed that cMET activation correlates with increased tumor relapse and a poor survival in pediatric patients with SHH medulloblastomas, thus defining a subset of patients that may benefit from cMET targeted therapy.

We selected foretinib, an FDA approved multikinase inhibitor with high affinity to the cMET receptor, to evaluate the effect of cMET targeting in SHH medulloblastoma. Foretinib suppressed cMET activation, decreased proliferation and induced apoptosis, both in medulloblastoma cell lines and in SHH medulloblastoma flank xenografts. Importantly, we characterized the pharmacokinetics of foretinib and demonstrated that it penetrates the blood-brain barrier and is well tolerated through intrathecal administration. Treatment of mouse intracranial xenografts and of an aggressive transgenic mouse model of metastatic SHH medulloblastoma (*Patched*$^{+/-}$ mouse with the Sleeping Beauty transposon system) with foretinib reduced primary medulloblastoma growth and invasion, decreased the incidence of metastases by 36% and increased survival by 45%.

To investigate potential novel small molecules to target Group 3 medulloblastomas we used a bioinformatic platform called the Connectivity Map (C-MAP). The C-MAP contains a collection of gene expression profiles from several human cell lines treated with a large number of compounds already FDA approved. Comparative analysis between the oncogenic gene signature of interest and the C-MAP database may highlight patterns of gene expression change and identify small molecules with potential predicted activity within a given cancer. We queried the C-MAP using the subgroup-specific gene expression signatures of the four medulloblastoma subgroups. Piperlongumine, a natural product extracted from the fruit of the *Piper longum*, was the top candidate drug for non-WNT tumors. We then selected compounds predicted to have specific antitumor activity for Group 3 medulloblastomas and the cyclin-dependent kinase (CDK) inhibitor alsterpaullone ranked number one. To validate our findings we used two established Group 3 medulloblastoma cell lines (D425 and D458) and a medulloblastoma stem cell line derived from a patient with a Group 3 tumor (M441). The C-

MAP predicted drugs were able to decrease cell proliferation *in vitro* and to reduce tumor growth and increase survival in Group 3 medulloblastoma mouse xenografts. Alsterpaullone showed the highest efficacy both *in vitro* and *in vivo* in the patient derived medulloblastoma stem cell line. Interestingly, the chemical genomic profiling of Group 3 medulloblastoma cells treated with alsterpaullone confirmed inhibition of cell cycle-related genes and showed down-regulation of *MYC,* the hallmark oncogene of Group 3 tumors.

We used a gene expression-based approach to identify molecular targeted therapy to treat medulloblastoma. Our results demonstrate the preclinical efficacy of two small molecule inhibitors: foretinib in metastatic SHH medulloblastomas and alterpaullone in Group 3 tumors. Given the dismal outcome and lack of options for these patients, the results from our studies provide strong rationale for advancing both compounds as targeted agents into clinical trials for patients with these highly aggressive subgroups of medulloblastoma.

Keywords: medulloblastoma subgroups, genomics, HGF/cMET pathway, foretinib, alsterpaullone

Resumo

O meduloblastoma é o tumor cerebral maligno mais comum na população pediátrica. O tratamento convencional dos doentes com meduloblastoma inclui resseção cirúrgica máxima, radioterapia do crânio e do neuroeixo (em crianças com idade superior a 3 anos) e quimioterapia de alta dose. A sobrevida global em doentes submetidos a protocolos de tratamento convencional atinge os 70-80% mas a maioria dos sobreviventes apresenta sequelas graves dos tratamentos incluindo problemas no desenvolvimento, defeitos cognitivos, neurológicos e neuroendócrinos.

Durante muito anos o meduloblastoma foi considerado uma entidade única, um tumor de pequenas células azuis na observação histológica, oriundo do cerebelo. Recentemente, estudos de genómica integrada identificaram pelo menos quatro subgrupos moleculares de meduloblastoma – WNT, sonic hedgehog (SHH), Grupo 3 e Grupo 4 – que apresentam características distintas no que diz respeito ao perfil transcriptómico, anomalias genéticas, dados demográficos e sobrevida. Doentes com meduloblastomas do tipo WNT têm muito bom prognóstico. Doentes com tumores do tipo SHH e Grupo 4 têm um prognóstico intermédio. Os meduloblastomas do Grupo 3 são caracterizados por amplificações frequentes ou expressão aberrante do oncogene *MYC*, uma elevada incidência de metástases na altura do diagnóstico e um mau prognóstico apesar de terapias agressivas. Embora a presença de doença disseminada na altura do diagnóstico seja um factor conhecido de baixa sobrevida, os mecanismos de disseminação são pouco conhecidos e as lesões metastáticas são geneticamente divergentes do seu tumor primário. Assim, questionámos se seria possível usar a genómica na descoberta de pequenas moléculas inibidoras dirigidas aos subgrupos moleculares de meduloblastoma.

Para responder à nossa pergunta utilizámos duas abordagens: 1) uma terapia dirigida à via de sinalização do factor de crescimento dos hepatócitos (HGF)/cMET, conhecida pelo seu importante papel na patogénese do meduloblastoma, usando um inibidor do receptor cMET, foretinib e 2) um rastreio farmacológico *in silico* com base na expressão genética para identificar pequenas moléculas inibidoras com efeito antitumoral selectivo nos meduloblastomas do Grupo 3.

A sinalização aberrante através da via de transdução de sinal (HGF)/cMET está envolvida na progressão tumoral e metastização de vários cancros humanos. cMET é um receptor transmembranar que é activado através da fosforilação de resíduos de tirosina, após

interacção com o seu ligando HGF. O recrutamento de proteinas efectoras citoplasmáticas após a activação de cMET desencadeia a activação de múltiplas vias de sinalização incluindo MAPK (mitogen activated protein kinase) e PI3K (phosphoinositide 3-kinase). No meduloblastoma a activação de cMET tem sido associada a crescimento e invasão tumoral. Para determinar a importância de *cMET* nos diferentes subgrupos de meduloblastoma, analizámos a expressão de mRNA em três grupos independentes de doentes com meduloblastomas primários (grupo de descoberta de Boston, n = 199; grupo de validação 1, grupo multicêntrico obtido de Heidelberg, n = 439; grupo de validação 2, grupo multicêntrico obtido do Medulloblastoma Advanced Genomics International Consortium - MAGIC, n = 285) e demonstrámos que cMET é um marcador do meduloblastoma do tipo SHH. A análise imunohistoquímica de cMET activado (ou cMET fosforilado) noutro grupo independente de doentes (n = 385) validou estes resultados e revelou que a activação de cMET se correlaciona com o aumento de recidivas tumorais e com uma baixa sobrevida em doentes pediátricos com meduloblastoma do tipo SHH, definido assim um subgrupo de doentes que pode beneficiar de terapêutica dirigida a cMET.

Seleccionámos foretinib, um inibidor de múltiplas cinases aprovado pela FDA e com elevada afinidade para cMET, para avaliar o efeito da terapia dirigida a cMET no meduloblastoma do tipo SHH. Foretinib bloqueou a activação de cMET, reduziu a proliferação celular e induziu apoptose, tanto em linhas celulares de meduloblastoma como em tumores implantados no flanco de ratinhos. Importa salientar que caracterizámos a farmacocinética do foretinib e demonstrámos que este fármaco penetra a barreira hemato-encefálica e é bem tolerado quando administrado por via intratecal. O tratamento com foretinib em ratinhos com meduloblastomas implantados no cerebelo e num modelo de ratinho transgénico com uma forma agressiva de meduloblastoma metastizado do tipo SHH (ratinho transgénico *Patched*$^{+/-}$ com sistema de transposão do tipo *Sleeping Beauty*) reduziu o crescimento e invasão em meduloblastomas primários, diminuiu a incidência de metástases em 36% e aumentou a sobrevida em 45%.

Para investigar potenciais novas pequenas moléculas dirigidas aos meduloblastomas do Grupo 3, usámos uma plataforma bioinformática chamada Connectivity Map (C-MAP). O C-MAP contém uma colecção de perfis de expressão génica de múltiplas linhas celulares humanas tratadas com um elevado número de compostos aprovados pela FDA. A análise comparativa entre assinaturas genéticas oncogénicas de interesse e a base de dados C-MAP pode detectar padrões de mudança de expressão génica e identificar pequenas moléculas com

potencial actividade num determinado cancro. Assim, questionámos o C-MAP usando as assinaturas genéticas específicas dos quatro subgrupos de meduloblastoma. Piperlongumine, um produto natural extaído do fruto do *Piper longum*, foi identificado como o melhor candidato para os diferentes subgrupos de meduloblastoma, à excepção do tipo WNT. De seguida, seleccionámos compostos com potencial actividade antitumoral específica para os meduloblastomas do Grupo 3, tendo um inibidor das CDKs (cyclin-dependent kinases), alsperpaullone, sido o melhor classificado. Para validar os nossos resultados usámos duas linhas celulares estabelecidas representativas dos meduloblastomas do Grupo 3 (D425 e D458) e uma linha celular pluripotente obtida de um doente com um tumor do Grupo 3 (M441). Os fármacos predictos pelo C-MAP foram eficazes na diminuição da proliferação celular *in vitro* bem como na redução do crescimento tumoral e no aumento da sobrevida em ratinhos com meduloblastomas do Grupo 3 implantados no cerebelo. O composto alsterpaullone revelou-se o mais eficaz, quer *in vitro* quer *in vivo*, na linha celular pluripotente obtida de um doente. É interessante salientar que a caracterização do perfil químico e genómico de células de meduloblastoma do Grupo 3 tratadas com alsterpaullone confirmou a inibição de genes relacionados com o ciclo celular e a regulação negativa de *MYC*, o oncogene característico dos meduloblastomas do Grupo 3.

Usámos no nosso estudo uma abordagem com base na expressão genética para identificar terapêuticas dirigidas para o tratamento do meduloblastoma. Os resultados apresentados demonstram a eficácia pré-clínica de duas pequenas moléculas inibidoras: foretinib para o tratamento do meduloblastoma metastático do tipo SHH e alsterpaullone para o tratamento de meduloblastomas do Grupo 3. Tendo em conta o prognóstico sombrio e a falta de opções terapêuticas nestes doentes, os resultados dos nossos estudos constituem forte evidência para que estes compostos sejam incluídos como terapias dirigidas em ensaios clínicos para doentes diagnosticados com estes subgrupos agressivos de meduloblastoma.

Palavras-chave: subgrupos de meduloblastoma, genómica, via de sinalização HGF/cMET, foretinib, alsterpaullone

Chapter 1
Introduction

1.1 The Genomic Landscape of Medulloblastoma[i]

Medulloblastoma is the most common malignant brain tumor in childhood, comprising 20% of all primary pediatric brain tumors, although it can arise from infancy to adulthood[1]. The incidence of medulloblastoma in children has been estimated between 5.0 and 6.6 per million per year[2,3] and in adults between 0.57 and 0.58 per million per year[4]. The current treatment protocol for medulloblastoma includes surgical resection, radiation (for children older than 3 years of age) and chemotherapy with 5-year survival rates ranging between 50 and 80%. Among long-term survivors, a major concern is the sequelae induced by treatment including endocrinologic, neurocognitive and behavioral dysfunction[5].

Medulloblastoma arises in the cerebellum and originates from primitive pluripotent precursor cells of the ventricular zone and the external granular layer[6]. Medulloblastoma formation is strongly associated with dysregulation of pathways involved in the normal development of the cerebellum, including the Sonic hedgehog (SHH), Wingless (WNT) and Notch pathways[7].

The World Health Organization (WHO) classified medulloblastoma as a grade IV embryonal neoplasm comprising five histological variants: classic, desmoplastic/nodular, anaplastic, large cell and medulloblastoma with extensive nodularity[8]. Classic medulloblastomas are composed of densely packed, poorly differentiated cells, and areas of

---

[i] Claudia C. Faria, Christian A. Smith and James T. Rutka (2013). New Molecular Targets and Treatments for Pediatric Brain Tumors, Evolution of the Molecular Biology of Brain Tumors and the Therapeutic Implications, Dr. Terry Lichtor (Ed.), ISBN: 978-953-51-0989-1, InTech, DOI: 10.5772/53300.

Claudia C. Faria, Yuzo Terakawa and James T. Rutka (2014). Neurogenetic Basis of Pediatric Neurosurgical Conditions, Principles and Practice of Pediatric Neurosurgery, 3rd ed, Leland Albright, Ian F. Pollack, P. David Adelson (Editors), Thieme Medical Publishers (in press).

Homer-Wright rosettes. The desmoplastic/nodular variant includes pale nodular areas (pale islands) with patterns of neuronal differentiation surrounded by hyperchromatic cells densely packed. Anaplastic medulloblastomas are characterized by large pleomorphic nuclei. Tumor cell "wrapping" and mitotic figures are abundant. Large cell tumors are composed of enlarged round cells with prominent nuclei and pronounced mitotic and apoptotic figures. Tumors with both large cell and anaplastic regions can be encountered. Medulloblastoma with extensive nodularity shows a lobular architecture with long reticulin-free areas between the nodules. Clinical studies suggest a favorable outcome associated with desmoplastic medulloblastoma and a significant worst prognosis with the anaplastic subtype[9].

Medulloblastoma has been reported in the setting of several hereditary cancer syndromes including Li-Fraumeni syndrome, Gorlin syndrome, Turcot syndrome and Rubinstein–Taybi syndrome[10]. The Li-Fraumeni syndrome is associated with germline mutations in the *TP53* gene. Among many other cancers, patients with Li-Fraumeni syndrome have an increased risk to develop embryonal tumors (including medulloblastoma) and choroid plexus carcinoma. Gorlin syndrome (nevoid basal cell carcinoma syndrome) patients have germline mutations in the *PTCH1* gene, a component of the SHH signaling pathway, and up to a 5% risk of developing medulloblastoma. Germline mutations in the *SUFU* gene, a downstream mediator of the SHH pathway, have also been shown in patients with medulloblastoma[11]. Germline mutations of the *APC* gene, a component of the WNT signaling pathway, are seen in patients with Turcot syndrome who have an increased risk for colorectal carcinoma and brain tumors, predominantly medulloblastoma. Children with Rubinstein-Taybi syndrome have a complex developmental disorder that includes broad thumbs and toes, characteristic facies, severe developmental delay, and a predisposition to malignancy, including medulloblastoma, oligodendroglioma and meningioma. This syndrome is secondary to deletion/mutation of the *Crebs binding protein* (*CBP*) gene which functions in three pathways involved in medulloblastoma pathogenesis (SHH, WNT and TP53)[12].

Recent efforts of multiple independent groups have reached to a consensus that medulloblastoma comprises four distinct molecular variants named WNT, SHH, Group 3 and Group 4[13]. The subgroups have different demographics, genetic profiles and prognosis[14]. This may explain why patients with the same histological disease have different clinical outcomes and a variable response to current treatments including surgery, whole-brain radiation and intensive chemotherapy. **Figure 1.1** summarizes the main features of the four medulloblastoma subgroups.

1.1.1 WNT Medulloblastomas

WNT medulloblastomas are frequent in older children and teenagers and are rarely seen in infants. Patients within this subgroup have usually a very good outcome with survival rates over 90%. However, Remke *et al*. showed that this is only true for pediatric cases as adult WNT patients exhibit survival rates of approximately 80%[15]. Histologically, WNT tumors are almost always of the classic variant and they rarely disseminate.

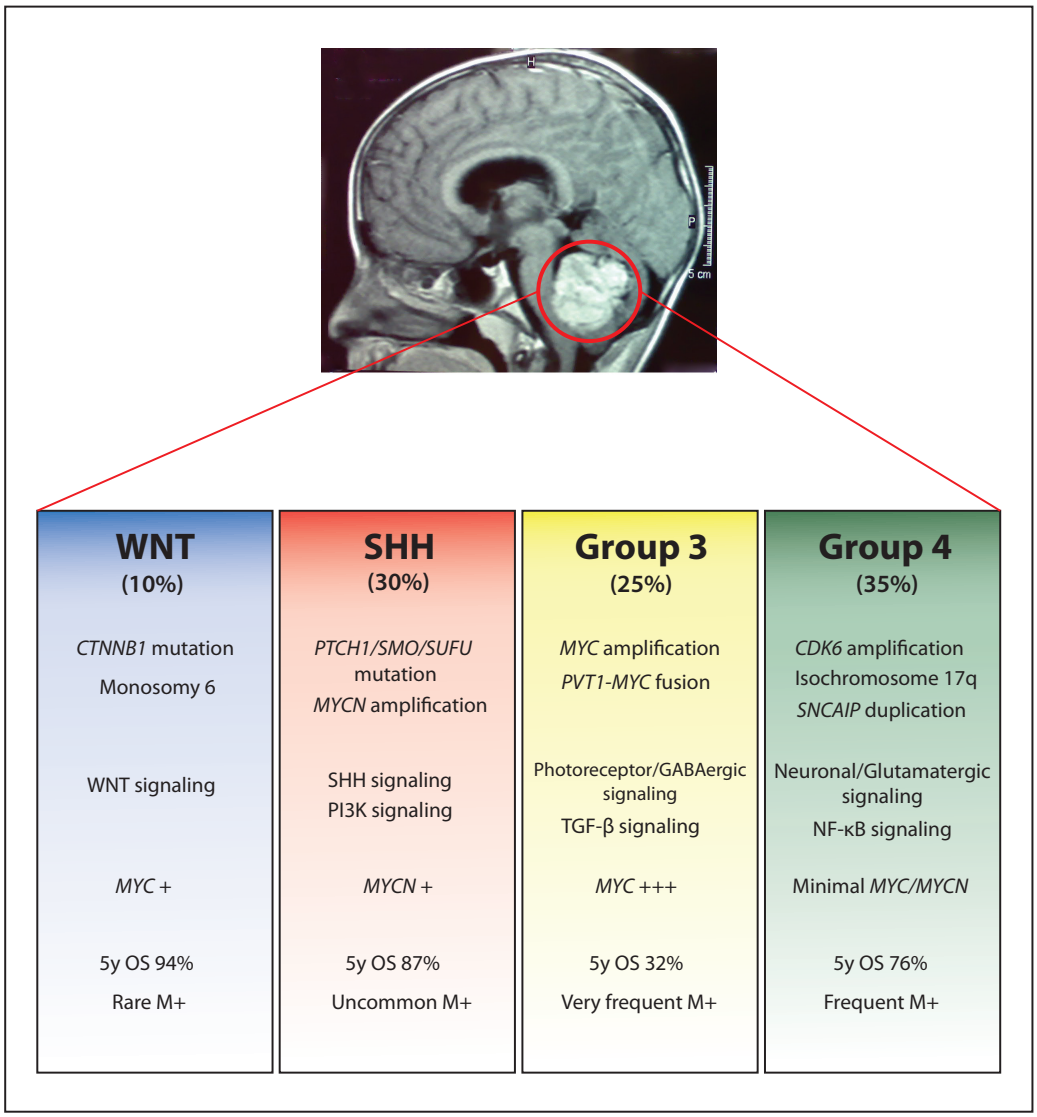

Figure 1.1: Features of the four medulloblastoma subgroups, including molecular genetics and clinical outcome.

This subgroup is enriched in genes of the WNT pathway. Specifically gene expression changes involve a combination of increased expression of inhibitors of WNT signaling (e.g. *WIF1, DKK1, DKK2, AXIN2*) and potential promoters of WNT signaling (e.g. *WNT16, LEF1*)[16]. *CTNNB1* mutation is the most common genetic event in WNT medulloblastomas and promotes the accumulation of β-catenin in the nucleus. Positive nuclear immunostaining for β-catenin is now routinely used as a marker of WNT pathway activation and is associated with better survival rates[17]. After *CTNNB1*, the *DDX3X* (DEAD-box RNA helicase) gene is the most frequently mutated in medulloblastoma and occurs in 50% of WNT tumors[18]. WNT medulloblastomas often carry *TP53* mutations and they confer a more favourable outcome[19]. Almost all patients with WNT medulloblastomas have monosomy 6 (deletion of one copy of chromosome 6), although the role of this chromosomal aberration remains undefined[20].

Recently, a mouse model of WNT medulloblastoma was generated and the cell of origin for this subgroup was elucidated. Mice with transgenic expression of a *CTNNB1* mutation in the context of a *TP53* deletion developed classic medulloblastoma, arising from progenitor cells in the lower rhombic lip of the dorsal brainstem[21].

The overall favourable outcome of WNT tumors suggests that this subgroup of patients may be considered for the de-escalation of therapy in future clinical trials.

1.1.2 SHH Medulloblastomas

SHH medulloblastomas have an intermediate prognosis with a 5-year overall survival (OS) of approximately 75%. Age distribution in these tumors is bimodal. They are frequently found in infants and adults but are rare in childhood. Prognostic factors such as desmoplasia and metastatic status are age-dependent. Desmoplasia is associated with a poor outcome only in children, while metastasis at presentation constitutes a negative prognostic factor only in adults[22]. SHH medulloblastomas include tumors of the four main histological variants (classic, nodular desmoplastic, large-cell anaplastic and medulloblastoma with extensive nodularity), although nodular desmoplastic histology is almost exclusively seen in this subgroup.

SHH-driven medulloblastomas exhibit aberrant expression of SHH pathway genes including *PTCH1, SUFU, SMO* and *GLI2*. Germline mutations affecting *PTCH1* or *SUFU* predispose patients with Gorlin syndrome to develop medulloblastoma. Amplifications and somatic copy number aberrations (CNAs) of SHH target genes such as *MYCN* and *GLI2* are also seen in this subgroup. An interesting association of SHH medulloblastoma and

deregulation of the PI3K signaling pathway has been recently reported. The alterations include amplifications of insulin-like growth factor 1 receptor (*IGF1R*) and focal deletions of *PTEN*[23]. When compared to WNT medulloblastoma genome, the SHH subgroup contains significant more gains and losses of chromosomal regions, including deletion of chromosome 9q and 10q. In an attempt to simplify the molecular subgrouping of medulloblastomas, different laboratories used formalin-fixed paraffin-embedded tissues (FFPE) to test a variety of markers for SHH medulloblastomas including SFRP1, GLI1 and GAB1[16,24,25].

Of note is the fact that the transcriptomes of pediatric and adult SHH tumors have different expression profiles with increased levels of genes related to extracellular matrix function in the first group and elevated levels of *HOX* family genes and genes involved in tissue development in the second group[22,26]. The clinical and molecular distinction of infant and adult SHH medulloblastomas suggests a disparate underlying biology and raise the question of possible different responses to current targeted therapies.

The cells of origin of SHH medulloblastoma are the cerebellar granule neuron precursors (CGNPs) of the external granule cell layer (EGL) of the cerebellum[27] and those of the cochlear nuclei of the brainstem[28]. SHH medulloblastomas can also be initiated from neural stem cells in the subventricular zone[29].

Several mouse models of SHH-dependent medulloblastoma are available for basic and preclinical research. The most common initiating events in these models include *Ptch1* inactivation and smoothened (*Smoa1*) activation[18].

1.1.3 Group 3 Medulloblastomas

Group 3 medulloblastomas have the worst prognosis of all subgroups. These tumors are restricted to children and infants, frequently have a large-cell anaplastic histology and 40 to 45% are disseminated at the time of diagnosis. One of the features of this subgroup is the amplification of *MYC*. In a recent study including a cohort of over 1,000 medulloblastoma samples, Northcott *et al.* identified recurrent fusions involving *MYC* and *PVT1* in about 60% of *MYC*-amplified tumors[23]. *PVT1* gene is adjacent to *MYC* on chromosome 8q24.21 and encodes several microRNAs that seem to promote *MYC* oncogenic properties[30]. This study also identified for the first time the TGF-β pathway as a potential target in Group 3 medulloblastoma. The genome of Group 3 tumors is highly unstable often exhibiting gains in chromosomes 1q, 7 and 17q (frequently isochromosome 17q), as well as deletions in chromosomes 10q, 11, 16q and 17p.

Recently, mouse models of MYC-driven Group 3 medulloblastoma, combined with Trp53 inactivation, were published. The cells of origin of these tumors were prominin 1-positive, lineage-negative neural stem cells and the CGNPs of the EGL[31,32]. Since *TP53* mutations are not seen in Group 3 medulloblastomas other candidates to cooperate with MYC in the process of tumorigenesis are being studied.

1.1.4 Group 4 Medulloblastomas

The most common medulloblastoma subgroup is Group 4 and, curiously, it is the least well understood. Group 4 tumors can be found across all age groups although children have an intermediate prognosis while adults may do significantly worse[15]. The expression of follistatin-related protein 5 (FSTL5) was identified as a marker of high-risk Group 4 patients[33]. These tumors are usually of the classic variant and show dissemination in one third of the patients. Recurrent amplifications of *MYCN* and cyclin-dependent kinase 6 (*CDK6*) are frequent in this subgroup as well as isochromosome 17q (i17q). Recently, a novel and frequent somatic CNA was described in Group 4 medulloblastomas. It is a duplication of *SNCAIP*, a gene involved in Parkinson's disease and located on chromosome 5q23.2. Duplication of *SNCAIP* is restricted to Group4α, a subtype of Group 4 medulloblastoma with a mostly balanced genome[23]. The NF-κB pathway was also identified as a new targetable pathway in this subgroup of tumors. However, there are currently no mouse models of Group 4 tumors and its cell of origin is still unknown.

Despite the potential for prognostic subgrouping based on molecular signatures or immunohistochemistry, clinical application of these findings is in its infancy. No consensus on a prognostic algorithm currently exists, although efforts to merge clinical and molecular features for risk stratification in clinical trials is underway.

1.2 The Role of HGF/cMET Pathway Signaling in Human Medulloblastoma[ii]

Medulloblastoma is associated with dysregulation of pathways that normally lead to cerebellum development. Over the past few years, different signaling pathways have been shown to play a critical role in medulloblastoma formation and progression. The hepatocyte growth factor (HGF)/cMET signaling pathway has been implicated in different processes including development and tumorigenesis but only recently has it been demonstrated in medulloblastoma pathogenesis. The receptor tyrosine kinase cMET is normally activated by ligation through its ligand HGF, secreted as a precursor that is proteolytically cleaved in an active form by the serine protease hepatocyte growth factor activator. HGF is a member of the plasminogen-related growth factor family and was originally identified as a growth factor for hepatocytes and as a fibroblast-derived cell motility or scatter factor. The interplay between cMET and its ligand mediate downstream events that, in the central nervous system, play a critical role in cerebellar granule cell precursors proliferation and survival. Dysregulation of this pathway can promote tumorigenesis through cell migration, invasion and metastasis, angiogenesis and prevention from apoptosis. cMET has been found to be overexpressed in a variety of malignancies where its activation can occur by HGF ligation or through ligand independent mechanisms, including mutations and amplifications.

It was shown that medulloblastoma tumor cell lines and surgical tumor samples express HGF and cMET. Furthermore, overexpression of cMET is associated with poor clinical outcome. Treatment of medulloblastoma cell lines with HGF induced tumor cell proliferation, anchorage-independent growth and reduced apoptosis in response to chemotherapy. *SPINT2*, a tumor supressor gene silenced by promoter methylation in medulloblastoma, was identified by our group as a key regulator of HGF/cMET pathway[34]. Several therapeutic strategies aiming to target and limit the signaling cascade of HGF/cMET were examined with the cMET inhibitors being the most promising. Targeting the HGF/cMET pathway, alone or in combination with standard therapies is likely to improve present treatments in MET-dependent malignancies such as medulloblastoma.

[ii] Claudia Faria, Christian Smith and James Rutka (2011). The Role of HGF/c-Met Pathway Signaling in Human Medulloblastoma, Molecular Targets of CNS Tumors, Dr. Miklos Garami (Ed.), ISBN: 978-953-307-736-9, InTech, DOI: 10.5772/23296.

1.2.1 The HGF/cMET Pathway Signaling

The HGF/cMET pathway has been associated with normal development, organ regeneration and cancer. cMET is a high affinity tyrosine kinase receptor for hepatocyte growth factor (also known as scatter factor, capable of inducing dissociation and motility). cMET is generally expressed in epithelial cells and is activated by HGF produced in surrounding mesenchymal cells or released into the circulation.

During embryogenesis the HGF/cMET signaling is necessary for the development of the placenta, liver, kidney and neuronal tissue but also for the directional migration of skeletal muscle cells[35]. In adult tissues, this pathway has been implicated in regeneration and wound healing[36,37]. Therefore, the HGF/cMET axis is a key player in cell proliferation, survival and migration and, when dysregulated, can give origin to a variety of cancers.

1.2.1.1 Structure of HGF and cMET

HGF is a multidomain protein similar to plasminogen, a circulating proenzyme that promotes the lysis of fibrin blood clots in its active form as plasmin. HGF is synthesized as a single-chain inactive precursor and it is converted by serine proteases into an active form with two chains (α and β chain) linked by a disulfide bond. HGF consists of six domains: an amino-terminal hairpin loop domain, four kringle domains (K1-K4) and a serine protease homology (SPH) domain which lacks enzymatic activity (**Figure 1.2**).

cMET, the HGF receptor, is a disulfide-linked heterodimer which results from cleavage of a precursor into an extracellular α chain and a transmembrane β chain. The extracellular region of cMET is composed of three domains: the Sema domain (homologous to the Sema domain of the semaphorins and plexins) that includes the entire α chain and part of the β chain; the PSI domain (also present in the plexins, semaphorins and integrins); and four IPT domains (immunoglobulin-like also found in plexins and transcriptional factors). The intracellular region of cMET consists of three portions: a juxtamembrane sequence that has the role to downregulate kinase activity upon phosphorylation of Ser975; a catalytic region that activates kinase activity following phosphorylation of Tyr1234 and Tyr1235; and a carboxy-terminal multifunctional docking site that contains two docking tyrosines (Tyr1349 and Tyr1356) essential for downstream signaling[38].

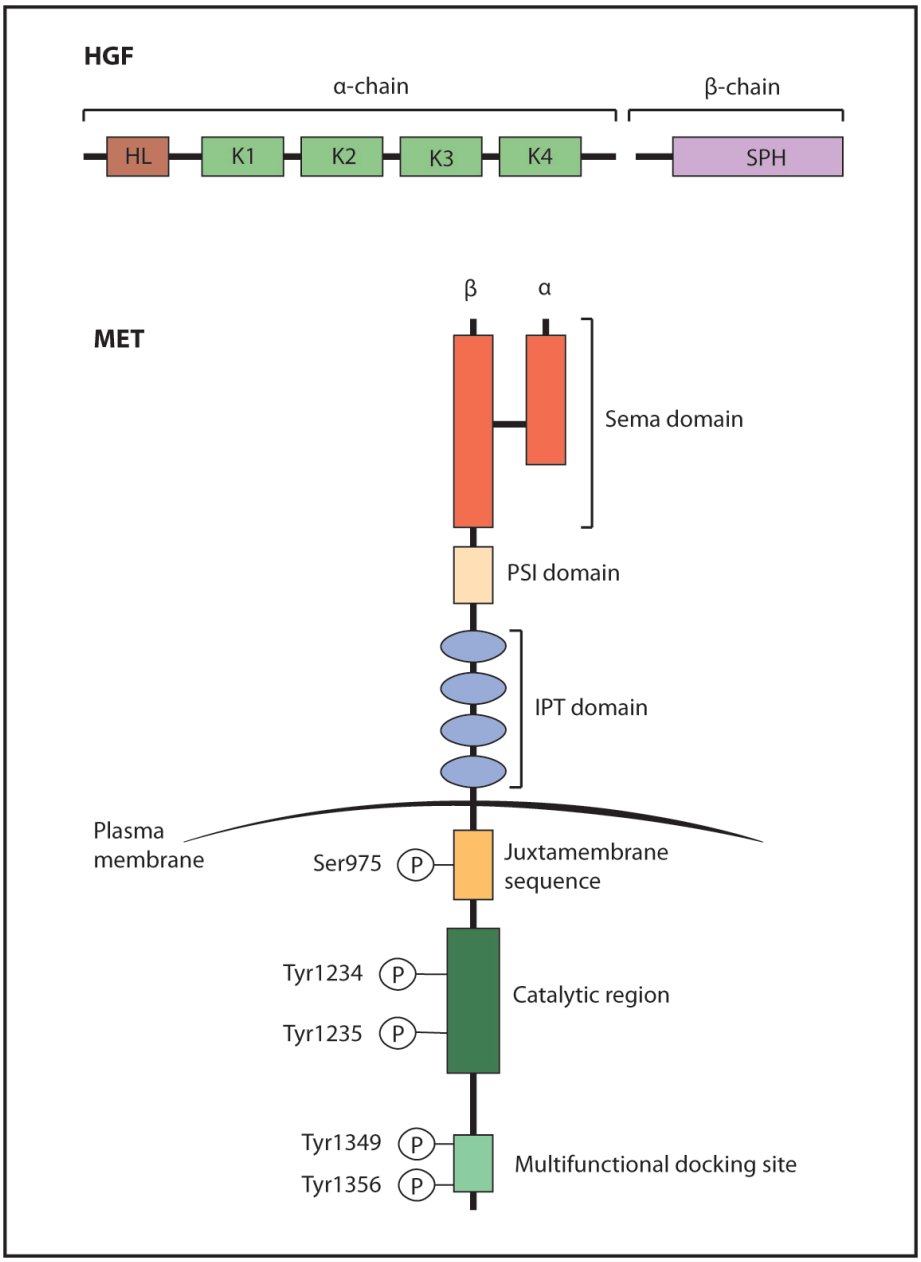

Figure 1.2: HGF and cMET structures.

1.2.1.2 cMET Signal Transduction

To activate the cMET receptor, the single chain HGF precursor is cleaved into a heterodimeric active form by a protease called HGF activator (HGFA)[39]. This process is regulated by a protein family of serine protease inhibitors called SPINT1 and SPINT2[40,41]. Inhibiting the activation of HGF by HGFA, SPINT1 and -2 limit signaling through the HGF/cMET pathway.

Following HGF binding, the kinase activity of cMET is switched on. This process starts with receptor dimerization and trans-phosphorylation of two tyrosine residues in the catalytic region (Tyr1234 and Tyr1235) and is followed by phosphorylation of two additional tyrosines in the carboxy-terminal tail (Tyr1349 and Tyr1356). These tyrosines create docking sites for a variety of adaptor proteins and direct kinase substrates including the growth factor receptor-bound protein 2 (GRB2), Grb2-associated adaptor protein (GAB1), son of sevenless (SOS), SRC homology protein tyrosine phosphatase 3 (SHP2), phosphatidylinositol-3-kinase (PI3K) and signal transducer and activator of transcription 3 (STAT3). This leads to the activation of downstream signaling pathways that include the mitogen-activated protein kinase (MAPK), PI3K/AKT and STAT pathways, which mediate cMET-dependent cell proliferation, survival, migration and invasion (**Figure 1.3**).

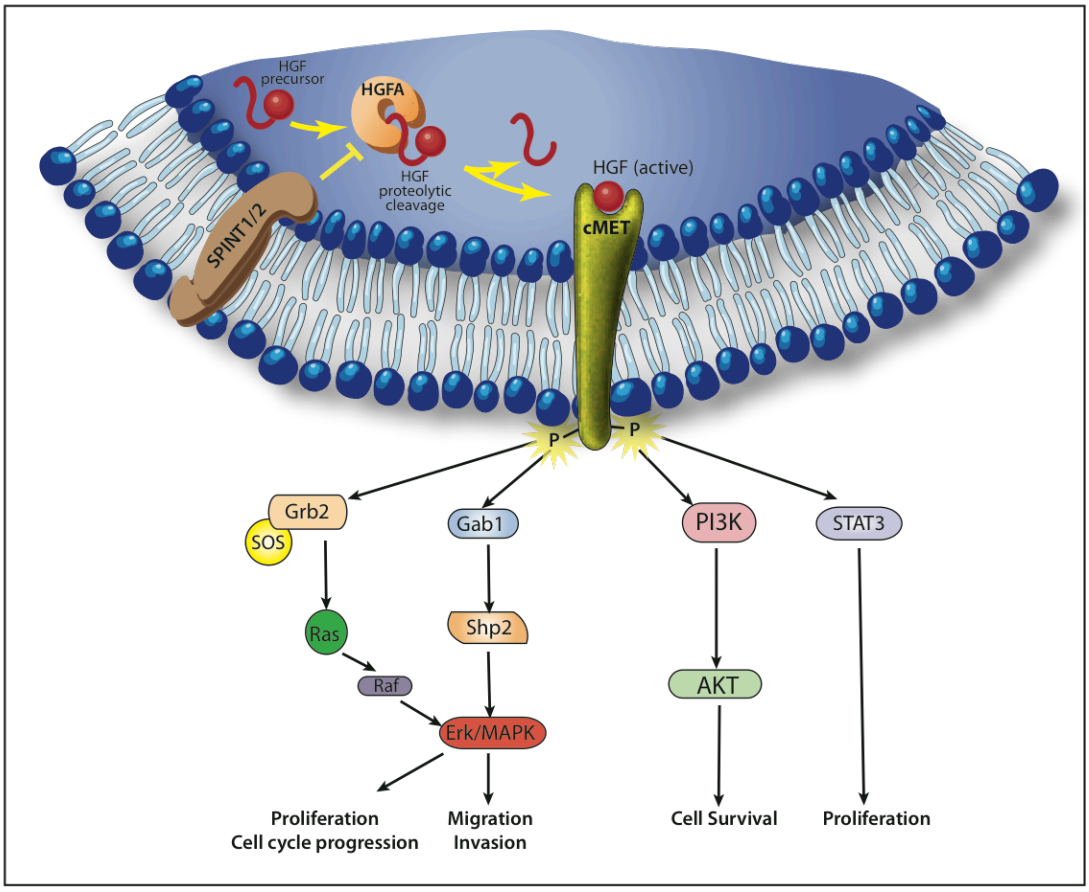

Figure 1.3: The HGF/cMET signaling pathway.

The activation of MAPK cascade will sequentially activate different protein kinases whose terminal effectors include extracellular signal-regulated kinases (ERK1 and ERK2), jun amino-terminal kinases (JNK1, JNK2 and JNK3) and p38. These downstream elements will activate cell cycle regulators leading to cell proliferation and will promote alterations in cytoskeletal functions that control cell migration and invasion. PI3K/AKT activation mediates cell survival and resistance to apoptosis through inactivation of the pro-apoptotic protein BCL-2 antagonist of cell death (BAD) and degradation of the pro-apoptotic protein p53[42]. Upon activation of STAT3 by the cMET receptor at the plasma membrane, it translocates to the nucleus to operate as a transcription factor regulating the expression of genes implicated in cell proliferation and differentiation[43].

Other molecules that interact with the cMET receptor include the epidermal growth factor receptor (EGFR), the α6β4 integrin, the semaphoring receptors of the plexin B family and the variant of the hyaluronan receptor CD44 (that links the extracellular matrix and the intracellular cytoskeleton)[44-46]. This crosstalk of cMET with different surface proteins highlights the dynamic environment at the plasma membrane and contributes to cMET associated biological responses[47].

1.2.1.3 Regulation of cMET Signaling

It has been shown that the signaling network around the tyrosine kinase receptor cMET is more complex than the known process of recruiting signaling effectors at the plasma membrane and subsequently stimulating intermediates in the cytosol. In fact, this view has been expanded by the finding that cMET signals can also originate from endosomal compartments and by a series of other events.

Upon HGF binding, cMET is internalized by clathrin-mediated endocytosis and recruited into peripheral early endosomes. This process is mediated by protein kinase Cε (PKCε) that promotes the transfer of active ERK to focal adhesions and, subsequently, the HGF-induced cell migration. From the peripheral endosomes, cMET travels along the microtubule network to late perinuclear compartments in a process mediated by PKCα. This juxtanuclear accumulation of cMET is a determinant step for activation and nuclear translocation of STAT3[48,49].

Downregulation of cMET signaling involves trafficking and degradation of ligand-activated receptors in the lysosomes. This process is initiated by the association of cMET with casitas B-lineage lymphoma (CBL) and endocytic adaptors. Following endocytosis, cMET

accumulates in multivesicular bodies that later fuse with lysosomes and lead to protein degradation. cMET can also undergo sequential proteolytic cleavage at two juxtamembrane sites. The first cleavage occurs in the extracellular domain and is mediated by a desintegrin and metalloprotease (ADAM) originating a 'decoy' fragment that sequesters the ligand and interferes with the receptor's activity. The second cleavage is performed in the intracellular domain, by a γ-secretase and yields a fragment that is destroyed in the proteasome[50] (**Figure 1.4**).

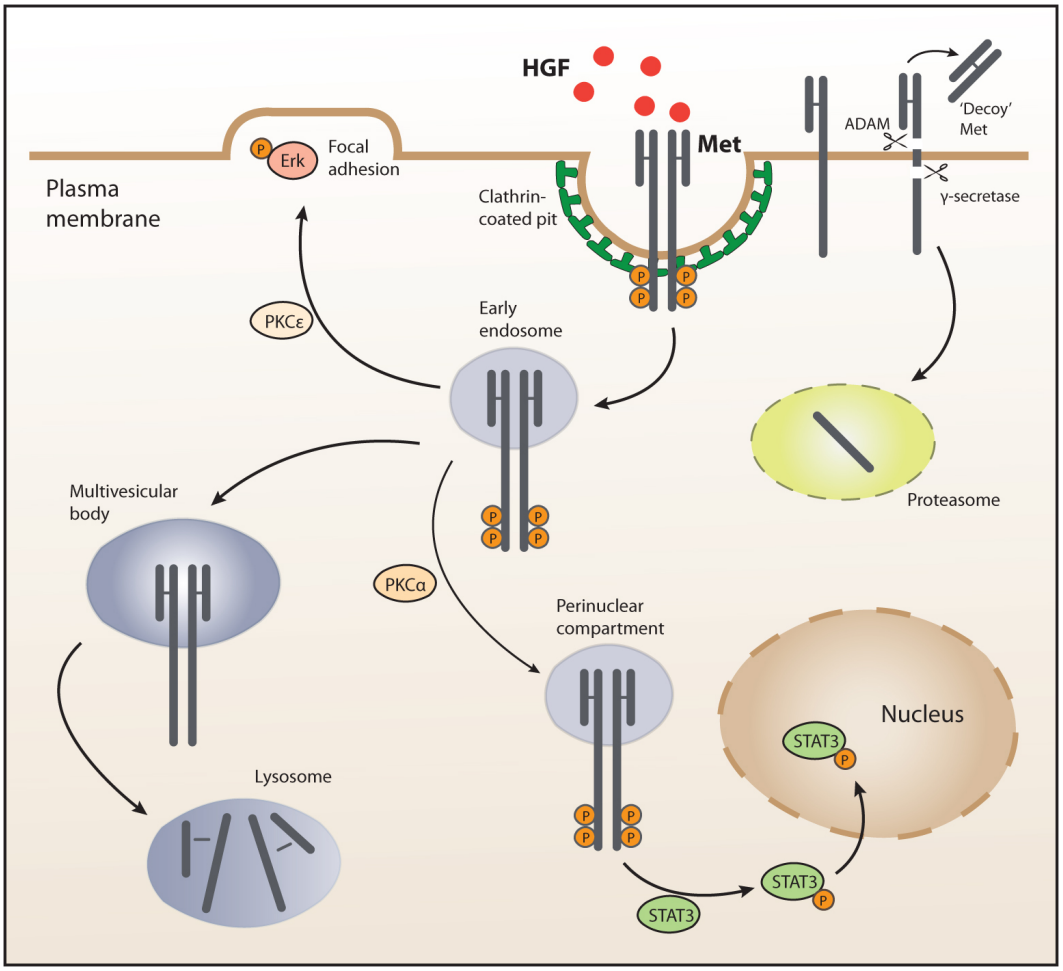

Figure 1.4: Mechanisms of cMET signaling regulation.

1.2.2 HGF, cMET and Cancer

The dysregulation of HGF/cMET signaling has emerged as a key player in several human malignancies, particularly in invasion and metastasis. Human cell lines overexpressing either HGF and/or cMET become tumorigenic and metastatic when implanted into nude

mice[51]. Moreover, transgenic mice expressing the receptor or the ligand develop metastatic tumors[52]. On the contrary, downregulation of HGF or cMET expression in human tumor xenografts decreases tumor growth[53]. There are three biological mechanisms underlying the tumorigenicity of cMET: a) the establishment of HGF/cMET autocrine loops; b) the overexpression of HGF or cMET; and c) the presence of activating mutations in the cMET receptor[54].

An autocrine mechanism of cMET activation is found in some human tumors. For example, osteosarcomas and rabdomyosarcomas are derived from mesenchymal cells which physiologically produce HGF. Glioblastomas and breast carcinomas are derived from ectodermal tissues that normally express cMET but not HGF. Experimental models of HGF/cMET autocrine loops were also able to generate invasive tumors *in vitro* and in transgenic mice[55]

The most frequent mechanism of cMET dysregulation found in human tumors is the overexpression of the receptor or its ligand. A large number of studies showed that HGF and cMET are expressed in a wide variety of human tumors and in their metastasis. These include carcinomas of the breast, colon, lung, ovary, liver, kidney, upper gastrointestinal tract, pancreas and prostate but also sarcomas, haematopoietic malignancies, melanomas and glioblastomas[42].

It has also been shown that high expression levels of cMET and its ligand correlate with increased aggressiveness of tumors and patients poor prognosis[42]. For example, in colorectal cancer patients, cMET is a powerful prognostic factor for early stage invasion and metastasis[56]. Moreover, in a study including 74 clinical samples of low-grade and high-grade gliomas the authors described a correlation of HGF and cMET expression levels with tumor grade[57].

The compelling evidence that links cMET with human cancer relies in the cMET-activating mutations found in hereditary renal papillary carcinoma. These mutations were also found in sporadic tumors such as renal carcinoma, gastric cancer, childhood hepatocellular carcinoma and in head and neck squamous cell carcinomas[47,55].

The association between cancer and blood coagulation disorders has been known for many years. In fact, approximately 50% of all patients with malignant tumors and up to 90% of those with metastasis have coagulopathies[58]. Interestingly, Boccaccio *et al*. showed in a mouse model that activation of the oncogene cMET induced cancer and a trombohemorrhagic syndrome through transcriptional upregulation of the procoagulation factors plasminogen activator inhibitor type 1 (PAI-1) and cyclooxygenase-2 (COX-2). Upon a first phase

characterized by a hypercoagulation state due to cMET signaling activation, the mice developed a hemorrhagic diathesis due to exhaustion of the hyperactivated hemostatic system[59]. At the early step of this process, hypoxia induces transcription of cMET that, subsequently, activates the transcription of genes involved in hemostasis, such as *PAI-1* and *COX-2*. The activation of the coagulation cascade will lead to fibrin deposition around cells forming an extracellular matrix that will promote angiogenesis and cell migration[60].

HGF/cMET signaling has also a role in angiogenesis either by direct influence of cMET activation in vascular endothelial cells, or by regulation of the expression levels of other angiogenic factors in tumor cells. It was previously shown that the HGF/cMET interaction stimulates proliferation and migration of endothelial cells *in vitro* and induces blood vessel formation *in vivo*[61]. Zhang *et al*. described the "angiogenic switch" in tumor cells upon HGF stimulation by simultaneous upregulation of the proangiogenic vascular endothelial growth factor (VEGF) and downregulation of thrombospondin 1 (TSP-1), an angiogenesis inhibitor[62]. This process has distinct mediators: while VEGF is modulated by MAPK, PI3K and STAT3, TSP-1 is targeted only by MAPK. An interesting example of this regulation was found in human glioma cells where stimulation with HGF increased the expression levels of VEGF and tumor-associated angiogenesis. The use of HGF and cMET inhibitors in experimental tumor models significantly reduced tumor growth and tumor vessel formation[57]. Recently, a new key player of the HGF/cMET pathway was described. Metastasis-associated in colon cancer-1 (*MACC1*) was identified by genome-wide expression analysis in primary and metastatic colon carcinomas. Its expression in human tumor samples was found to be an independent prognostic factor for metastasis formation and metastasis-free survival. The experimental studies showed that MACC1 promotes proliferation, invasion and HGF-induced scattering in vitro and tumor growth and metastasis in xenograft models[63]. The authors proposed a positive feedback mechanism where MACC1 acts as a transcriptional regulator of the cMET gene. The stimulation of the cMET receptor with HGF causes the translocation of MACC1 from the cytoplasm into the nucleus. There, MACC1 activates the transcription of the *cMET* gene by binding to its promoter[64]. The increased amounts of cMET receptor will be able to bind more HGF molecules thereby enhancing the pathway signaling and promoting cell proliferation, migration and metastasis.

1.2.3 HGF/cMET Signaling in Medulloblastoma

1.2.3.1 HGF/cMET Pathway in Cerebellar Development

During embryonic development, the progenitor cells localized in the ventricular zone of the cerebellum (also called primary germinal zone), along the fourth ventricle, migrate radially to give rise to Purkinje cells, neurons of the cerebellar nuclei and different types of cerebellar interneurons. Simultaneously, the progenitor cells in the rombic lip migrate dorsally to originate in the EGL or secondary germinal zone. The peak of proliferation of these cells occurs between postnatal day (P) P5 and P8 in the mouse. Through a tightly regulated mechanism, the progenitor cells in the EGL become postmitotic, differentiate and migrate inwards to give origin to the internal granule layer (IGL), a process that is compete by P20 in the mouse[65].

During the early postnatal period, multiple mitogenic pathways, such as SHH, WNT and Notch, promote the rapid expansion of progenitor cells in the EGL. It is believed that this vast population of cells includes subgroups of progenitors with distinct genetic properties, that give origin to the different medulloblastoma subtypes[7].

The HGF/cMET pathway also plays a critical role in cerebellar development. The knockout mice for HGF, cMET and SPINT2 are all embryonic lethal[66-68]. Comparing the regional expression of HGF and cMET in both developing and adult rat brains, Achim and co-workers found expression of HGF in the parietal cortex, striatum and cerebellar deep gray matter in developing but not in adult brain. Abundant expression of cMET was also detected in the newborn cortex, thalamus and brainstem[69]. The analysis of HGF and cMET expression in the central nervous system of different mammalian species showed that their neuronal expression is highly conserved during evolution, a sign that they mediate important functions[70].

Leraci *et al*. described the expression of cMET in the proliferating cells of the external granule layer of the cerebellum and increased proliferation after stimulation of primary cultures of granule cells with HGF. In addition, transgenic mice with partial loss of cMET function had a smaller cerebellum with abnormal foliation and balance impairment[71]. HGF has also been proposed to mediate neurotrophic functions during neurogenesis both in the central and peripheral nervous systems. In fact, it was shown that HGF is a chemoattractant and promotes survival of motor neurons in the embryo. Furthermore, stimulation of sensory and sympathetic neurons with HGF enhances survival, differentiation and axonal growth[72].

Exploring the neuroprotective role of HGF, different groups showed that HGF treatment of primary cerebellar granule neurons prevents apoptotic cell death through activation of the PI3K/AKT pathway signaling[73-75].

1.2.3.2 HGF/cMET Pathway in Medulloblastoma Formation

HGF/cMET signaling has an important role in tumorigenesis and metastatic behavior in several human malignancies but its role in medulloblastoma pathogenesis was only recently described.

Studying a series of 14 human medulloblastoma samples by comparative genomic hybridization Tong *et al.* found amplification of the *cMET* oncogene on chromosome 7q in 38.5% of cases[76]. Other group showed a correlation between the expression of HGF and cMET in human medulloblastoma samples and patient clinical outcome[77]. When they stimulated medulloblastoma cells with HGF there was an activation of downstream effectors, evidenced by cMET, MAPK and AKT phosphorylation. Up-regulation of the pathway was also able to induce cell proliferation, cell cycle progression, anchorage-independent growth and resistance to chemotherapy-induced apoptosis in medulloblastoma cell lines. In vivo models overexpressing HGF also had increased tumor growth and invasion[77]. More recently, the same group identified an association between HGF/cMET signaling and c-MYC in medulloblastoma. They found that HGF induced MYC expression both at transcriptional and post-transcriptional levels, leading to cell cycle progression, cell proliferation and apoptosis[78].

Although the anti-apoptotic functions of HGF/cMET pathway seem to be predominant, Li *et al.* described enhanced cell death in Daoy cell lines after cMET activation. Apoptotic cell death can be induced by two different pathways: the intrinsic mitochondrial pathway and the extrinsic death receptor pathway. In malignant tissues, the tumor necrosis factor-related apoptosis–inducing ligand (TRAIL) has the potential to activate the death receptor pathway upon binding of death receptors DR4 and DR5, which leads to downstream caspase activation and apoptosis[79]. Li and co-workers found that increased apoptosis of medulloblastoma cell lines after stimulation with HGF was induced by TRAIL and mediated by DR5 overexpression[80]. Moreover, the treatment of those cells with a specific cMET inhibitor (PHA665752) reduced apoptosis indicating that it requires activation of the canonical receptor tyrosine kinase[80].

Using an epigenome-wide screening our group identified an inhibitor of HGF/cMET signaling. *SPINT2*, a tumor suppressor gene, was downregulated in 73.2% of primary

medulloblastoma samples while *cMET* was upregulated in 45% of cases. *SPINT2* was silenced by promoter hypermethylation in 34.4% of primary tumor samples[34]. A single nucleotide polymorphism (SNP) array analysis identified hemizygous deletions in the *SPINT2* locus on chromosome 19q13.2 and gains in the *HGF* and *cMET* loci on chromosome 7q. The experimental studies using medulloblastoma cells transfected with SPINT2 showed decreased proliferation, migration and anchorage-independent growth in vitro and increased survival times in mouse xenografts[34]. Although SPINT2 downregulation has already been implicated in other human cancers[81-83] this was the first report to establish its role in medulloblastoma pathogenesis.

Binning *et al*. showed that HGF and SHH cooperate to transform cerebellar neural progenitors in transgenic mice, leading to medulloblastoma initiation and growth. Furthermore, the treatment of mice bearing SHH+HGF induced tumors with a monoclonal antibody against HGF (L2G7) prolonged survival by increasing apoptosis[84]. Previous studies had already shown that systemic administration of L2G7 to mouse xenografts of human HGF+/cMET+ glioblastomas improved survival and reduced tumor growth[85].

Knowing that a procoagulant state is often the first manifestation of a malignancy and that it is due to the expression of specific proteins such as tissue factor (TF), Provencal and colleagues analyzed the expression of this protein in human medulloblastoma samples and observed a strong correlation between cMET and TF expression levels. Furthermore, the stimulation of Daoy cells with HGF increased the expression of TF and the treatment of those cells with physiological amounts of TF activator (factor VIIa) increased their migratory potential[86]. It was hypothesized that the acquisition of a procoagulant phenotype by medulloblastoma favors its dissemination because the enrichment of the tumor environment with fibrin protects the cancer cells from the immune system and forms a matrix for cell migration[86]. The same group found that upregulation of TF upon cMET pathway activation was associated with increased resistance to the chemotherapeutic drug etoposide[87]. This observation suggested that the combination of anticoagulant drugs and chemotherapy could improve the efficacy of chemotherapeutic agents. In fact, this regimen was already tested in metastatic breast cancer with encouraging results[88].

These findings show the importance of the HGF/cMET pathway signaling in medulloblastoma malignancy. Furthermore, they also provide validation of this pathway as a target for new and promising therapies using small molecular inhibitors and antibodies, some of them already in clinical trials for other cancers.

1.2.4 Inhibitors of HGF/cMET Pathway in Cancer Therapy

The evidence that the HGF/cMET pathway is involved in the progression and dissemination of several malignancies has generated considerable interest in HGF and cMET as major targets in cancer therapy and drug development. Different strategies are being explored and some of them are already being tested in clinical trials. We can consider three main groups of drugs: a) HGF and cMET antagonists or competitors; b) Monoclonal antibodies directed against HGF and cMET; and c) Small molecule tyrosine kinase inhibitors.

The use of molecular targeted therapies against HGF and cMET in medulloblastoma was only recently reported. Our group demonstrated the efficacy of a highly specific small molecular inhibitor (PHA665752) in the treatment of medulloblastoma cell lines by reducing cell proliferation, migration and anchorage-independent growth[89]. Another group used an orally available small molecule inhibitor of cMET (SGX523) in medulloblastoma cells and human glioblastoma xenografts. They reported decreased cell proliferation, migration and invasion in the *in vitro* studies and significant reduction of *in vivo* tumor growth[90]. The HGF-neutralizing monoclonal antibody, L2G7, was also tested in monotherapy and in combination therapy in genetically engineered mice with medulloblastomas induced by SHH and HGF. The authors reported tumor growth inhibition and increased survival with L2G7 monotherapy[91].

Strategies using combined regimens targeting multiple receptor tyrosine kinases are currently under study. This can be achieved in two different ways either by a combination of highly selective agents or by using a single agent that targets multiple specific members of the cMET pathway. The use of broad-spectrum agents may have the advantage of reducing drug interactions, but it may also affect other unintended kinases. Stommel *et al*., studying glioma cell lines, xenografts and human primary glioblastomas, showed simultaneous activation of multiple receptor tyrosine kinases and better responses to combined treatment when compared to monotherapy[92].

We provide a brief summary of the latest advances in HGF/cMET targeted therapy (**Table 1.1**).

Table 1.1: Summary of the HGF/cMET inhibitors.

Compound	Mechanism of Action	Stage of development	References
Biological antagonists			
NK2	Inhibits HGF activity	Preclinical	93,94
NK4	Inhibits HGF binding to cMET	Preclinical	95-97
Uncleavable HGF	Inhibits proteolytic HGF activation	Preclinical	98
Decoy MET	Inhibits HGF binding and cMET dimerization	Preclinical	99
Antibodies			
AMG102 (Amgen)	Anti-HGF (IgG2)	Phase II trial	100-102
L2G7 (Galaxy Biotech)	Anti-HGF (IgG1)	Preclinical	85,91,103
MetMAb (Genentech)	Anti-cMET	Phase II trial	104
Small molecule inhibitors of cMET			
PHA665752 (Pfizer)	Selective inhibitor (cMET)	Preclinical	78,89
PF2341066 (Pfizer)	Selective inhibitor (cMET and ALK)	Phase II/III	105-107
ARQ197 (ArQule)	Selective inhibitor (cMET)	Phase II	108,109
SGX523 (SGX Pharmaceuticals)	Selective inhibitor (cMET)	Phase I (discontinued)	90,110
XL184 (Exelixis)	Multikinase inhibitor (cMET, VEGFR, Ret, Kit, Flt-3, Tie-2)	Phase II/III	(http://clinicaltrials.gov)
XL880 (Exelixis)	Multikinase inhibitor (cMET, VEGFR, PDGFR, Ron, Kit, Flt-3, Tie-2)	Phase II	111 (http://clinicaltrials.gov)
MP470 (Supergen)	Multikinase inhibitor (cMET, PDGFR, Ret, Kit, Flt-3)	Phase I	112-114

VEGFR, vascular endothelial growth factor receptor; Ret, rearranged during transfection; Kit, stem cell factor receptor; Flt-3, FMS-like tyrosine kinase 3; Tie-2, angiopoietin receptor 2; PDGFR, platelet-derived growth factor receptor; Ron, recepteur d'origine nantais

1.2.4.1 HGF and cMET Antagonists

HGF and cMET antagonists or decoys are molecules that bind to the receptor with high affinity without activation of downstream signaling. The activation of cMET by HGF implies the dimerization of the receptor upon binding of the two chains of the ligand. HGF has a high affinity site located in the α–chain and a low affinity site in the β–chain, which only becomes accessible after pro-HGF activation[115]. This means that the inactive form of HGF or HGF fragments can interact with cMET binding to the high affinity site but they cannot induce cMET signaling because they are unable to promote receptor dimerization.

Examples of HFG competitors are NK2, NK4 and uncleavable HGF. NK2 is a naturally occurring HGF fragment and NK4 is a synthetic truncated form of HGF that contains only the α–chain. This is by far the best studied HGF antagonist and it was shown that it inhibits cell invasion and angiogenesis in vitro and in xenografts[95]. Uncleavable pro-HGF is an unprocessable form of HGF that competes with active HGF for cMET binding and with pro-HGF proteases for HGF proteolytic activation.

Decoy MET is an enzymatically inactive molecule that corresponds to the extracellular domain of the receptor. It interacts with HGF and full-length cMET, sequestering the ligand and interfering with the receptor dimerization.

1.2.4.2 Monoclonal Antibodies Directed Against HGF and cMET

The use of monoclonal antibodies has the following advantages: specificity against HGF and cMET; a relatively longer half-life when compared to other inhibitors; and the potential to induce a host immune response against the tumor cells[116].

AMG102 is a fully human IgG2 antibody against HGF that was found to enhance the effects of temozolomide and docetaxel *in vitro* and in xenograft models of gliomas[101]. A Phase I study used a combination of AMG102 and the antiangiogenic drugs bevacizumab and motesanib in the treatment of patients with advanced solid tumors, showing a stable disease in most patients[117]. This molecule has also been tested in Phase II clinical trials for advanced glioblastomas and renal cell carcinomas and a preliminary analysis in glioma patients suggested that AMG102 has limited efficacy as monotherapy[118]. Therefore, the most recent clinical trials will use AMG102 in combination therapy (http://clinicaltrials.gov). L2G7 is another anti-HGF antibody that proved to be effective reducing subcutaneous and intracranial glioma xenografts and to increase survival[85].

The initial efforts to develop antibodies against cMET were unsuccessful because they tended to behave as agonists rather than antagonists, due to its bivalent structure that acts as a natural dimerizing agent. To circumvent this problem a 'one-armed' antibody (OA-5D5; MetMAb), consisting of a monovalent Fab fragment, was developed. It binds to cMET with high affinity preventing HGF interaction and subsequent downstream signaling. Martens *et al.* infused MetMAb intratumorally, reporting almost complete inhibition of tumor growth in a glioblastoma mouse model[104]. Phase II clinical trials using MetMAb in combination with bevacizumav and paclitaxel for metastatic breast cancer and with erlotinib for advanced non-small cell lung cancer have been initiated (http://clinicaltrials.gov).

1.2.4.3 Small Molecule Tyrosine Kinase Inhibitors

Small molecule inhibitors target the ATP-binding site of the cMET receptor, blocking its transphosphorylation. These molecules can also be classified according to their specificity for cMET. Highly selective drugs may not be desirable as inhibition of multiple kinases may be more efficient and reduce the development of resistance. On the other hand, off-target inhibition of essential kinases may also be deleterious. With the recent advances in research and the ongoing clinical trials the small molecule inhibitors have emerged as promising drugs[119].

PHA665752 is a cMET selective inhibitor that was found to be effective in tumor cell lines and xenografts, particularly in a subset of cancers with amplification of the *cMET* gene[89,120]. Due to its low oral bioavailability another drug (PF2341066) with identical structure but more favorable pharmacokinetic properties was designed. PF2341066 selectively targets cMET and anaplastic lymphoma kinase (ALK) and was shown to have antitumor cytoreductive activity and antiangiogenic activity in several cancer models[105-107]. A Phase II study in non-small-cell lung cancer reported encouraging results with a disease control rate of 87%[121]. The drug is now in Phase III trials. Interestingly, PF2341066 is also being tested in Phase I/II studies in children with recurrent solid tumors, primary central nervous system tumors and anaplastic large cell lymphoma (http://clinicaltrials.gov).

ARQ197 is a highly selective, non-ATP competitive drug with reported clinical activity in several types of solid tumors. A Phase II trial in patients with non-small-cell lung cancer reported improved survival in patients treated with ARQ197 and erlotinib when compared to erlotinib monotherapy[121]. SGX523 is an orally available ATP-competitive molecule with high selectivity for Met. Although the initial results with in vitro and in vivo

models of medulloblastomas and gliomas looked promising because of its efficacy in reducing tumor growth, the drug was discontinued from a Phase I trial due to renal toxicity[122].

XL184 and XL880 are orally available, non-selective inhibitors, with high binding affinity to both cMET and VEGFR and to a lesser extent to other receptor tyrosine kinases such as PDGFR, Ret, Kit, Flt-3 and Tie-2[123]. XL184 is being evaluated in a Phase III study in patients with advanced medullary thyroid cancer and in Phase II studies in patients with glioblastoma multiforme and non-small-cell lung cancer that has progressed after previous benefit with erlotinib. XL880 has been tested in Phase II clinical trials in metastatic gastric cancer, papillary renal cell carcinoma and head and neck squamous cell cancer (http://clinicaltrials.gov).

MP470 is a multi-kinase inhibitor, orally available, that was reported to radiosensitize glioblastoma cell lines, in vitro and in vivo models, through the suppression of RAD51, a DNA repair related protein[113]. Additional Phase I clinical studies used MP470 in monotherapy or in combination with standard chemotherapies in patients with metastatic solid tumors and lymphoma (http://clinicaltrials.gov).

1.2.5 Conclusion and Future Directions

The HGF/cMET signaling pathway plays a significant role in cancer and has emerged recently as a promising target in the treatment of several malignancies. It was shown that HGF and cMET are key players in cerebellum development and that their dysregulation is involved in medulloblastoma formation and progression.

Advances in understanding the molecular mechanisms and genetic profiles underlying the different subtypes of medulloblastoma created an urgent need for new and less toxic targeted therapies. HGF/cMET inhibitors used in the treatment of gliomas *in vitro* and *in vivo* showed efficient reduction in tumor growth and are, therefore, being evaluated in clinical trials. Our preliminary data using a cMET selective inhibitor in medulloblastoma cell lines showed that the HGF/cMET pathway is a novel and promising therapeutic target in this disease.

In the future we will test a panel of available HGF and cMET inhibitors using orthotopic xenograft models and our transgenic medulloblastoma mouse model. We hope that the results of our pre-clinical studies will provide the basis for future clinical trials where the HGF and cMET inhibitors could synergize with current therapies to increase survival and improve the quality of life of children with brain tumors.

1.3 Novel Therapies and Next Generation Clinical Trials in Medulloblastoma[iii]

1.3.1 Advances in Medulloblastoma Clinical Trials

The treatment of medulloblastoma includes surgery with maximal safe tumor resection and adjuvant chemotherapy with or without craniospinal irradiation, depending on patient age at diagnosis. Despite advances in these treatment modalities challenges remain to effectively treat some patients, especially those with recurrent or refractory medulloblastoma. Current medulloblastoma protocols separate children with standard-risk disease (absence of metastatic disease and residual tumor < 1.5 cm^2) from those with high-risk disease (metastatic disease and/or residual tumor >1.5 cm^2)[124]. More recently, the tumor histology was introduced in the staging system with patients with large cell/anaplastic histology being at greater risk of tumor relapse and hence, classified as high-risk[125,126].

Table 1.2 summarizes the most relevant clinical trials over the past years for standard-risk, high-risk and recurrent medulloblastoma.

1.3.1.1 Standard-risk patients

The conventional treatment for standard-risk medulloblastoma has consisted of complete surgical resection followed by craniospinal radiation therapy with a total dose of 54-56 Gy (36 Gy to the craniospinal axis with a boost of 18-20 Gy to the posterior fossa) and chemotherapy. The 5-year progression free survival using this therapeutic regimen was 85%[127]. However, it has been recognized over the years that a high proportion of medulloblastoma survivors have significant long-term sequelae, mostly induced by craniospinal irradiation. Neurocognitive impairment occurs in a dose dependent manner and is more pronounced in children of younger age[128]. Other late side effects include hearing loss, growth and endocrinological deficits, gonadal dysfunction and secondary tumors[129].

[iii] Claudia C. Faria, Roberto J. Diaz and James T. Rutka (2014). Novel Therapies and Next Generation Clinical Trials in Medulloblastoma, Medulloblastoma Book, Dr. Dimitris Kombogiorgas (Ed.), Nova Science Publishers (in press).

Table 1.2: Clinical trials in medulloblastoma.

Therapeutic Regimen	Clinical Trial	Number of MB patients	Results	Reference
Standard-risk medulloblastoma				
CSI (36 Gy) + vincristine	Phase II	63 (48 standard-risk)	90% 5-year PFS	1994 [127]
CSI (23.4 Gy) + vincristine	Phase III	379	81% 5-year EFS	2006 [130]
CSI (25 Gy) + 8 drugs in one day + etoposide and carboplatin	Phase II	136	64.8% 5-year EFS 73.8% OS	2005 [131]
CSI (23.4 Gy), high-dose chemotherapy and SCR	Phase II	134 (86 standard-risk)	85% 5-year OS 83% 5-year EFS	2006 [132]
Conformal radiotherapy	Clinical study	86	83% 5-year EFS	2008 [133]
STRT vs HFRT	Phase II	340	STRT: 77% 5y EFS, 87% 5y OS HFRT: 78% 5y EFS, 85% 5y OS	2012 [134]
High-risk medulloblastoma				
CSI (36 Gy) + vincristine	Phase II	63 (15 high-risk)	67% 5-year PFS	1994 [127]
8-in-1 chemotherapy or VCP + radiotherapy	Phase III	203 (83 high-risk)	40% 5-year PFS (M2) 57% 5-year PFS (M1)	1999 [135]
Post-op neoadjuvant chemo vs immediate pot-op radiotherapy	Phase II	137 (19 high-risk)	66% 3-year PFS (all patients) 30% 3-year PFS (M2/3)	2000 [136]
CSI (36-39.6 Gy), high-dose chemo and SCR	Phase II	134 (48 high-risk)	70% 5-year OS 70% 5-year EFS	2006 [132]
Post-op neoadjuvant chemotherapy + CSI	Phase III	68	43.9% 5-year OS 34.7% 5-year EFS	2005 [137]
Intensive sequential chemotherapy + HART	Phase III	33	72% 5-year PFS 73% 5-year OS	2009 [138]
Topotecan + CSI + high-dose chemo + SCR	Phase II	53 (19 high-risk)	73.7% 2-year PFS	2001 [139]
Induction chemo + single myeloablative cycle + SCR	Phase II	21	48% 3-year PFS 60% 3-year OS	2004 [140]

Recurrent medulloblastoma				
Thiotepa and etoposide + SCR	Phase I	6	2 patients with PR	1996 [141]
Cyclophosphamide and melphalan + SCR	Phase I	8	1 patient with CR 4 patients with PR	1996 [142]
Carboplatin, thiotepa and etoposide + SCR	Phase I	23	34% 3-year PFS 46% 3-year OS	1998 [143]
Carboplatin, thiotepa and etoposide + SCR	Phase II	25	24% 10-year PFS and OS	2010 [144]
Busulfan and thiotepa + SCR	Phase II	39	50-77% 5-year OS	2007 [145]
Temozolomide	Phase II	25	1 patient with CR 2 patients with PR	2007 [146]
Temozolomide and etoposide (oral)	Phase I	14	1 CR, 2 PR, 7 SD, 3 PD	2010 [147]
Etoposide (oral)	Phase II	4	3 patients with PR	1997 [148]
Etoposide, Cisplatinum and CSI	Phase II	28	57.6% 5-year PFS 80% 5-year OS	2012 [149]
Irinotecan	Phase II	3	2 patients with SD	2002 [150]
Irinotecan	Phase II	25	4 patients with PR	2007 [151]
Irinotecan and carboplatin	Phase I	2	1 patient with CR 1 patient with PR	2009 [152]
Irinotecan and temozolomide	Phase II	66	33% objective response	2013 [153]

Medulloblastoma (MB); Craniospinal irradiation (CSI); Progression-free survival (PFS); Event-free survival (EFS); Overall survival (OS); Standard fractionated radiotherapy (STRT); Hyperfractionated radiotherapy (HFRT); Stem cell rescue (SCR); Vincristine, lomustine (CCNU) and prednisone (VCP); eight drugs in one day (8-in-1); M1: microscopic tumor cells in the cerebrospinal fluid; M2: gross nodular seeding in the cerebellum, cerebral subaracnoid space, or in the third or fourth ventricles; M3: gross nodular seeding in the spinal subaracnoid space; Hyperfractionated accelerated radiotherapy (HART); Stem cell rescue (SCR); Partial response (PR); Complete response (CR); Stable disease (SD); Progressive disease (PD)

In order to reduce morbidity and improve the quality of life of patients with medulloblastoma, subsequent studies attempted to reduce the dose of craniospinal irradiation from 36 Gy to 23.4 Gy. This therapeutic approach reduced long-term neurocognitive deficits in children younger than 8 years[154]. A phase III study enrolled 421 patients with standard-risk medulloblastoma (379 patients were eligible). All patients received weekly vincristine concurrent with reduced-dose craniospinal irradiation, followed by a multidrug therapy with

cisplatin/vincristine/lomustine or cisplatin/vincristine/cyclophosphamide. The 5-year event-free survival using this regimen was over 80% and the adjuvant chemotherapy did not influence outcome[130].

A study from the French Society of Pediatric Oncology included 136 patients with a standard-risk medulloblastoma and a median age of 8 years. The treatment included 8 drugs in one day followed by etoposide or carboplatin, both administered before radiotherapy. The overall survival rate was 73.8% and the event-free survival rate was 64.8%[131].

Another study used risk-adapted radiotherapy in 134 patients with medulloblastoma (86 standard-risk treated with 23.4 Gy and 48 high-risk treated with 36-39 Gy) followed by four cycles of high-dose chemotherapy and stem cell or bone marrow rescue. The reported 5-year overall survival was 85% for standard risk patients and 70% in high-risk patients[132].

To limit the irradiated volume and the subsequent neurocognitive deficits, a protocol using conformal radiotherapy to the posterior fossa (36 Gy) and to the primary site (55.8 Gy) was used in 86 patients with standard-risk medulloblastoma. The irradiation to the primary site targeted the tumor surgical bed surrounded by a 2 cm margin. In this study, the control of the disease was comparable to that after radiation of the entire posterior fossa, with a 5-year event free survival of 83%[133].

A recent multicenter prospective randomized trial compared the event-free survival (EFS) and OS of 340 children treated with hyperfractionated radiotherapy (HFRT) and standard fractionated radiotherapy (STRT), followed by conventional chemotherapy. The survival rates did not differ significantly between the two therapeutic regimens, after a median follow up of 4.8 years. The reported 5-year EFS was 77% in the STRT group and 78% in the HFRT group; the 5-year OS was 87% and 83%, respectively[134].

1.3.1.2 High-risk patients

There is no standard chemotherapeutic regimen for patients with high-risk medulloblastoma. Despite high doses of radiation and intense adjuvant chemotherapy the prognosis of these patients is still very poor. Over the years, several clinical trials used different treatment schedules to achieve better control of the disease.

The Children's Cancer Group 921 phase III trial randomized high-risk medulloblastoma patients into an "eight-drugs-in-one" chemotherapy before and after radiotherapy or weekly vincristine during radiotherapy followed by vincristine, lomustine (CCNU) and prednisolone (VCP regimen). For the 83 metastatic patients with 3 years of age

or older, the 5-year progression-free survival (PFS) was significantly lower than the standard-risk patients (70% M0; 57% M1; 40% M2)[135]. The German multicenter prospective trial HIT'91 compared post-operative neoadjuvant chemotherapy consisting of ifosfamide, etoposide, cysplatin, cytarabine and intravenous high-dose methotrexate, with immediate post-operative radiotherapy followed by maintenance chemotherapy with vincristine, cisplatin, and CCNU ("Philadelphia protocol"). The 3-year PFS rates were 66% for all randomized patients, 72% for patients without residual disease after surgery, 68% for patients with residual disease and 30% for patients with metastatic disease. Although neoadjuvant chemotherapy resulted in higher response rates and lower toxicity than maintenance chemotherapy, it induced an increased myelotoxicity of subsequent radiotherapy[136]. In the European phase III trial (PNET-3) M2/M3 stage medulloblastoma patients were treated with neoadjuvant chemotherapy (vincristine, carboplatin, etoposide and cyclophosphamide) followed by craniospinal irradiation (35 Gy). When compared with other multi-institutional series, the outcome for metastatic patients did not improve, with 5-year OS and EFS rates of 43.9% and 34.7%, respectively[137].

More recently, a study including 33 patients with metastatic medulloblastoma used hyperfractionated accelerated radiotherapy (HART) (39 Gy craniospinal with a posterior fossa boost up to 60 Gy) after intensive sequential chemotherapy for 2 months. Patients showing persistent metastatic disease before HART were consolidated with two myeloablative courses of chemotherapy (tiothepa) followed by circulating progenitor cell administration. The 5-year PFS and OS was 72% and 73%, respectively[138]. Other studies have reported encouraging results with high-dose chemotherapy and autologous stem cell rescue. This procedure requires induction, harvesting and re-administration of autologous stem cells to medulloblastoma patients that have been treated with high-dose chemotherapy. The patient's stem cells are mobilized with factors including granulocyte colony stimulating factor (G-CSF) or Plerixafor (AMD3100), collected from peripheral blood or bone marrow and re-infused. Strother et al. enrolled 19 high-risk medulloblastoma patients for treatment with topotecan, followed by craniospinal irradiation (36 to 39.6 Gy) and four cycles of high-dose chemotherapy, each followed by stem cell rescue. The 2-year PFS rate was 73.7%[139]. In another study, 21 young patients (between 7 months old and 10 years old) with disseminated medulloblastoma were treated with intensified induction chemotherapy (vincristine, cyclophosphamide, etoposide and methotrexate) followed by a single myeloablative chemotherapy cycle and autologous stem cell infusion. Patients older than 6 years old or with

residual disease after induction chemotherapy received craniospinal irradiation with a boost to the tumor bed. The reported 3-year OS was 60% and the PFS was 49%[140].

In a recent phase I/II study including 81 patients (median age of 8.7 years old) with metastatic medulloblastoma, Jakacki *et al.* evaluated the role of carboplatin as radiosensitizer during craniospinal irradiation. The study showed that carboplatin is well tolerated and may improve survival in patients with high-risk medulloblastoma at presentation[155].

1.3.1.3 Recurrent medulloblastoma

There is considerable ongoing debate about the best therapeutic approach for patients with recurrent or relapsed medulloblastoma. The outcome for patients with recurrent disease following previous craniospinal irradiation and who undergo retreatment with conventional therapy is less than 5%. Therefore, other therapeutic regimens have been extensively investigated to improve the outcome of these patients[156,157].

The first reports of patients with recurrent brain tumors salvaged with high-dose chemotherapy combined with autologous stem cell rescue were almost two decades ago[141-143]. These early series suggested that the best candidates for high-dose chemotherapy were patients with minimal residual disease[141]. One study including 8 patients with recurrent medulloblastoma showed significant improvement in survival after intensive chemotherapy and stem-cell rescue with an OS of 46% at 36 months post-treatment[143]. This study also suggested that patients previously treated with a combination of radiation and chemotherapy had a worse outcome than patients treated with previous chemotherapy only. Later, another study used the same regimen to treat 25 patients with recurrent medulloblastoma previously irradiated. The reported 10-year PFS and OS were both 24%[144].

In a multicenter study including 39 infants with local recurrence or progression of medulloblastoma, 70% of the patients could be salvaged by surgical resection followed by local irradiation and intensive chemotherapy with stem-cell rescue[145]. When infants had a metastatic relapse, 50% could be salvaged with high-dose chemotherapy and stem-cell rescue although the neurocognitive outcome was very poor[158]. Despite the fact that regimens with intensive chemotherapy and stem-cell rescue have greatly increased survival of patients with recurrent medulloblastoma, the rate of toxicity and mortality related to hepatic veno-oclusive disease, systemic infections and multi-organ failure were worrisome. This led investigators to design clinical trials using different therapeutic approaches.

Temozolomide is a well-known DNA damaging agent that effectively crosses the blood-brain barrier. Its efficacy is higher in patients with low levels of the DNA repair enzyme O6-methylguanine-DNA methyltransferase (MGMT). Temozolomide has been included, as a single agent or in combination with other drugs, in several clinical trials for recurrent medulloblastoma. A phase II study from the Children's Oncology Group treated 113 patients with recurrent central nervous system tumors with temozolomide administered as monthly 5-day courses, for up to 12 cycles. Among the 25 medulloblastoma patients treated, there was one complete response and two partial responses[146]. A recent pilot study treated patients with local recurrence of medulloblastoma with reirradiation and concomitant temozolomide, alone or in combination with other drugs, in a metronomic schedule. The results showed that temozolomide can be a radiosensitizer to radiotherapy[159].

The synergistic effect of temozolomide with other chemotherapeutic agents has also been investigated. Ruggiero *et al*. conducted a phase I trial in 14 children with progressive or relapsed medulloblastoma treated with temozolomide and etoposide, both administered orally. The results from this study revealed one complete response after 4 cycles, 2 partial responses after 1 cycle, 7 patients with stable disease and 3 patients with progressive disease[147]. Recently, Aguilera *et al*. reviewed 9 patients with recurrent medulloblastoma treated with bevacizumab, irinotecan, with or without temozolomide. This therapeutic regimen was well tolerated and the reported OS was 13 months. At 6 months, 55% of patients responded to treatment and three showed a complete response[160]. Another very recent phase II multicenter trial was conducted using a combination of temozolomide and irinotecan in pediatric patients with recurrent or refractory medulloblastoma. Although this therapeutic regimen was well tolerated, objective responses were only seen in 33% of patients. However, the combination of both drugs seemed to be more beneficial than previous reports using temozolomide or irinotecan as single agents[153].

Another option for patients with recurrent medulloblastoma is etoposide, a topoisomerase inhibitor. An early study including patients with relapsed medulloblastoma, previously treated with conventional therapy or that failed to respond to salvage therapy, showed benefit of oral etoposide[148]. Recently, a phase II trial of 28 adults with medulloblastoma evaluated the effect of etoposide and cis-platinum in combination with radiotherapy. The authors reported a PFS of 57.6% and an OS of 80%[149]. There are some reports of phase I/II trials in patients with refractory solid tumors, including some patients with medulloblastoma, that showed some efficacy of another topoisomerase inhibitor, irinotecan. In a phase II study including 22 patients with malignant brain tumors, two of three

patients with medulloblastoma treated with irinotecan showed disease stabilization[150]. Another phase II clinical trial with irinotecan (administered for 5 days and repeated every three weeks) involving 171 children with refractory solid tumors, reported a partial response in 4 patients with medulloblastoma[151]. A combination therapy of irinotecan and carboplatin was assessed in a phase I trial involving 28 patients with refractory tumors, including 2 medulloblastoma patients. In these patients, one complete response and one partial response were observed[152].

Despite the large number of chemotherapeutic agents available to treat recurrent medulloblastoma the results from clinical trials show a very low success rate. This may be due to various factors including changes in the eligibility criteria for patient's selection, the number of patients with medulloblastoma enrolled and tumor heterogeneity. It is anticipated that clinical trials taking into consideration the molecular subgroups of medulloblastoma, may lead to more promising results.

1.3.2 Emerging Targeted Therapies in Medulloblastoma

The most recent discoveries in the genomic landscape of medulloblastoma shed some light on possible novel targets for the treatment of this disease. Few clinical trials were undertaken using some of these targeted therapies.

The hedgehog pathway is known to have an important role during development and is aberrantly activated in 30% of medulloblastomas[22]. Hedgehog signaling is mainly regulated through a cascade of inhibitory signals. Binding of the hedgehog ligands (Sonic, Indian or Desert Hedgehog) to the Patched transmembrane receptor (PTCH1) relieves PTCH1 inhibition of the neighbouring Smoothened receptor (SMO). This leads to downstream activation of the cytoplasmic proteins GLI1 and GLI2, through an intermediate SUFU. Activated GLI1 and GLI2 then translocate to the nucleus and induce gene expression of regulators of the hedgehog pathway, including GLI1 and PTCH1. Due to the involvement of the hedgehog pathway in cancer, its pharmacological inhibition became an attractive tool to study antitumor activity and several compounds were developed.

Vismodegib is a potent SMO inhibitor that acts by binding to the extracellular domain of the receptor and induces a marked inhibition of downstream signaling[161]. Vismodegib was effective inducing tumor regression in a patient with metastatic medulloblastoma refractory to multiple therapies[162]. These findings prompted the establishment of phase I and phase II

clinical trials, some of them ongoing. A phase I trial assessed the safety of vismodegib in 68 patients with refractory solid tumors including 33 advanced basal cell carcinomas and one medulloblastoma[163]. One pitfall of vismodegib is the development of acquired resistance. The first identified mechanism of resistance was a missense mutation in the extracellular domain of SMO, which prevents the binding of vismodegib. The mutation occurs at the position 1697, predicted to change codon 473 from Asp to His (D473H)[164]. Another study reported various mechanisms of resistance to SMO inhibition using another Smoothened inhibitor, NVP-LDE225. Despite initial tumor regression, resistance developed shortly afterwards with mutations of SMO, amplifications of GLI2 and up-regulation of PI3K signaling pathway[165]. Therefore, tumors with amplifications in genes that encode key proteins downstream of the SMO receptor may have an inherent resistance to SMO inhibitors.

Other phase I/II trials using vismodegib to treat patients with recurrent or refractory medulloblastoma are in progress (see www.clinicaltrials.gov). A phase I/II trial to assess the efficacy of vismodegib in combination with temozolomide is recruiting patients with refractory medulloblastoma and concomitant activation of the Sonic Hedgehog pathway.

The significant antitumor properties of vismodegib along with the minor side effects that were reported with its administration make this drug attractive for future combination therapies. However, for young children one major concern using SMO inhibitors are the potential permanent defects in bone development induced by these drugs[166]. Appropriate patient selection will be crucial when enrolling patients for treatment with SMO inhibitors.

The Notch pathway has been implicated in the regulation and maintenance of normal neural stem cells. The activation of Notch signaling occurs upon binding of the Delta and Jagged ligands expressed in adjacent cells. This triggers proteolytic cleavage of the Notch receptor by ADAM family protease and gamma secretase with the subsequent release of the Notch intracellular domain. The intracellular domain translocates to the nucleus and activates transcription. Notch signaling dysregulation has been associated with several cancers including brain tumors (medulloblastoma, ependymoma and glioma)[167]. In medulloblastomas, Notch signaling seems to play a key role in the sonic hedgehog subtype[168] and is, therefore, an attractive therapeutic target.

MK-0752, a gamma secretase inhibitor, has been tested in phase I clinical trials. Fouladi et al. assessed the pharmacokinetics and toxicity of MK-0752 in 23 children with refractory or recurrent central nervous system tumors, including 4 medulloblastomas[169]. Another recent phase I trial enrolled 103 adult patients with advanced solid tumors. The

authors reported one complete response and 10 patients with stable disease among patients with malignant gliomas[170].

Finally, aberrant signaling via the EGFR family (also called ERBB receptors) has also been reported in brain tumors. High expression of EGFR has been associated with brainstem glioma and high expression of ERBB2 with medulloblastoma and ependymoma[171,172]. A phase I trial of children with refractory central nervous system tumors showed that lapatinib was well tolerated[173]. Later, a phase II study with lapatinib was conducted in 34 children with recurrent brain tumors (14 medulloblastomas, 10 ependymomas and 10 high-grade gliomas) but no objective responses were observed[174].

Several other molecular and pharmaceutical targets have been implicated in medulloblastoma pathogenesis. These include receptor tyrosine kinases, like cMET, PDGF, ERB and IGF1R, and some downstream effectors such as c-MYC, PI3K/AKT and STAT3. Preclinical studies were undertaken using human cells lines and mouse models of medulloblastoma. As the field moves forward and new drugs are being developed, it is anticipated that many more clinical trials will follow, taking into consideration the molecular biology of medulloblastomas.

1.3.3 Conclusions and Future Perspectives

The treatment of medulloblastoma has undergone tremendous change over the past several years. Advances in surgical techniques, radiation and chemotherapeutic protocols have significantly improved survival and quality of life of patients with medulloblastoma. However, the toxicity induced by therapy and the poor outcome of patients with recurrent or metastatic disease remains a challenge and warrants the development of new therapeutic avenues.

The recent identification of medulloblastoma subgroups has profoundly changed the way we should deal with this disease. The knowledge that the different subgroups have distinct outcomes has important clinical implications and has launched a debate about subgroup-specific therapy. WNT medulloblastoma patients, known to have an exceedingly good outcome, are now considered for de-escalation of therapeutic intensity. On the other hand, Group 3 patients, which have a very poor outcome, clearly need more intensified therapies or novel pharmacological approaches.

An overwhelming amount of data from whole genome and whole exome sequencing has been generated uncovering key pathways and genetic changes that are crucial for tumor

initiation and maintenance. *DDX3X* mutations in WNT tumors, *PVT1-MYC* fusion in Group 3 tumors and *SNCAIP* tandem duplication in Group 4 tumors are some examples of novel genetic events recently described. Preclinical studies with human cell lines and mouse models of medulloblastoma are currently ongoing to validate these and other molecular targets. Thus far, few drugs targeting specific pathways or receptors have completed phase I or phase II clinical trials, namely vismodegib (an inhibitor of SMO in hedgehog signalling), MK-0752 (an inhibitor of gamma secretase in Notch signalling) and lapatinib (an inhibitor of EGFR and ERBB2). However, their efficacy was limited when administered as single agents. Drug-acquired resistance has been a problem both in preclinical and in some human studies highlighting the importance of combination therapies in future clinical trials. Taking into consideration the heterogeneity and complexity of medulloblastoma it is very unlikely that this disease can be cured with single agent therapy.

Next generation clinical trials are making their way into the clinical arena. Meticulous patient selection, stratification based on molecular subgroup affiliation and the combination of conventional and targeted therapies are most likely the key to improve survival and quality of life of children with medulloblastoma.

1.4 Hypothesis and Aims

The objective of our work was to investigate whether we could use the gene expression signatures of medulloblastoma to identify novel subgroup-specific targeted therapies, focusing in subsets of patients with the worst prognosis. The design of our study included two different approaches for drug discovery: 1) targeting a pathway previously identified as relevant in medulloblastoma and 2) using computational tools to identify small molecules with the ability to revert the oncogenic gene signatures of medulloblastoma subgroups.

The HGF/cMET pathway is known to be involved in medulloblastoma pathogenesis. We aimed to determine the subgroup-specific role of cMET in medulloblastoma and its clinical relevance. Furthermore, we aimed to evaluate the *in vitro* and *in vivo* effect of small molecule inhibition in cMET signaling. Given the importance of cMET in the process of dissemination in human cancers and the lack of therapeutic options for patients with metastatic medulloblastoma, we hypothesized that cMET small molecule inhibition would impair tumor invasion and dissemination in mouse models of the disease. Since one of the principle concerns when evaluating new drugs to treat brain tumors is whether they cross the blood-brain barrier, we aimed to design a method, based on mass spectrometry technology, to detect and quantify drugs in the central nervous system.

Group 3 medulloblastomas are characterized by overexpression or amplification of the oncogene *MYC* and have the worst outcome of all medulloblastoma subgroups. Since the development of small molecule inhibitors of MYC has had limited success, an alternative approach is to target basic cellular processes that drive the oncogenesis of Group 3 tumors. The C-MAP is a bioinformatic tool that allows rapid *in silico* assessment of molecules with the ability to modulate biological processes or diseases. Therefore, we decided to query the C-MAP database using the gene expression profile of Group 3 medulloblastomas to identify novel small molecules with predicted efficacy against this aggressive tumor. Furthermore, we aimed to validate our findings by testing the best-ranked compounds against medulloblastoma cell lines and medulloblastoma mouse xenografts representative of Group 3 tumors.

Chapter 2
cMET Inhibition as a Molecular Therapy for Metastatic SHH Medulloblastoma[iv]

2.1 Introduction

Medulloblastoma has a high tendency to disseminate through the cerebrospinal fluid to the brain and the spinal cord leptomeninges. Dissemination is a known factor of poor survival, and occurs in one third of the children at the time of diagnosis and in two thirds by the time of relapse. Affected children are treated with craniospinal radiation and high-dose chemotherapy but the majority of survivors suffer from severe neurocognitive deficits induced by the deleterious effects of treatment on the developing nervous system[132]. The discovery of novel and less toxic therapies has been hampered by the poor understanding of the mechanisms of dissemination, and by the failure to account for the genetic divergence between metastatic lesions and their matched primary tumor. Recent studies have shed light into the candidate genes that drive leptomeningeal dissemination in medulloblastoma[175,176] but therapies that target both the primary and the metastatic compartment have not been identified.

The HGF/cMET pathway is essential for cell proliferation and migration during embryogenesis[66] and, in the central nervous system, it plays a critical role in cerebellar development[71]. Aberrant cMET signaling is known to be involved in tumor growth and metastatic behavior of several human cancers[38,42]. The transmembrane receptor cMET is activated through phosphorylation of tyrosine residues upon binding of its ligand HGF. These tyrosines recruit a variety of cytoplasmic effector proteins, including GRB2, GAB1, SRC and PLC. Phosphorylation of GAB1 upon binding to cMET at the plasma membrane can trigger multiple downstream effector cascades including MAPK and PI3K/AKT that function in

[iv] Bioinformatic analysis of medulloblastoma samples was performed by Adrian Dubuc and Marc Remke. Assistance with assays to assess cMET and PDGFRß signaling was obtained from Brian Golbourn, Roberto Diaz and Sameer Agnihotri. Amanda Luck helped with the genotyping of *Ptch*$^{+/-}$*/SB11/T2Onc* mice. Assistance with active caspase assays was obtained from Samantha Olsen. HPLC-MS/MS analysis of brain and plasma samples was performed by Denis Raynaud and Michael Leadly. Leoneardo Ermini performed the MALDI-TOF imaging. Assistance for immunostaining of human tissue microarrays was obtained from Andrey Korshunov and Nesrin Sabha.The remainder of experiments described in this chapter were performed by the candidate.

various cellular processes including cell proliferation, cell survival, migration and invasion[177]. In medulloblastoma, cMET activation has been associated with tumor growth and anaplastic histology[77]. cMET signaling is deregulated in medulloblastoma through multiple, independent molecular mechanisms including epigenetic silencing of an upstream inhibitor SPINT2[34,178]. The HGF/cMET axis cooperates with other important signaling pathways in medulloblastoma, namely MYC[80], SHH[84] and focal adhesion kinase (FAK)[179], to promote tumor formation and growth. Previous studies have shown that cMET inhibition can effectively decrease medulloblastoma cell migration and invasion[89].

Foretinib is an orally available multikinase inhibitor that targets cMET with high affinity (IC50 = 0.4 nmol/L)[111]. Foretinib has demonstrated antitumor activity in preclinical models of different tumor types such as ovarian cancer[180], pancreatic islet cancer[181] and hepatocellular carcinoma[182]. Partial response in a subset of patients was observed in a phase I clinical trial investigating the pharmacokinetics and safety of foretinib in patients with advanced solid tumors[183]. These findings led to a phase II clinical trial that demonstrated an association between the presence of MET germline mutations and the response to foretinib[184]. Other clinical trials are currently ongoing to determine the efficacy of foretinib in various solid, non-central nervous system tumors. To date, the ability of foretinib to penetrate the brain is unknown.

Foretinib also targets other tyrosine kinases with lower affinity, including the platelet derived growth factor receptor beta (PDGFRß) with an IC50 of 9.6 nmol/L. Interestingly, PDGFRß is known to be overexpressed in metastatic medulloblastoma[185,186] and targeting the receptor reduces proliferation and migration of medulloblastoma cell lines[187]. Activation of PDGFRß occurs through a similar mechanism to cMET receptor activation in which ligand binding (PDGF-BB) induces receptor autophosphorylation and activates downstream signaling via MAPK and AKT[188].

Therefore, we sought to establish the subgroup-specific role of cMET and PDGFRß in medulloblastoma, and to test the efficacy of foretinib to cross the blood-brain barrier and to target those pathways, both in the primary and in the metastatic compartments.

2.2 Methods and Materials

2.2.1 Tumor Material and Patient Characteristics

All tissues and clinicopathological information were serially collected in accordance with Institutional Review Boards from contributing institutions. Nucleic acid extractions were carried out as previously described[16].

2.2.2 Expression Profiling and Molecular Subgrouping

Expression of candidate genes was assessed using the R2 software (http://r2.amc.nl) in independent gene expression cohorts[15,16,20,23,33,189-192]. Expression of reported intermediates of MET signaling were visualized using heatmaps[38]. Associations between gene expression and subgroup affiliation were evaluated using one-way ANOVA. P-values < 0.05 were considered to be statistically significant.

2.2.3 Analysis of Somatic Copy Number Alterations

Somatic copy number alterations were assessed on the Affymetrix Single Nucleotide Polymorphism 6.0 array platform in 1,239 cases. Raw copy number estimates were obtained in dChip, followed by CBS segmentation in R as previously described[23].

2.2.4 Cell Lines and Animal Models

Human medulloblastoma cell lines (Daoy, ONS76 and D425) were kindly provided by Dr. Annie Huang, Hospital for Sick Children, Toronto, Canada. All cell lines were authenticated and tested by PCR. Daoy-GFP/Luciferase cells were generated as described previously[193]. Athymic nude mice were obtained from the Charles River Laboratory. *Ptch*$^{+/-}$*/SB11/T2Onc* mice [175] were generously provided by Dr. Michael Taylor, Hospital for Sick Children, Toronto, Canada.

2.2.5 Cell Culture Assays for cMET and PDGFRß Signaling

Foretinib was purchased from Selleck Chemicals, dissolved in DMSO (Sigma) and stored at -20ºC. To study the effect of foretinib in the cMET and PDGFRß pathways, medulloblastoma cells were serum starved for 24 hours in media with 0.1% (Daoy and ONS76) and 2% FBS (D425), pre-treated with increasing concentrations of foretinib or 1% v/v DMSO for 2 hours and stimulated with human recombinant HGF (20 ng/mL; Sigma-Aldrich) for 20 minutes or human PDGF-BB (20 ng/mL; Cell Signaling) for 10 minutes.

2.2.6 Migration and Invasion Assays

The protocols for migration and invasion assays were as described previously [194].

For the radial migration assays, 2,000 Daoy cells and 3,000 ONS76 cells per well were seeded through a cell sedimentation manifold (CSM Inc.) onto a 10 well Teflon-coated slides (CSM Inc.) previously coated with 0.1% BSA. After 24 hours of incubation at 37ºC, regular media was replaced by starved media (0.1% FBS) containing HGF (50 ng/mL) or PDGF-BB (50 ng/mL) in the presence or absence of foretinib. Cells were allowed to migrate for 24 hours and the radius of the migrating cells was measured and compared to the initial radius using a Leica Fluorescent Stereoscope (2.5X magnification).

For the invasion assays, Matrigel Invasion Chambers (8 μm pore size; BD Biosciences) were hydrated for 2 hours with DMEM. Daoy and ONS76 cells (50,000/chamber) were plated in the top chamber with starved media (0.1% FBS) containing dilutions of foretinib. The bottom chamber was loaded with serum free media (0.1% FBS) or serum free media supplemented with HGF (50 ng/mL) or PDGF-BB (50 ng/mL) and foretinib. After incubation at 37ºC for 16 hours, non-invading cells were removed and cells invading through the porous membrane were stained with DAPI and photographed with an Axiovert 200M (Carl Zeiss) microscope. The number of cells per 6 random fields was determined (10X magnification) using Volocity software (Perkin Elmer).

2.2.7 Immunoblotting

Cell lysates were obtained using RIPA buffer (Sigma) containing protease inhibitors (F. Hoffman-La Roche AG), 0.2 M sodium fluoride, 0.2 M sodium pyrophosphate and 0.2 M sodium orthovanadate. Protein concentration was determined using the Pierce BCA Protein

Assay Kit (Thermo Scientific). Proteins were electrophoresed on 7%, 7.5% or 10% SDS-PAGE gels, depending on the protein that was being detected, and transferred using a semidry transfer apparatus (Bio-Rad). The following antibodies were used: cMET (1:1,000; L41G3, Cell Signaling), phospho-cMET (1:1,000; Tyr1234/1235, Cell Signaling), PDGFRß (1:500; 28E1, Cell Signaling), phospho-PDGFRß (1:500; Tyr751, Cell Signaling), AKT (1:1,000; Cell Signaling), phospho-AKT (1:2,000; Ser473, Cell Signaling), p44/42 MAPK (1:1,000; Cell Signaling), phospho-p44/42 MAPK (1:2,000; Thr202/Tyr204, Cell Signaling), PARP (1:1,000; Cell Signaling), ß-actin (1:10,000; Cell Signaling), anti-rabbit IgG conjugated to horseradish peroxidase (1:5,000; Cell Signaling) and anti-mouse IgG conjugated to horseradish peroxidase (1:5,000; Amersham Biosciences). Western blot analysis and quantification was performed using the Fluorchem Q Imaging System (ProteinSimple).

2.2.8 Cell Proliferation Assays

Daoy, ONS76 and D425 cells were seeded in 96-well microplates at 2,500, 2,500 and 10,000 cells per well, respectively. These cells were treated with different concentrations of foretinib or DMSO and cell viability was determined for the indicated time points by MTS (3-(4,5-dimethylthiazol-2-yl)-5-(3-carboxymethoxyphenyl)-2-(4-sulfophenyl)-2H-tetrazolium) absorbance at 490 nm (CellTiter 96 Aqueous One Solution Reagent; Promega). Three independent experiments were performed with 16 repeats per treatment condition and per time point.

2.2.9 Active Caspase Assays

Daoy cells were seeded at 2,500 cells in 96-well microplates in the presence or absence of different concentrations of foretinib. The activity of caspases 3 and 7 was measured using the Apo-One® Homogeneous Caspase 3/7 assay (Promega). For the indicated time points, 100 µl of Apo-One solution was added to each well and the levels of fluorescence were measured after 12 hours of incubation.

2.2.10 Foretinib Pharmacokinetic Studies

Detection and quantification of foretinib was performed using a high-performance liquid chromatography tandem mass spectrometry (LC/MS/MS) method (Agilent 1290 HPLC

Agilent Technologies, Santa Clara, California, USA / QTRAP 5500 AB SCIEX, Framingham, Massachusetts, USA), with cabozantinib (Selleck Chemicals) as internal standard for brain homogenates and plasma.

Images of foretinib distribution in various mouse organs were acquired using a matrix-assisted laser desorption/ionization (MALDI) time-of-flight tandem mass spectrometer (AB SCIEX TOF/TOF 5800 System, AB SCIEX, Framingham, MA, U.S.A.).

Female 5-6 week old athymic nude mice (Charles River) were dosed with 30, 60 and 100 mg/kg of foretinib, by oral gavage. Mouse brains and matched blood samples were collected from animals (n = 3 per time point) at 5 hours, 10 hours and 5 days (after daily drug administration). Blood samples were collected by cardiac puncture into tubes containing EDTA and plasma was harvested by centrifugation at 800 x g for 15 minutes and stored at -80ºC. Animals were perfused with saline containing heparin (5U/mL) and brains were harvested, frozen in liquid nitrogen and stored at -80ºC. High-performance liquid chromatography tandem mass spectrometry (LC/MS/MS) was used to detect and quantify foretinib (Agilent 1290 HPLC Agilent Technologies, Santa Clara, California, USA / QTRAP 5500 AB SCIEX, Framingham, Massachusetts, USA). Cabozantinib (Selleck Chemicals) was used as internal standard for brain homogenates and plasma. At least 5 standards were run for each curve and the lower limit of quantitation (LLOQ) was 0.1 ng/mL. Foretinib concentration in whole brain was normalized by brain weight.

For matrix-assisted laser desorption/ionization with time-of-flight mass spectrometer (MALDI-TOF) imaging, brain, liver and kidney from foretinib treated and untreated mice were frozen rapidly in liquid nitrogen and stored at -80°C. Samples were mounted with optimal cutting temperature (OCT) compound (Sakura Finetek, Torrance, CA) for sectioning. Tissues were cut in 12 μm sections at -15°C and mounted onto indium tin oxide (ITO)-coated glass slides. A thin matrix layer of 2,5-dihydroxybenzoic acid (DHB) was applied to the sections using an automated MALDI plate matrix deposition system (TM-Sprayer™ , Leap Technologies, Carrboro, NC). A total of 5 mL of DHB solution (15 mg/mL in 50% acetonitrile/0.1% trifluoroacetic acid) was sprayed per slide during 4 passes at 140°C with a velocity of 400 mm/min and a line spacing of 3 mm. Images were acquired using a MALDI time-of-flight tandem mass spectrometer (AB SCIEX TOF/TOF 5800 System, AB SCIEX, Framingham, MA, U.S.A.). MALDI mass spectra were obtained using an Nd:YAG laser (349 nm) at 3 ns pulse width and 400 Hz firing rate. All data were acquired in the positive-ion reflector mode. An aliquot of pure Foretinib (Selleck Chemicals) was deposited on the ITO-coated slides as external standard and to compensate for mass shift. A total of 200 laser shots

per pixel were acquired (1 s/pixel) at a spacing of 100 mm between pixels. The mass spectrometric data was processed and images were visualized using TissueView software (AB SCIEX). The imaging experiments were repeated with tissues obtained from 3 animals treated and untreated with foretinib.

2.2.11 Medulloblastoma Xenografts and Transgenic Mouse Models

All mouse studies were approved and performed in accordance to the policies and regulations of the Institutional Animal Care and Use Committee of the University of Toronto and the Hospital for Sick Children, in Toronto.

Mouse subcutaneous xenografts (Daoy and ONS76) were established in athymic nude mice (Charles River Laboratories). Foretinib was given orally, every other day, for 9 days at 60 and 100 mg/kg. Intracranial xenografts of disseminated medulloblastoma were established by injecting Daoy medulloblastoma tumor cells into the fourth ventricle of athymic nude mice. Tumor growth and the presence of metastases were evaluated by weekly bioluminescence imaging using the IVIS Spectrum Optical In-vivo Imaging System (Caliper Life Sciences). Foretinib was administered daily by oral gavage, 6 days a week, for 2 weeks.

Osmotic pumps (Alzet, model 2004) were implanted in Ptch+/- mice with Sleeping Beauty (SB) transposition ($Ptch^{+/-}$/SB11/T2Onc) at post-natal day 30 to 35. Pumps loaded with foretinib (6 mg/kg) infused the drug into the cerebrospinal fluid (right lateral ventricle) for 28 days at a rate of 0.25 μl/hour.

Female 5-6 week old athymic nude mice (Charles River Laboratories) were used for flank and intracranial xenografts. Daoy (2×10^6) and ONS-76 (2.5×10^6) were injected in the right flank of animals as a 1:1 suspension in Matrigel (BD Biosciences). At day 16 (Daoy) and day 13 (ONS76) after cell inoculation animals were randomized to a vehicle or drug treatment group. Foretinib was administered by oral gavage at 60 and 100 mg/kg, every other day for 9 days. Tumor volume was assessed using a digital caliper and the formula: tumor volume = length (mm) x width2 (mm^2)/2. Tumors were excised at day 25 (Daoy) and day 21 (ONS76) post-injection.

For the intracranial xenografts of disseminated medulloblastoma, 5×10^5 Daoy GFP/Luciferase cells were injected into the fourth ventricle of nude mice using a stereotactic frame. Three days after cell inoculation bioluminescence imaging was conducted using the IVIS Spectrum Optical In-vivo Imaging System (Caliper Life Sciences). Animals that had a

detectable signal were randomized to a foretinib (n = 11) or a DMSO (n = 11) treatment. Foretinib at 60 mg/kg was given orally once daily, 6 days a week, for 2 weeks. Tumor growth and dissemination were assessed by weekly bioluminescence imaging (BLI). Animals were euthanized upon signs of sickness or loss of weight greater than 20%. Brains and spinal cords of all animals were harvested and fixed in 10% formalin. Three serial sections of the brain and multiple sections of the cervical, thoracic and lumbar spinal cord (minimum of 30 sections per spinal cord region) were analyzed.

We used $Ptch^{+/-}$ mice with Sleeping Beauty (SB) transposition ($Ptch^{+/-}$/SB11/T2Onc) as a spontaneous mouse model of metastatic medulloblastoma. Osmotic pumps (Alzet, model 2004) were implanted in animals at post-natal day 30 to 35 and brain infusion cannulas were placed in the right lateral ventricle. Pumps were previously loaded with 6 mg/kg of foretinib and infused the drug for 28 days at a rate of 0.25 μl/hour. Mouse brains and spinal cords were harvested and sectioned as described above.

2.2.12 Immunohistochemistry

The protocol for immunohistochemistry was performed as previously described[195]. The following antibodies were used: Ki-67 (1:1,000; Novus), cleaved caspase 3 (1:800; Cell Signaling), phospho-cMET (1:100; Tyr1234/1235, Cell Signaling) and phospho-PDGFRß (1:200; Tyr751, Abcam). For immunohistochemical quantification, four 20X magnification fields per tumor were used and a total number of 3 mice per group were assessed.

2.2.13 Statistical Analysis

Survival curves according to p-cMET status were generated using the Kaplan-Meier estimate and a log-rank test. The comparison between binary and categorical patient characteristics was performed using the two-sided Fisher's exact test. To analyze contiguous variables, the Mann-Whitney U test was used.

Results from experiments were expressed as mean ± SEM. For multiple group comparisons, analysis of variance (ANOVA) was conducted followed by a post-Tukey test (to identify differences among sub-groups) or a post-Dunnetts test (to compare groups to one control group). Direct comparisons using an unpaired two-tailed Student's t-test were conducted where appropriate. Statistical analysis was performed using GraphPad Prism 5 Software. We considered a P-value inferior to 0.05 as significant.

2.3 Results

2.3.1 cMET and PDGFRß are Highly Expressed in SHH Medulloblastomas

We evaluated the expression of *cMET* and *PDGFRβ* in a discovery cohort of primary medulloblastomas from Boston (n = 199)[191]. *cMET* expression was highly upregulated in most SHH medulloblastomas and in a subset of Group 3 tumors (**Figure 2.1A**). PDGFRß was expressed across all medulloblastoma subgroups, with higher levels of expression in SHH tumors (**Figure 2.1B**). We confirmed our results using a multicentre validation cohort of 439 cases profiled on the Affymetrix 133plus 2.0 arrays obtained from the German Cancer Research Centre, Heidelberg (validation cohort 1)[20,189,190,192](**Figures 2.1C and 2.1D**).

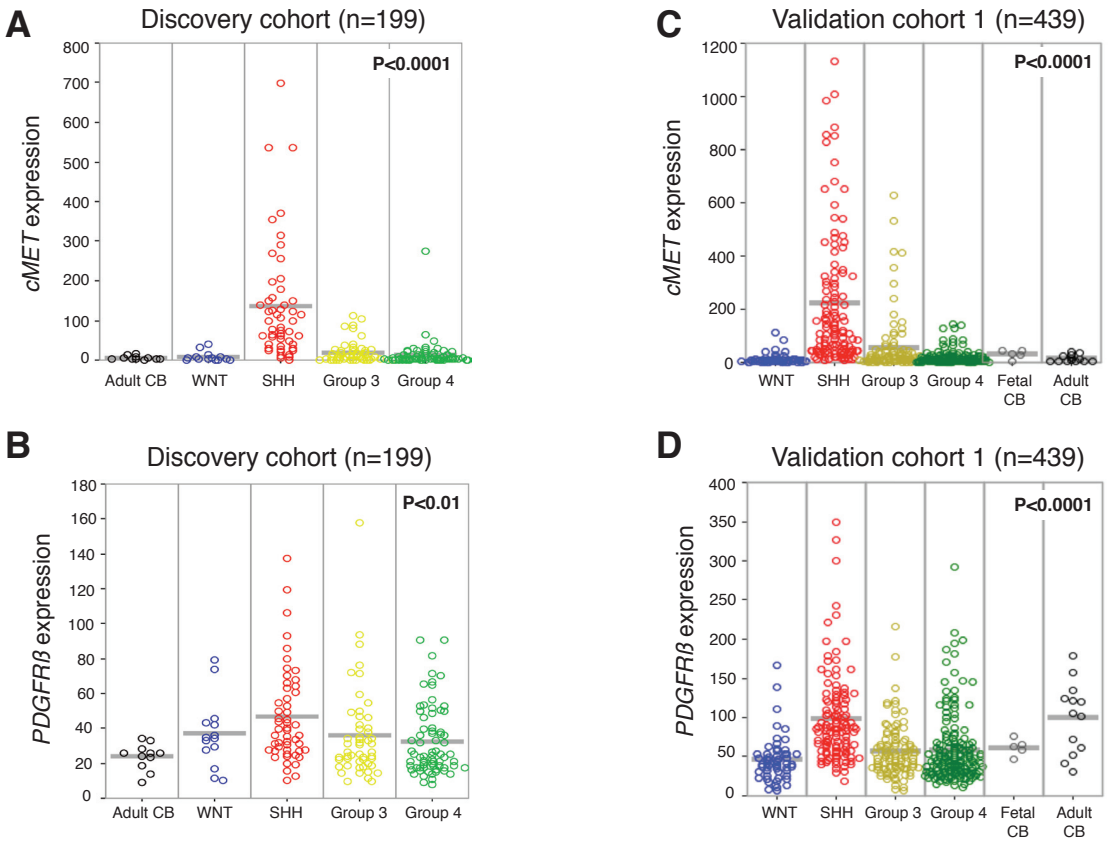

Figure 2. 1: *cMET* and *PDGFRβ* expression accross medulloblastoma subgroups.
Expression of (**A**) *cMET* (P < 0.0001) and (**B**) *PDGFRβ* (P < 0.01) mRNA in a discovery cohort of primary medulloblastomas (Boston; n = 199). *cMET* (**C**) (P < 0.0001) and *PDGFRβ* (**D**) (P < 0.0001) expression analysis in a validation cohort with 439 cases (validation cohort 1: multicentre cohort obtained from Heidelberg).

To identify molecular markers of cMET pathway activation in SHH medulloblastomas, we interrogated three independent datasets (discovery cohort from Boston; validation cohort 1 from the German Cancer Research Centre, Heidelberg; and validation cohort 2: multicentre cohort from the Medulloblastoma Advanced Genomics International Consortium - MAGIC) using a group of genes known to activate cMET signaling[38,177]. In addition to cMET, GAB1 expression was highly and specifically up-regulated in SHH-driven medulloblastomas, across the three non-overlapping cohorts, when compared to normal cerebellum and to non-SHH medulloblastomas (**Figures 2.2A–F**).

To investigate possible mechanisms leading to cMET and PDGFRß overexpression, we examined the subgroup-specific CNAs encompassing the *MET* loci (7q31.2) and the *PDGFRβ* loci (5q31), in a large cohort of 1,239 medulloblastomas[23]. There were no focal gains or amplifications of *cMET* (**Figure 2.3A**) and very infrequent copy number gains affecting the *PDGFRβ* loci (**Figure 2.3B**).

2.3.2 Identification of Biological Pathways and Processes Associated with High cMET and Low cMET SHH Medulloblastomas

To identify signaling pathways and biological processes discriminating high cMET and low cMET SHH medulloblastomas we performed Gene Set Enrichment Analysis between tumors with the highest (n = 13) and the lowest (n = 13) cMET expression across a series of 51 primary SHH medulloblastomas[23]. Gene sets were compiled from Gene Ontology (GO), Kyoto Encyclopedia of Genes and Genomes (KEGG), the National Cancer Institute (NCI), Protein Families (PFAM) and Biocarta pathway databases. To visualize significant gene sets (FDR < 0.25; P < 0.01) as interaction networks we used Cytoscape and Enrichment Map (**Figure 2.4**). High cMET SHH medulloblastomas were characterized by gene sets involved in organ development and morphogenesis, cell migration (cell motility and extracellular matrix components), cell cycle and DNA repair, T-cell differentiation, transcription (transcription factor activity, RNA processing, nuclear and RNA transport) and mitochondrial function. Low cMET SHH medulloblastomas were defined by numerous networks including neural development (neurogenesis, cell morphogenesis and polarity), neurotransmission (neurotransmitter release and activity, ion transport, calcium signaling, chemical homeostasis, cytoplasmic vesicle formation), amino acid and nucleotide metabolism, ribonucleotide biosynthesis, smooth muscle contraction and Ras-GTPase activity.

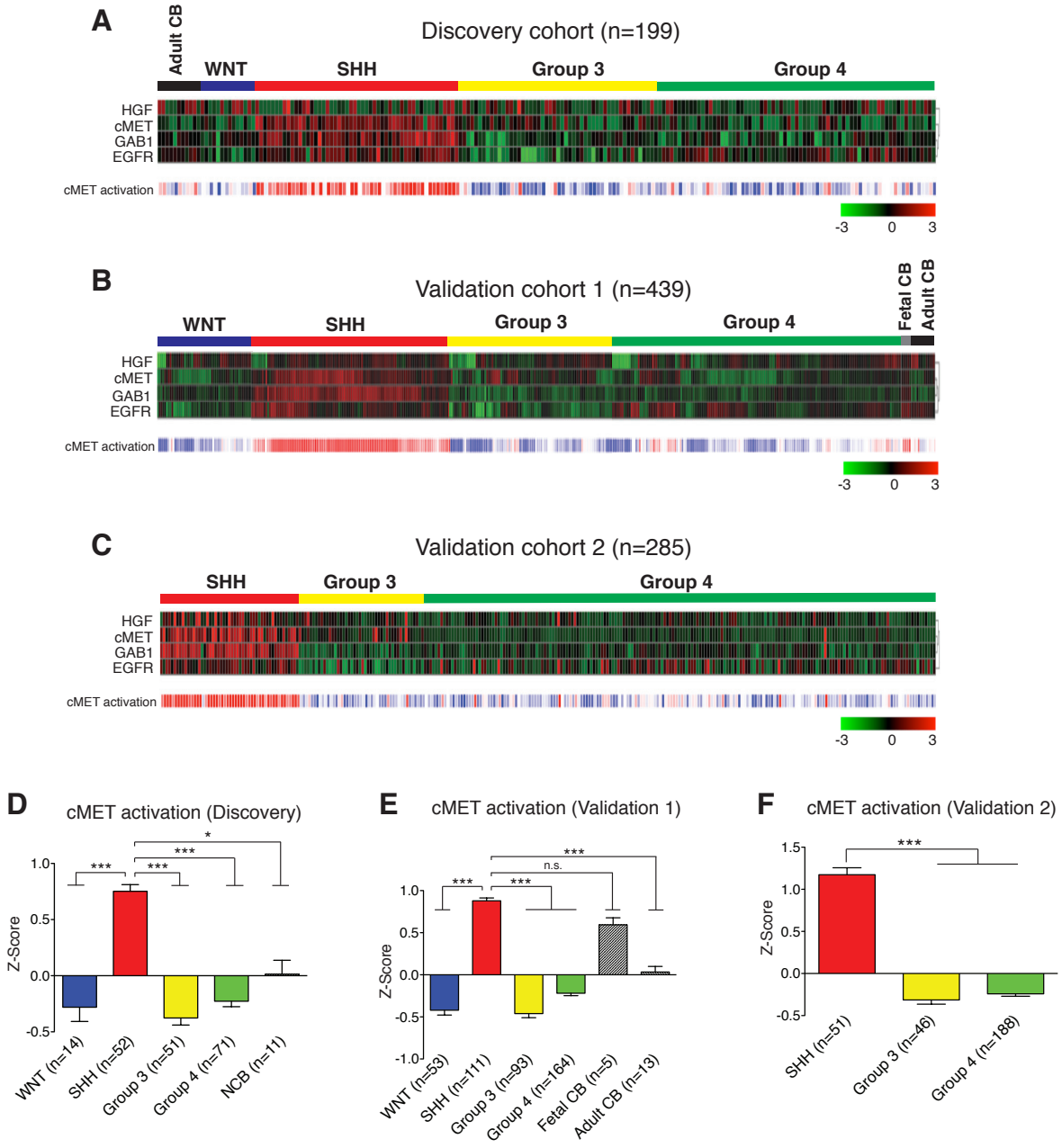

Figure 2.2: *cMET* as a signature gene in SHH medulloblastoma.

(**A – C**), heatmaps illustrating aberrant overexpression of cMET activators in SHH medulloblastomas, in three non-overlapping cohorts of patients, (**A**) discovery cohort (Boston; n=199), (**B**) validation cohort 1 (multicentre cohort obtained from Heidelberg; n=439) and (**C**) validation cohort 2 (Medulloblastoma Advanced Genomics International Consortium – MAGIC; n=285). (**D – F**), Z-scores demonstrating cMET activation in SHH tumors when compared to other medulloblastoma subgroups and normal cerebellum (CB), in all datasets (*P < 0.05; ***P < 0.001).

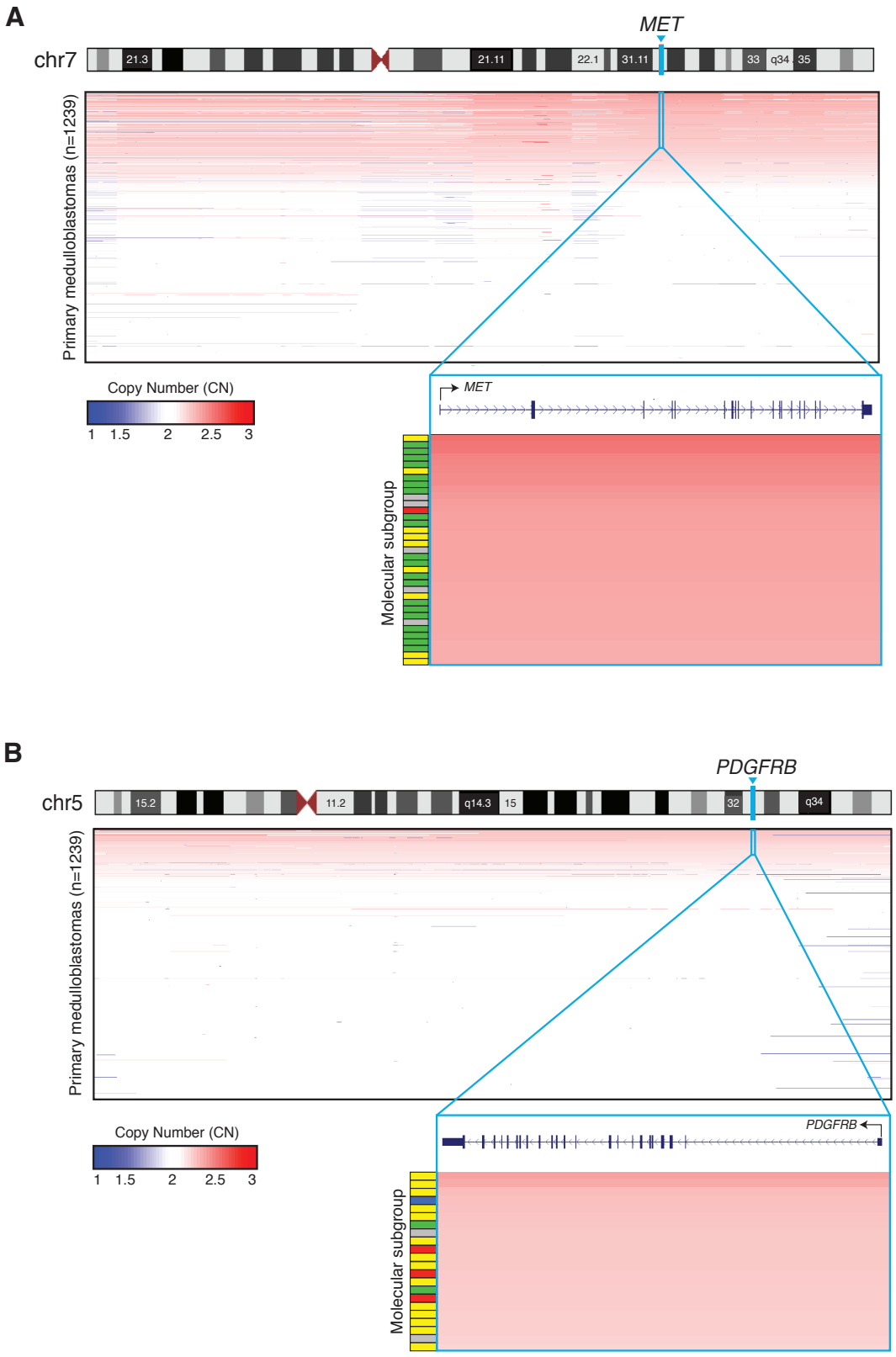

Figure 2.3: **Subgroup-specific copy number aberrations in primary medulloblastomas.** Copy number aberrations in (**A**) the *MET* loci (7q31.2) and in (**B**) the *PDGFRß* loci (5q31). Molecular subgroups: WNT (blue), SHH (red), Group 3 (yellow) and Group 4 (green).

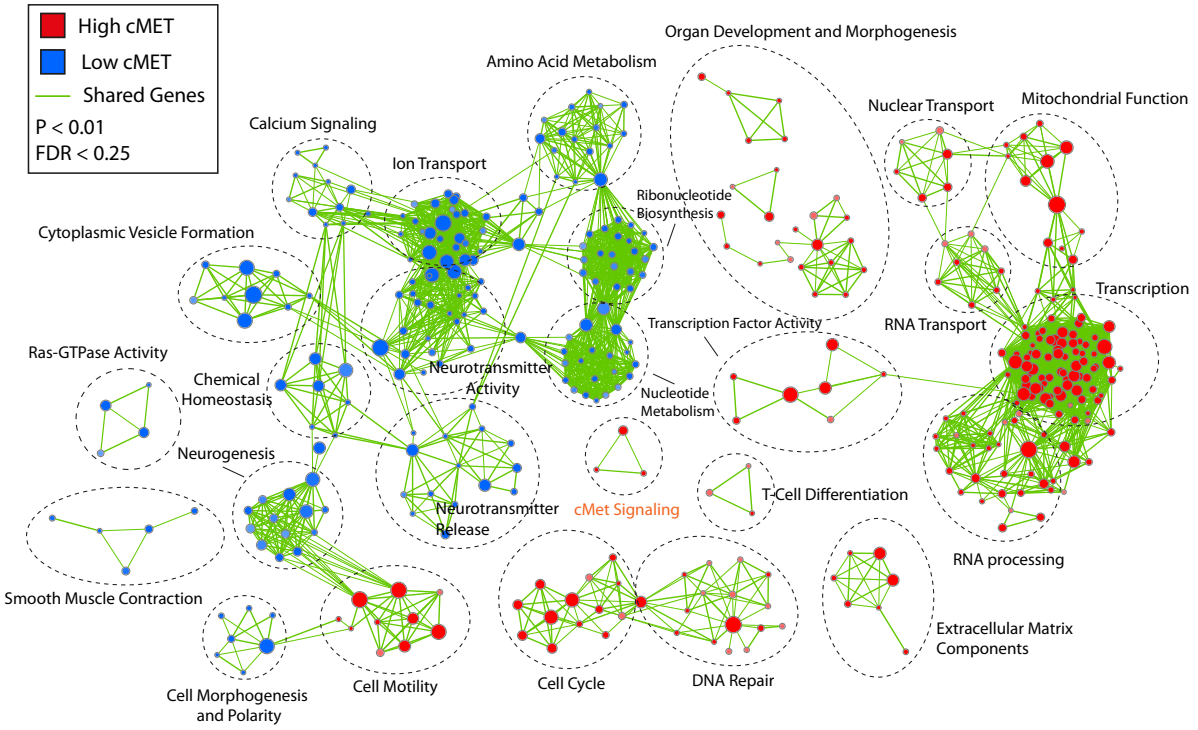

Figure 2.4: Biological pathways and processes associated with high cMET and low cMET SHH medulloblastomas.

Gene Set Enrichment Analysis (GSEA) comparing high cMET (red) against low cMET (blue) SHH medulloblastomas and identifying distinct pathways and biological processes between both subgroups (FDR < 0.25; P < 0.01). For visualization of the GSEA results, Cytoscape and Enrichment Map were used. The enriched gene sets were represented as nodes, grouped by their similarity, and mapped as a network. The total number of genes within each gene set determines the size of the node.

2.3.3 High p-cMET Levels Correlate with Recurrence and Poorer Survival in SHH Medulloblastomas

To evaluate the clinical significance of cMET, we stained medulloblastoma tissue microarrays (TMA) comprised of an independent cohort of 385 patients, for the activated cMET receptor or phosphorylated cMET (p-cMET). Eighty percent (104/128) of SHH tumors and approximately 25% (16/62) of Group 3 tumors showed high p-cMET staining (**Figure 2.5A**). Interestingly, there was a significant correlation (P = 0.041) between high p-cMET and

an increased 5-year rate of recurrence across all subgroups of pediatric medulloblastomas (**Figure 2.5B**). These trends were most pronounced (P = 0.011) across pediatric SHH tumors (**Figure 2.5C**).

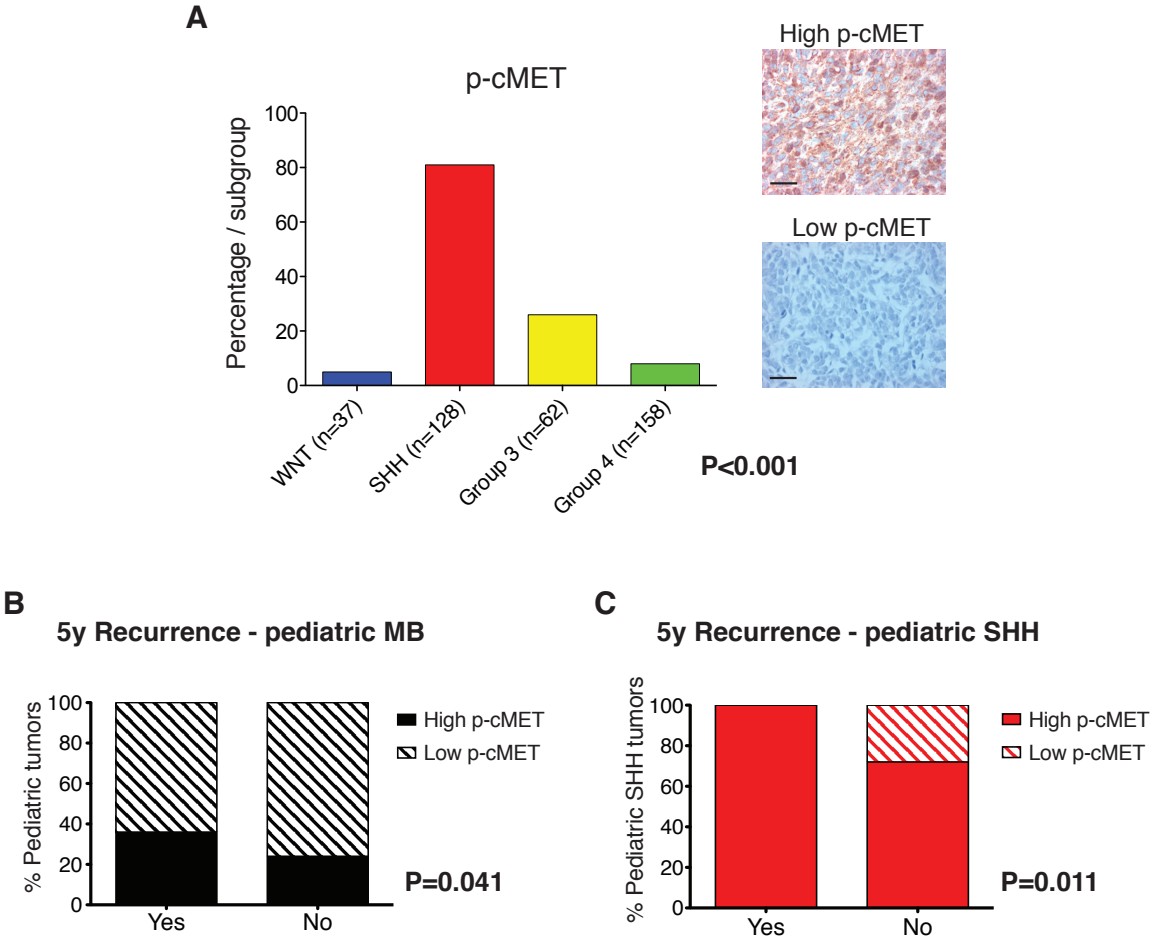

Figure 2.5: cMET pathway activation as a hallmark of SHH medulloblastomas.
(**A**) Immunopositivity for activated cMET (phosphorylated cMET or p-cMET) is a hallmark feature of SHH medulloblastomas identified by immunohistochemistry of medulloblastoma tissue microarrays in a cohort of 385 patients. Representative photographs of tumors with high p-cMET and low p-cMET staining are shown. Scale bar: 100 μm. (**C and D)** In pediatric medulloblastomas, high p-cMET correlates with an increased 5-year recurrence rate (**B**) across all subgroups (P = 0.041) and particularly, in (**C**) the SHH subgroup (P = 0.011).

High p-cMET across medulloblastoma subgroups was associated with older age at diagnosis (**Figures 2.6A and 2.6B**) and desmoplastic histology (**Figures 2.6C and 2.6D**), most likely due to a subgroup-specific enrichment with SHH patients. There was no

association of p-cMET expression and the presence of metastases or *TP53* mutational status in SHH tumors (**Figures 2.6E and 2.6F**).

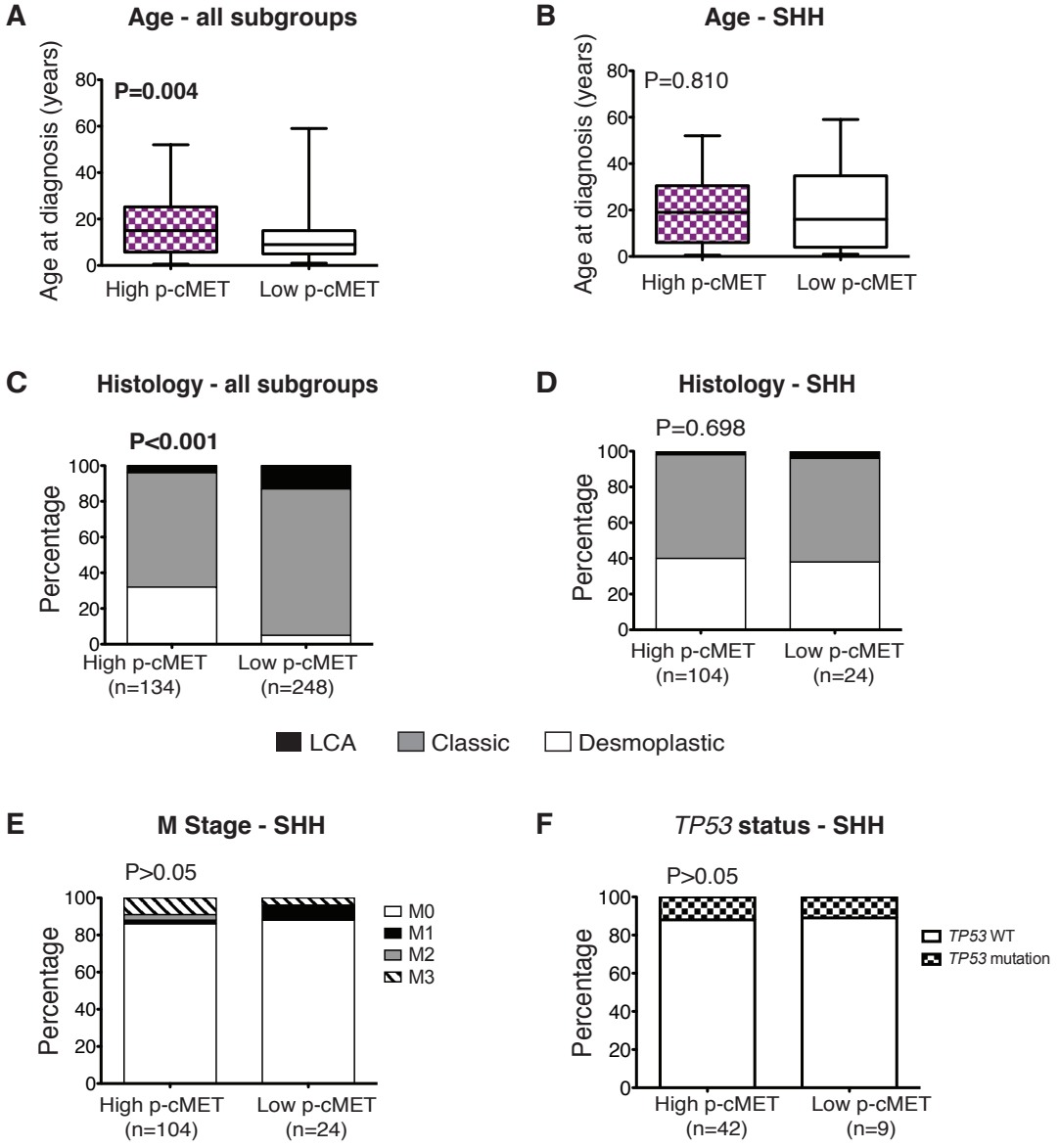

Figure 2.6: Clinicopathological correlations of SHH medulloblastomas according to p-cMET status.

(**A and B**) Box plots demonstrating the association of p-cMET expression and age (**A**) across medulloblastoma subgroups and (**B**) within the SHH subgroup. Statistical significance was determined by a Mann-Whitney *U* test. (**C and D**) Distribution of histological variants across (**C**) all medulloblastoma subgroups and (**D**) SHH subgroup. P-values were determined by Fisher's exact test. (**E and F**) Association of p-cMET expression in SHH medulloblastomas with (**E**) metastatic status and (**F**) *TP53* mutational status. Statistical significance was calculated by Fisher's exact test.

A striking association between p-cMET expression and outcome was noted in SHH medulloblastomas. Specifically, high p-cMET expression in SHH tumors was associated with a significantly (P = 0.007) shorter progression-free survival (**Figure 2.7A**), particularly in the pediatric cohort (P = 0.002) (**Figure 2.7B**). A trend toward a worse overall survival was also observed in these patients (**Figures 2.7C and 2.7D**).

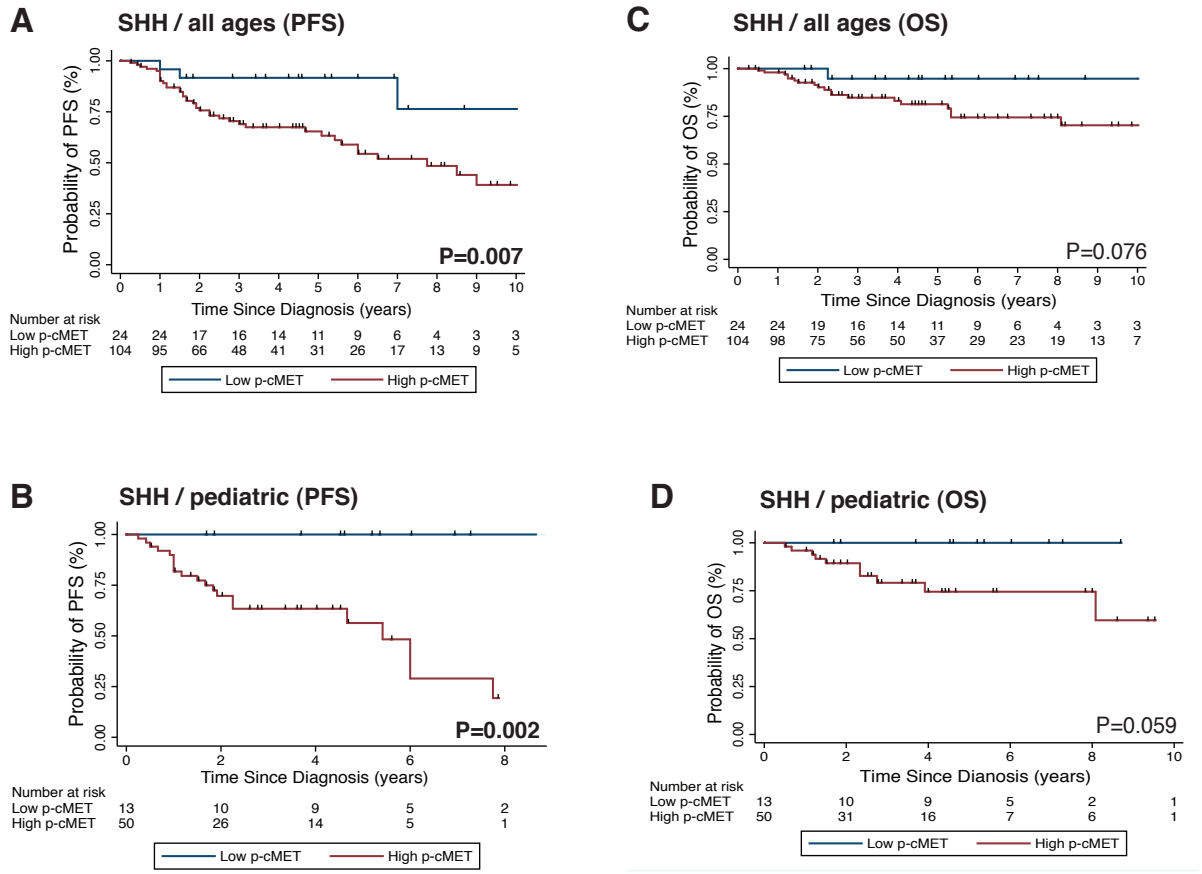

Figure 2.7: cMET pathway activation identifies subgroups of SHH medulloblastoma with distinct clinical outcomes.

(**A – D**) Kaplan-Meier survival curves demonstrate that SHH medulloblastomas with high p-cMET have a poorer progression-free survival, particularly within the pediatric cohort. Statistical significance of recurrence was determined by a Fisher's exact test and survival by a log-rank test. PFS, progression-free survival; OS, overall survival.

Interestingly, considering the metastatic status within SHH medulloblastomas, the prognostic impact of high p-cMET expression was still observed. High p-cMET correlated (P = 0.022) with a poor outcome in non-metastatic SHH patients (**Figures 2.8A and 2.8B**). A trend toward a worse survival was observed in patients with high p-cMET and leptomeningeal dissemination at diagnosis (**Figures 2.8C and 2.8D**).

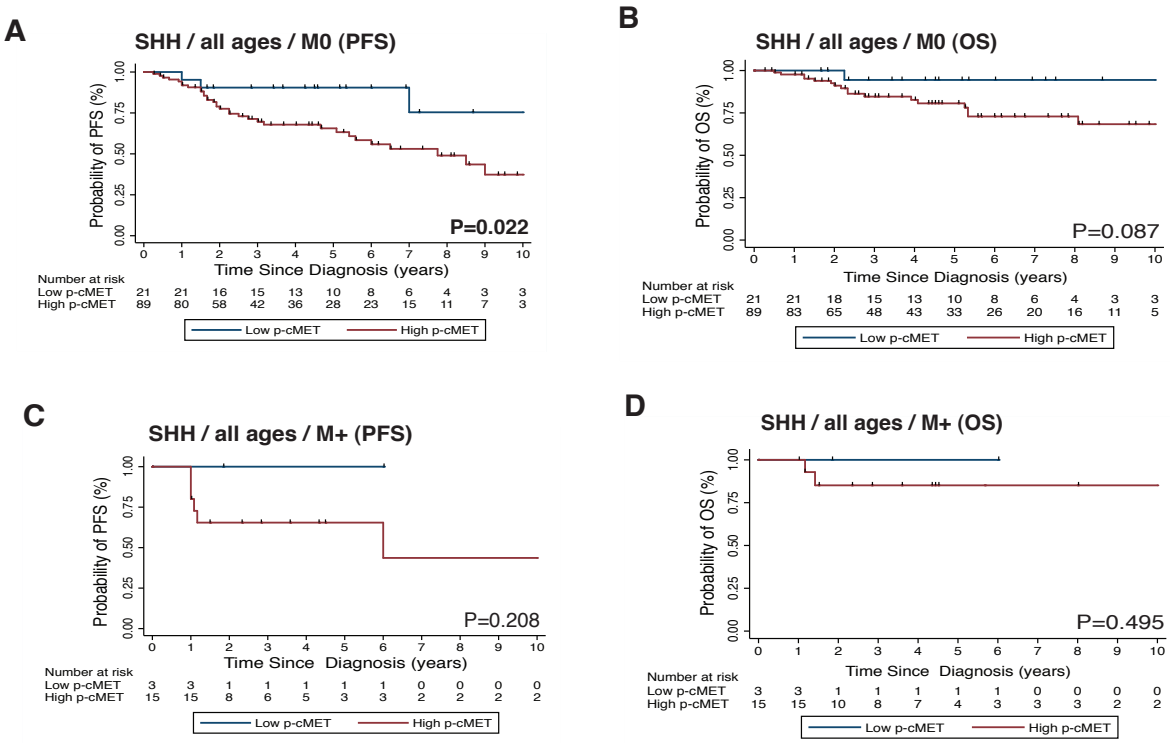

Figure 2.8: Prognostic impact of leptomeningeal dissemination according to p-cMET status in SHH medulloblastomas.

Kaplan-Meier survival curves displaying progression-free survival and overall survival according to p-cMET status in (**A and B**) non-metastatic SHH medulloblastomas (M0) and (**C and D**) metastatic SHH medulloblastomas (M+) across all ages. Statistical significance of recurrence was determined by a Fisher's exact test and survival by a log-rank test. PFS, progression-free survival; OS, overall survival.

Survival differences could not be determined in adult SHH medulloblastoma patients according to p-cMET status (**Figures 2.9A and 2.9B**). In Group 3 medulloblastomas, expression of p-cMET had no prognostic relevance and did not correlate with metastatic status.

Thus, we conclude that activated cMET defines distinct prognostic patient cohorts with higher recurrence rate and poorer prognosis in SHH subgroup of medulloblastomas.

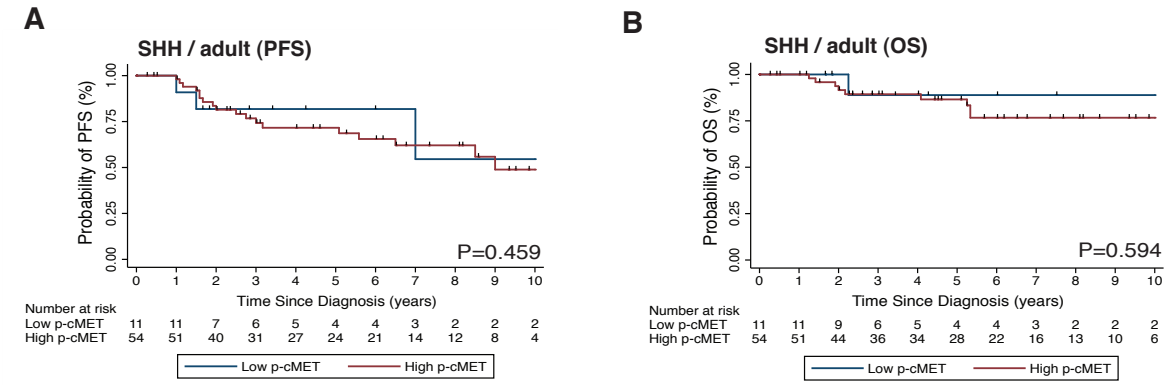

Figure 2.9: Prognostic impact of p-cMET status in adult SHH medulloblastomas.
Kaplan-Meier survival curves displaying (**A**) progression-free survival (PFS) and (**B**) overall survival (OS) according to p-cMET status in adult SHH medulloblastomas. Statistical significance of recurrence was determined by a Fisher's exact test and survival by a log-rank test.

2.3.4 Foretinib Inhibits cMET and PDGFRß Pathway Activity

Based on the elevated expression levels of cMET and PDGFRß in SHH and Group 3 medulloblastomas we sought to evaluate the antitumoral effect of foretinib against medulloblastoma cell lines representative of these two subgroups. Daoy, ONS76 and D425 human medulloblastoma cell lines have transcriptional and cytogenetic features that suggest they are originally derived from SHH (Daoy and ONS76) and Group 3 (D425) tumors[196]. Furthermore, they express different levels of the tyrosine kinase receptors cMET and PDGFRß (**Figure 2.10A**). First, we evaluated the ability of foretinib to inhibit the cMET and the PDGFRß pathway activity in the context of HGF or PDGF-BB stimulation. Foretinib potently inhibited the HGF-induced cMET pathway activation, as evidenced by the suppression in cMET phosphorylation ($P < 0.01$) and also by the decrease in the phosphorylation of downstream effectors AKT and MAPK (**Figures 2.10B and 2.10C**). The inhibitory effect of foretinib in PDGF-BB-induced PDGFRß pathway activation resulted in inhibition of PDGFRß phosphorylation and only moderate inhibition of downstream signaling (**Figures 2.11A and 2.11B**).

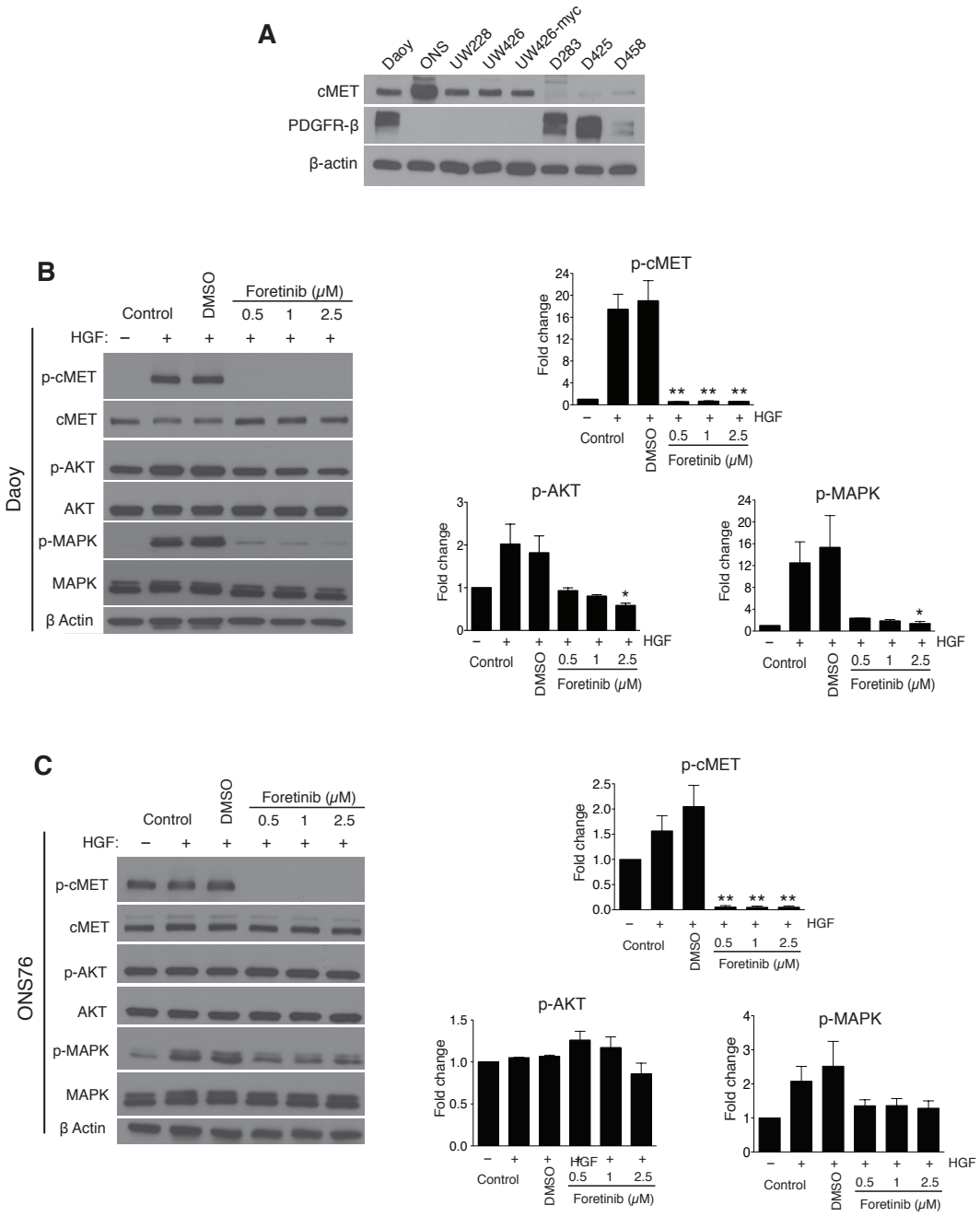

Figure 2.10: cMET pathway targeting by foretinib in human medulloblastoma cell lines.

(**A**) Western blot of cMET and PDGFRß expression in several medulloblastoma cell lines showing variable expression levels. (B) Daoy and (C) ONS76 cells were serum starved for 24 hours, pre-treated with different concentrations of foretinib and stimulated with HGF (20 ng/mL). The phosphorylation levels of cMET, AKT and MAPK were determined using Western blot and chemoluminescence densitometric analysis. Fold change in densitometric analysis represents the phosphorylated proteins compared to total proteins. Data represent mean of triplicates ± SEM (*P < 0.05; **P < 0.01).

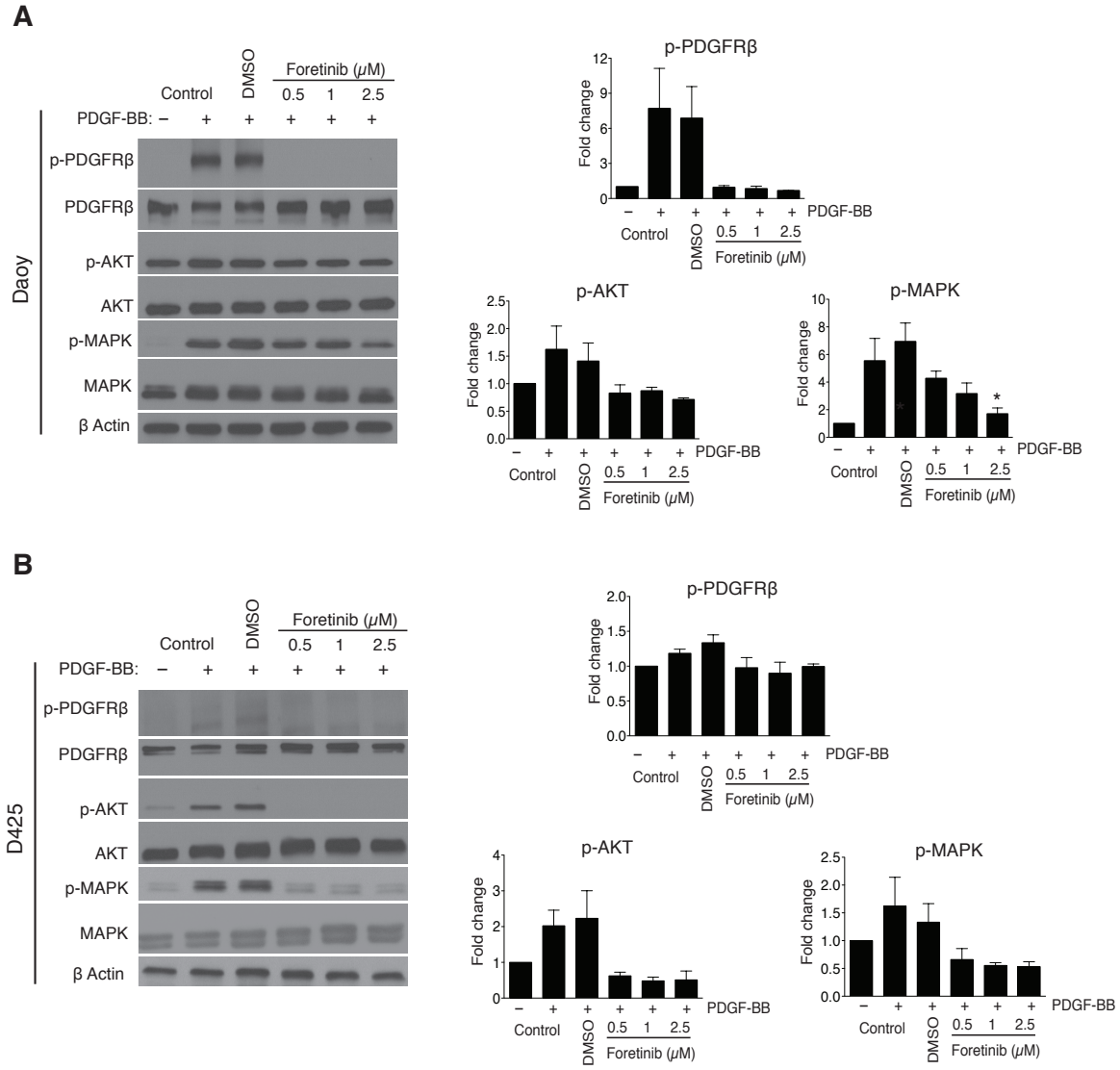

Figure 2.11: PDGFRß pathway inhibition by foretinib in human medulloblastoma cell lines. Serum starved (**A**) Daoy and (**B**) D425 medulloblastoma cells were pre-treated with foretinib for 2 hours and stimulated PDGF-BB (20 ng/mL). Inhibition of PDGFRß pathway and downstream signaling were determined by Western blot and chemoluminescence densitometric analysis. Fold change in densitometric analysis represents the phosphorylated proteins compared to total proteins. Data represent mean of triplicates ± SEM (*P < 0.05).

Furthermore, a significant ($P < 0.001$) anti-proliferative effect was observed in foretinib treated Daoy, ONS76 and D425 medulloblastoma cells (**Figures 2.12A – C**). The reduction in cell proliferation was matched by an induction of apoptosis as shown by the increase in PARP cleavage (**Figures 2.12D – F**) and in caspase 3 and 7 activity (**Figures 2.12G and 2.12H**).

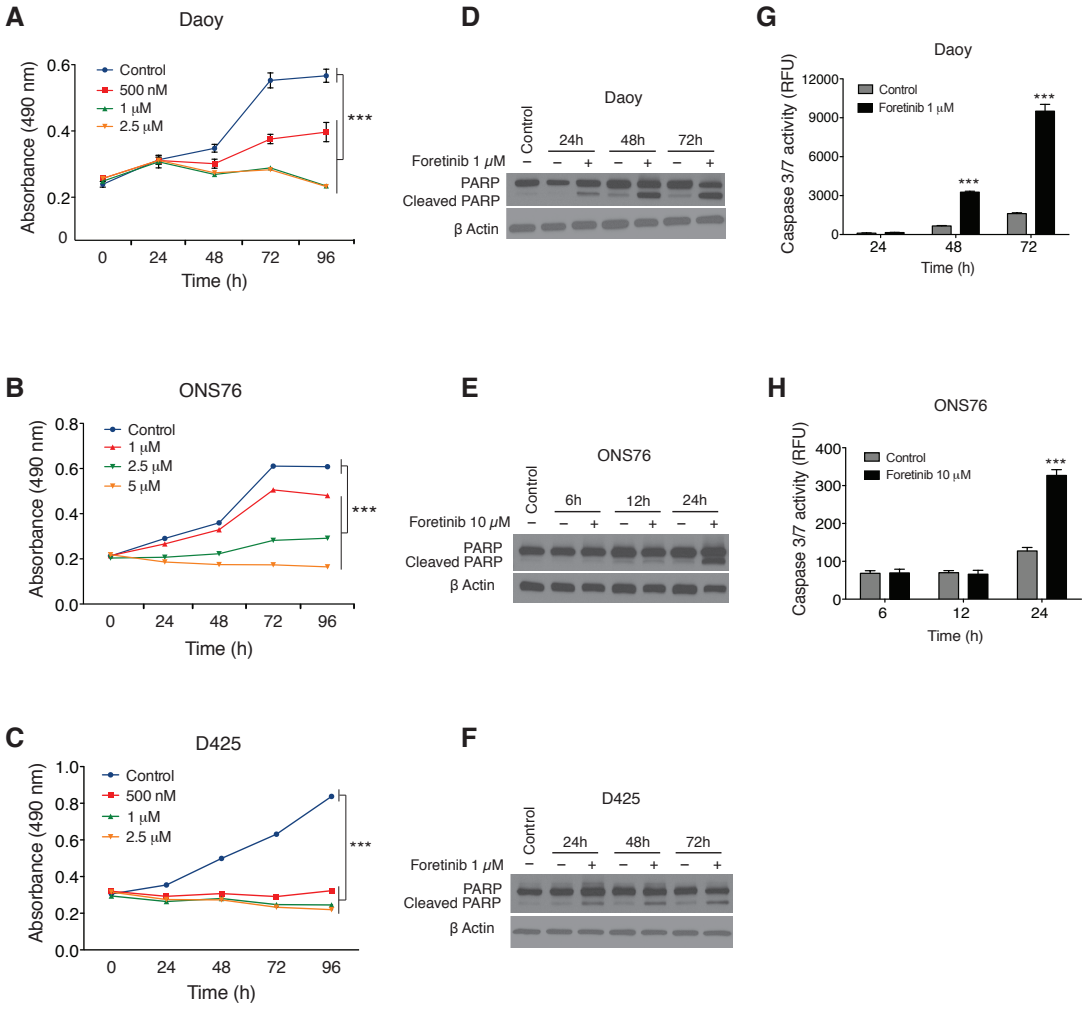

Figure 2.12: Anti-proliferative and pro-apoptotic effects of foretinib in human medulloblastoma cells.

Viability of (**A**) Daoy, (**B**) ONS76 and (**C**) D425 cells treated with varying concentrations of foretinib and measured over 96 hours by MTS assay. Data represent mean of triplicates ± SEM (***$P < 0.001$). (**D – F**) Western blot showing PARP and cleaved PARP antibodies probing cell lysates from Daoy, ONS76 and D425 cells treated with foretinib for different time points. (**G and H**) Cleaved caspase 3/7 assays demonstrating induction of apoptosis after foretinib treatment in Daoy and ONS76 cells. RFU: Relative Fluorescence Units. Data represent mean of triplicates ± SEM (***$P < 0.001$).

Foretinib potently inhibited HGF-mediated migration (**Figures 2.13A – 2.13D**) and invasion (**Figures 2.14A and 2.14B**) of Daoy and ONS76 cells for all drug concentrations. In contrast, a significant reduction in migration and invasion mediated by PDGF-BB was only seen with 2.5 µM of foretinib (**Figures 2.13E and 2.14C**). Collectively, these results suggest that foretinib exhibits a significant in vitro inhibitory activity in medulloblastoma cells, mainly through blockade of the cMET pathway.

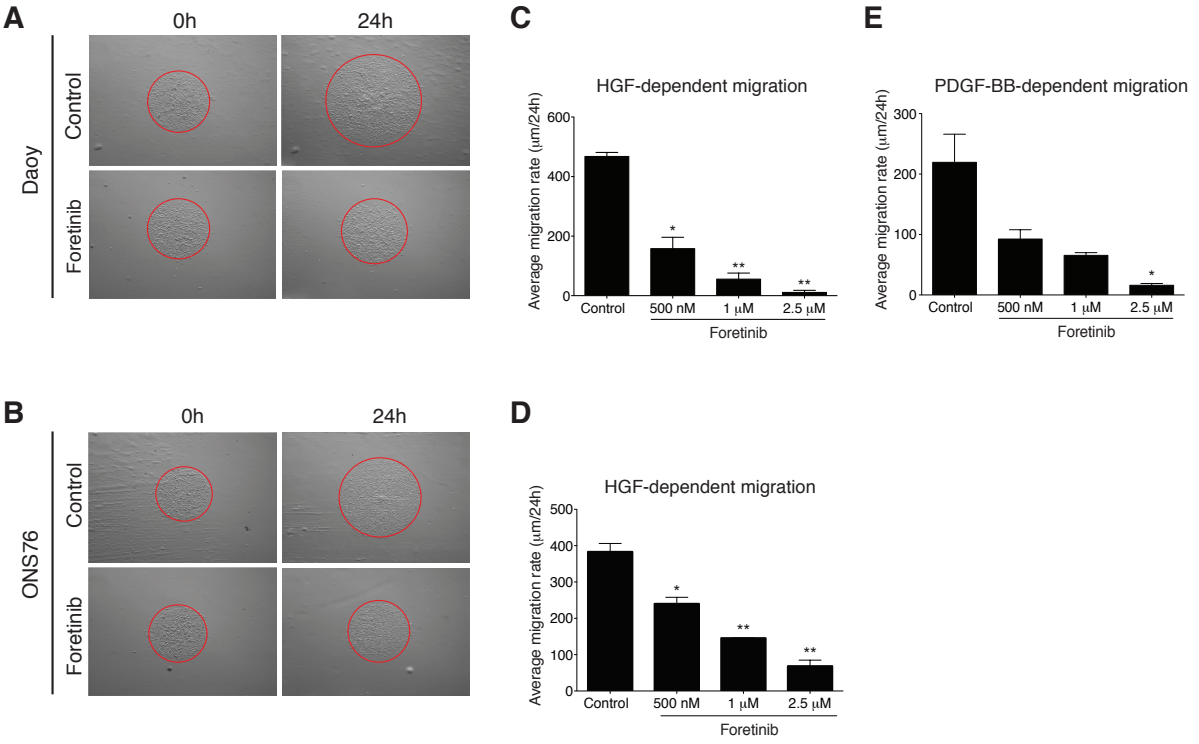

Figure 2.13: Effect of cMET and PDGFRß inhibition in medulloblastoma migration. Representative images of radial migration assays with (**A**) Daoy and (**B**) ONS76 cells under HGF stimulation (2.5X magnification). Foretinib inhibits (**C and D**) HGF and (**E**) PDGF-BB-dependent cell migration. Data represent mean of triplicates ± SEM (*P < 0.05; **P < 0.01).

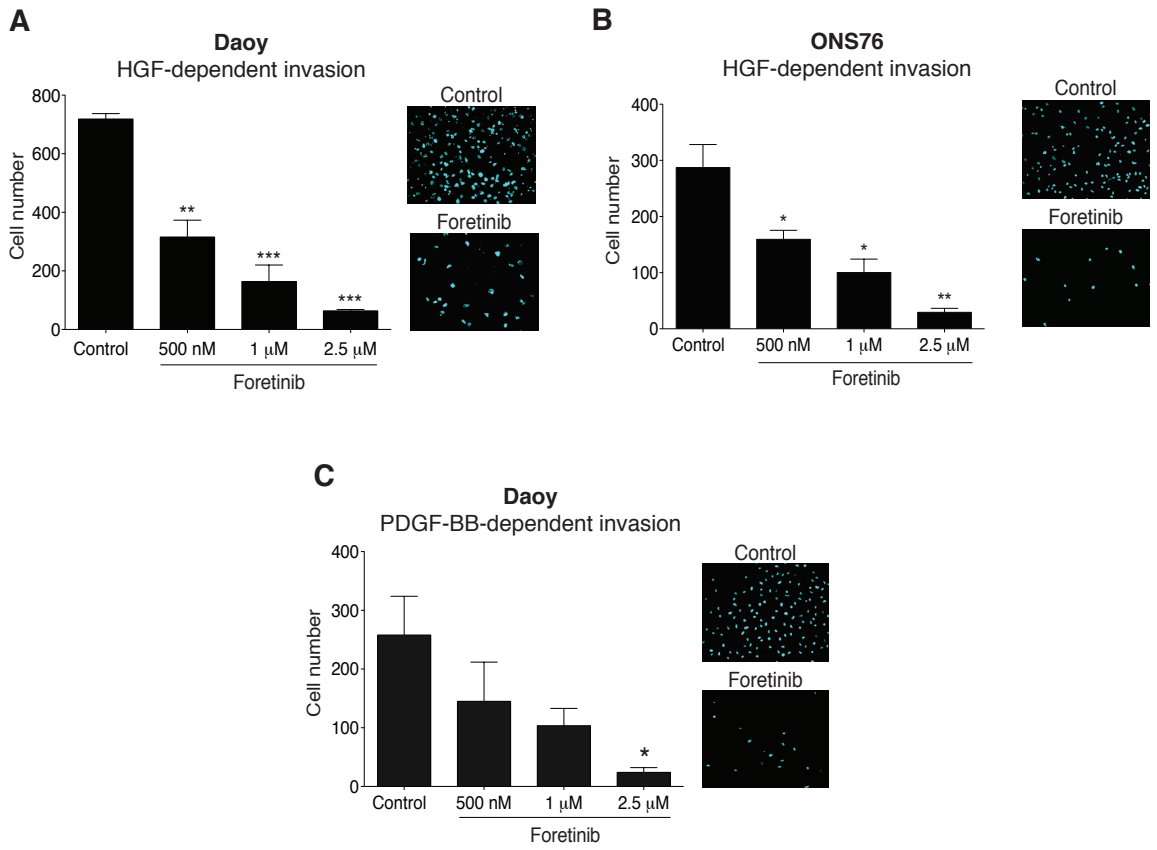

Figure 2.14: Effect of cMET and PDGFRß inhibition in medulloblastoma invasion.
Foretinib reduces (**A and B**) HGF and (**C**) PDGF-BB-dependent medulloblastoma cell invasion. Representative photographs are shown with the nuclei stained with DAPI. The number of cells per 6 random fields was determined (10X magnification). Data represent mean of triplicates ± SEM (*P < 0.05; **P < 0.01; ***P < 0.001).

2.3.5 Foretinib Induces Medulloblastoma Regression *In Vivo*

Having assessed the efficacy of foretinib in vitro, we sought to investigate its antitumor activity in vivo using subcutaneous xenograft models of SHH medulloblastoma. Daoy and ONS76 cells were implanted in the flank of nude mice and animals with established tumors were treated by oral gavage with vehicle (DMSO) or foretinib (60 and 100 mg/kg), once every other day for 9 days. Therapy with foretinib significantly induced tumor regression at all drug concentrations administered. At the end of treatment, tumor volumes were reduced by 37% and 46% with 60 and 100 mg/kg of foretinib, respectively, in Daoy xenografts (**Figures 2.15A and 2.15B**) and by 50% in ONS76 xenografts (**Figures 2.16A and 2.16B**). Foretinib was well tolerated as mice body weights were maintained during the treatment period for all cohorts (**Figures 2.15C and 2.16C**).

Medulloblastoma tumor growth inhibition in mice treated with foretinib was associated with concomitant reduction in cMET and PDGFRß pathway activity (**Figures 2.15D and 2.16D**). Compared to tumors treated with vehicle, foretinib treatment resulted in a potent inhibition of cMET phosphorylation in all cohorts (**Figures 2.15E and 2.16E**) and a moderate reduction in PDGFRß activation (**Figure 2.15F**). Tumors treated with foretinib also displayed significant dose-dependent decrease in cell proliferation (**Figures 2.15G and 2.16F**), and increase in apoptosis (**Figures 2.15H and 2.16G**).

These studies demonstrate that foretinib has a significant in vivo antitumor effect in medulloblastoma allografts, through a potent suppression of the cMET pathway activity and a moderate inhibition of PDGFRß signaling.

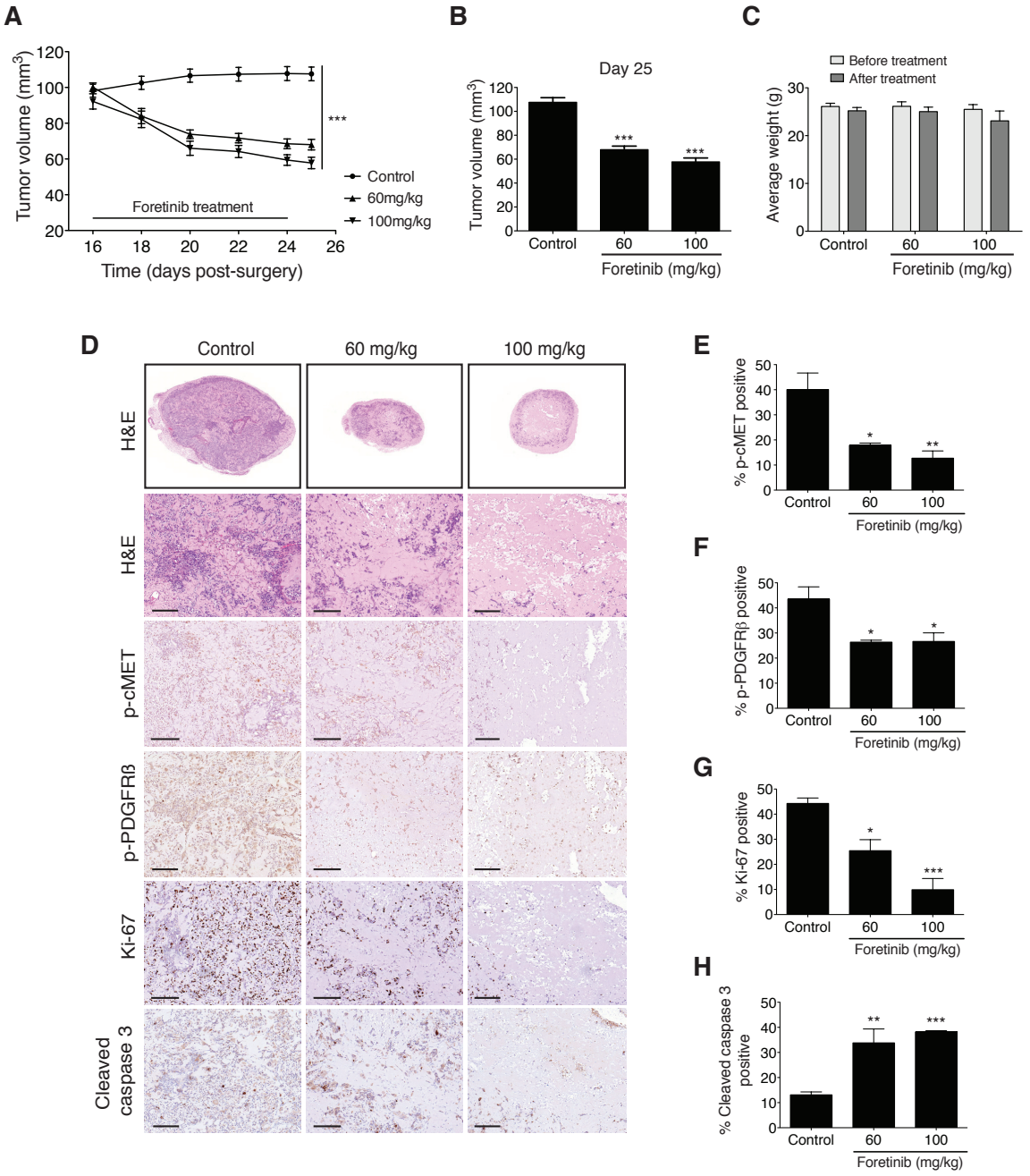

Figure 2.15: Foretinib induces regression of Daoy medulloblastoma flank xenografts.

Nude mice with Daoy hindflank xenografts were treated with vehicle control (10% DMSO, n = 6) or foretinib (60 and 100 mg/kg; n = 6 per group), once every other day for 9 days. Effect of foretinib on tumor growth was compared during treatment (**A**) and in the end of treatment (**B**). Data represent group means ± SEM (***P < 0.001). (**C**) Average animal body weight before and after therapy. (**D**) Flank tumors treated with foretinib show inhibition of p-cMET and p-PDGFRß, decreased cell proliferation (Ki-67 staining) and increased apoptosis (cleaved caspase 3 staining). Scale bar: 100 µm. (**E – H**) Immunohistochemical quantification of p-cMET, p-PDGFRß, Ki-67 and cleaved caspase 3. Data represent mean ± SEM (*P < 0.05; **P < 0.01; ***P < 0.001).

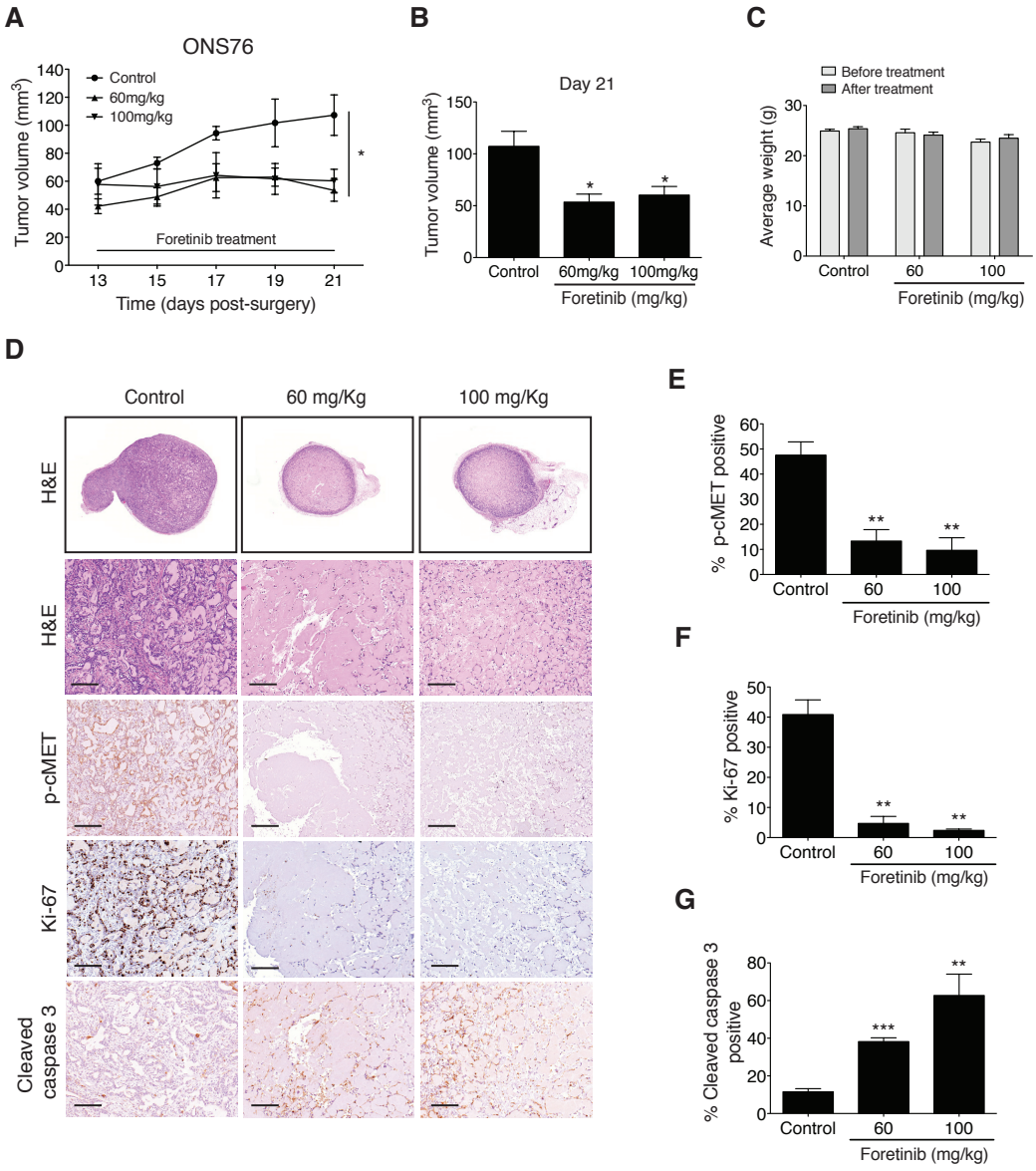

Figure 2.16: Foretinib reduces tumor growth in ONS76 medulloblastoma flank xenografts. (**A and B**) Effect of foretinib in ONS76 mouse flank xenografts treated with 60 and 100 mg/kg by oral gavage, once every other day for 9 days (n = 6 in each group). Data represent group means ± SEM (*P < 0.05). (**C**) Differences in mean body weight between vehicle treated and foretinib (60 and 100 mg/kg) treated mice were not statistically significant by 1 way ANOVA (P > 0.05) followed by Tukey's Multiple Comparison Post-Test (P > 0.05 for all pairwise comparisons). Data represent group mean ± SEM. (**D**) ONS76 flank tumors treated with foretinib show potent inhibition of p-cMET, decreased cell proliferation (Ki-67 staining) and increased apoptosis (cleaved caspase 3 staining). Scale bar: 100 μm. (**E – G**) Immunohistochemical quantification of p-cMET, Ki-67 and cleaved caspase 3. Data represent mean ± SEM (**P < 0.01; ***P < 0.001).

2.3.6 Characterization of Foretinib Pharmacokinetics and Brain Permeability

To further evaluate the potential clinical relevance of foretinib in brain tumor treatment, we assessed the pharmacokinetics of the drug and its ability to penetrate into the brain. Nude mice were treated by oral gavage with 30, 60 and 100 mg/kg of foretinib, and blood and the perfused brains were harvested at specific time points (after 5 hours, 10 hours and 5 days of daily treatment). Foretinib was detected in samples from treated animals using high-performance liquid chromatography with tandem mass spectrometry (LC/MS/MS). Maximum concentrations of foretinib in the plasma and in the brain of mice occurred 5 hours after oral administration with no difference between dose levels (**Figures 2.17A and 2.17B**).

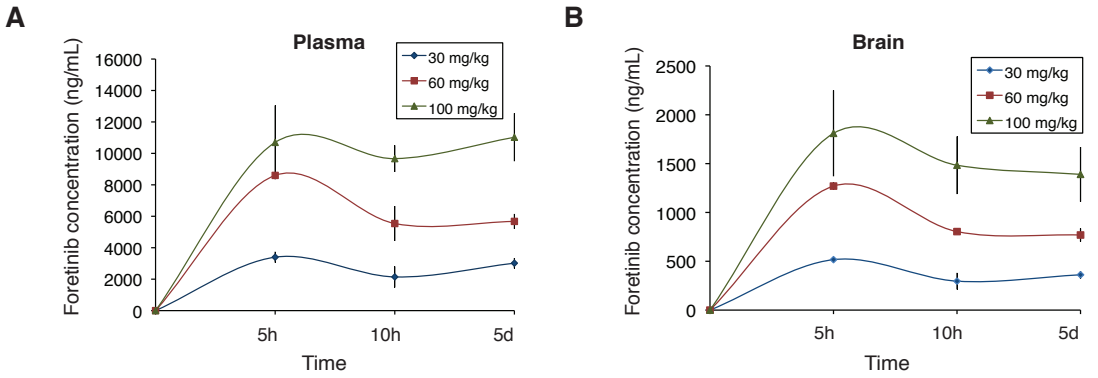

Figure 2.17: Pharmacokinetics of foretinib in preclinical mouse models.
Concentration-time profile of foretinib determined by high-performance liquid chromatography with tandem mass spectrometry (LC/MS/MS) method in the plasma (**A**) and in the brain (**B**) of mice, after oral administration of 30, 60 and 100 mg/kg of foretinib. Data represent mean of quadruplicates ± SEM.

The same pharmacokinetic features in the plasma were previously reported in a phase I clinical trial of foretinib in adult patients with advanced solid tumors outside the central nervous system [183]. This study established a dose of 3.6 mg/kg of oral foretinib as the maximum tolerated dose in human studies. The concentration of foretinib used in our mouse studies that better resembles the recommended dose in humans is 60 mg/kg since it has a human equivalent dose of 4.8 mg/kg[197]. Furthermore, after 5 consecutive days of treatment with 60 mg/kg of oral foretinib, the penetration of the drug in the brain was approximately 14% (**Table 2.1**).

Table 2.1: Foretinib concentrations in mouse brain, mouse plasma and the brain/plasma ratio after administration of 30, 60 and 100 mg/kg by oral gavage

Foretinib concentration	Brain (ng/mL)	Plasma (ng/mL)	Ratio
30 mg/kg (oral gavage)			
5 h	517 ± 20	3400 ± 345	0.152
10 h	296 ± 85	2143 ± 670	0.138
5 d	362 ± 38	3018 ± 328	0.120
60 mg/kg (oral gavage)			
5 h	1270 ± 40	8600 ± 50	0.148
10 h	804 ± 23	5540 ± 1110	0.145
5 d	769 ± 67	5675 ± 475	0.135
100 mg/kg (oral gavage)			
5 h	1810 ± 440	10700 ± 2350	0.169
10 h	1483 ± 295	9667 ± 848	0.153
5 d	1390 ± 280	11025 ± 1525	0.126

NOTE: The results are the mean of measurements of 3 mice ± SEM.

We then assessed the distribution of foretinib in different mouse organs using matrix-assisted laser desorption/ionization with time-of-flight mass spectrometer (MALDI-TOF) imaging. This technique allows direct imaging of compounds in tissue sections and uses mass spectrometry to confirm the presence of specific molecules. Foretinib produces a strong signal and the mass spectrum shows three well-defined peaks corresponding to the natural isotopic distribution of the drug (**Figures 2.18A and 2.18B**). Five hours after oral administration of foretinib, when it reaches the maximum plasma concentration, the drug is seen in the liver and also in the renal cortex (**Figure 2.18C**). The concentration of foretinib in the brain after oral gavage was below the threshold detection of MALDI-TOF imaging.

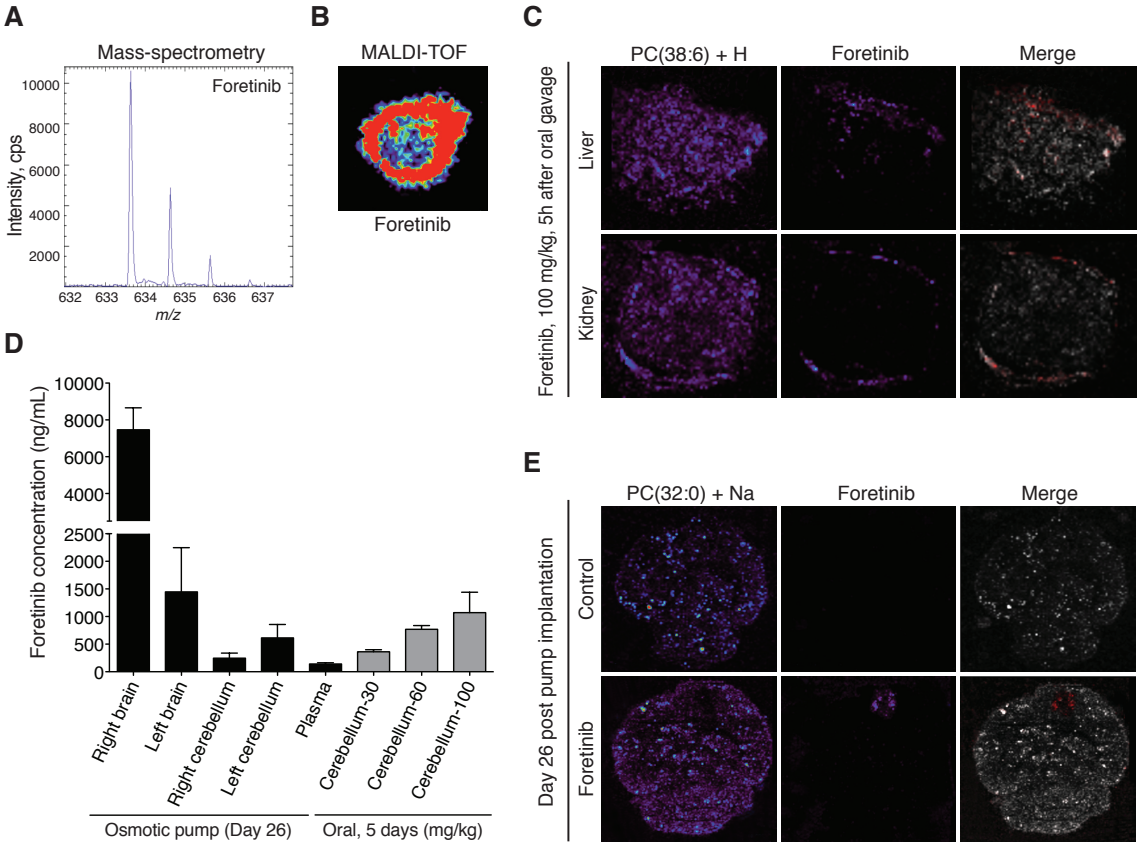

Figure 2.18: Distribution of foretinib in preclinical mouse models.
(**A and B**) Identification of foretinib by matrix-assisted laser desorption/ionization with time-of-flight mass spectrometer (MALDI-TOF) imaging. *m/z*: mass-to-charge. (**C**) Distribution of foretinib in the liver and kidney of mice 5 hours after oral administration of 100 mg/kg. (**D**) Comparison of foretinib concentration (ng/mL) in different areas of the brain after intrathecal therapy (osmotic pumps) versus oral gavage. Data represent mean of triplicates ± SEM. (**E**) foretinib imaging with MALTI-TOF in the mouse brain after local delivery by osmotic pump.

To explore the potential use of foretinib for intrathecal therapy in neuro-oncology we delivered the drug into the lateral ventricles of mice using osmotic pumps and assessed toxicity, drug quantification and distribution in the brain. In order to mimic human intrathecal chemotherapeutic regimens[198], we delivered 6 mg/kg of foretinib for 28 days at a rate of 0.25 µl/hour, which represents 10% of the oral dose of 60 mg/kg previously tested. Foretinib injected into the right lateral ventricle of mice was distributed through the cerebrospinal fluid to the supra- and infratentorial compartments. Interestingly, the concentration of foretinib in

the cerebellum after oral administration of 60 mg/kg for 5 consecutive days was similar to the concentration of the drug obtained by local delivery of a single dose of 6 mg/kg over a period of 26 days (**Figure 2.18D**). Foretinib was clearly detected by MALDI-TOF imaging in the right frontal lobe of mice due to its very high concentration at the drug delivery site (**Figure 2.18E**). The drug was well tolerated and the mice did not display any signs of central nervous system toxicity.

Collectively, these studies demonstrate for the first time, to our knowledge, that foretinib crosses the blood-brain barrier and can be safely administered as intrathecal therapy.

2.3.7 Foretinib Reduces SHH Medulloblastoma Growth and Dissemination in Mouse Xenografts

Having established that foretinib can effectively be delivered in the brain, we investigated its efficacy in mouse models of disseminated medulloblastoma. Daoy cells expressing luciferase were orthotopically implanted into the fourth ventricle of nude mice. Animals with a detectable signal by bioluminescence at 3 days post inoculation were treated by oral gavage either with vehicle (DMSO) or 60 mg/kg of foretinib once daily, 6 days a week, for 2 weeks. The weekly evaluation of tumor growth and dissemination by bioluminescence showed a significant reduction in tumor size and metastases in the animals treated with foretinib (**Figures 2.19A and 2.19B**), as confirmed by the smaller increase in the total photon flux from luciferase expressing Daoy xenografts (**Figure 2.19C**). Histological examination (H&E stain) of brains and spinal cords of animals in the control group showed a higher number of metastases in the ventricles and leptomeningeal spaces, as well as surrounding the spinal cord and the nerve roots, when compared to foretinib treated animals (**Figures 2.19D and 2.19E**). Since all animals developed hydrocephalus due to injection of tumor cells into the cerebrospinal fluid, we could not evaluate survival using this mouse model.

These results demonstrate that foretinib is effective in reducing tumor growth and treating established medulloblastoma metastases in orthotopic mouse models of disseminated medulloblastoma.

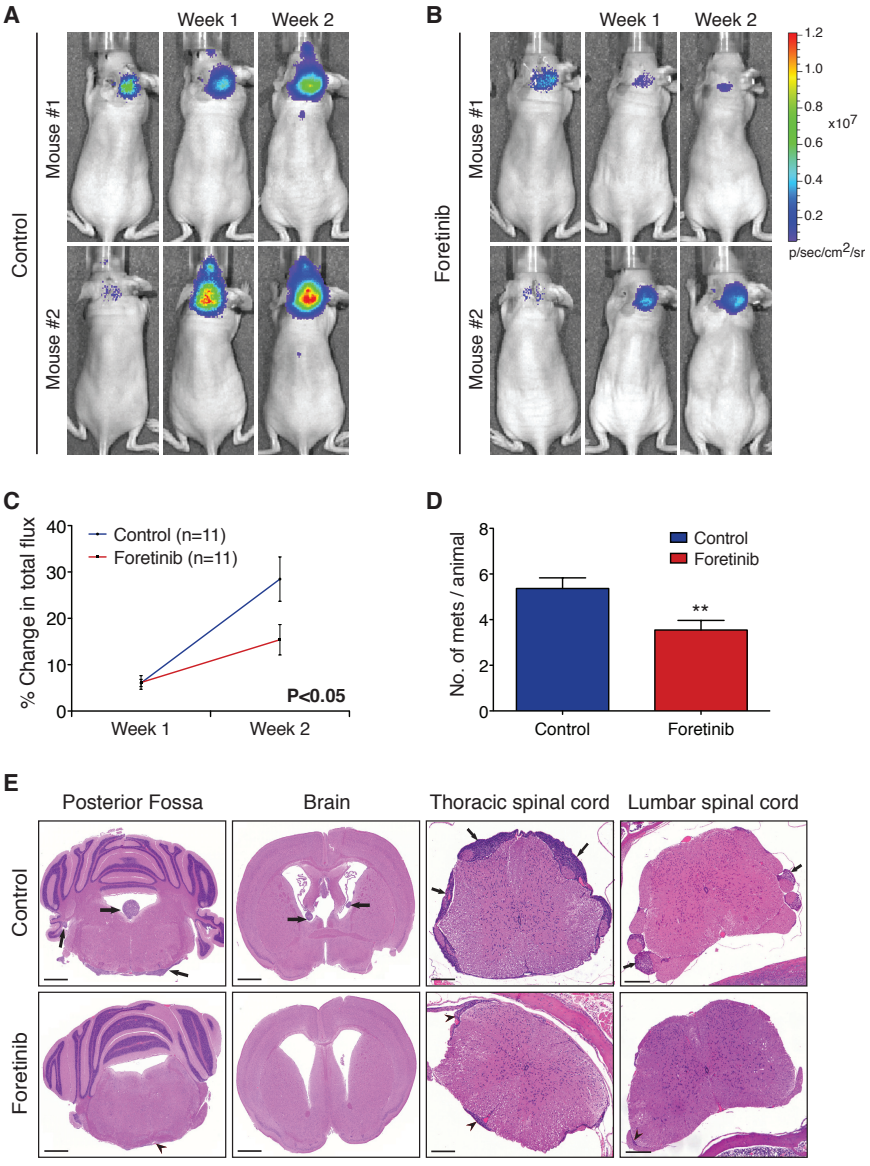

Figure 2.19: Foretinib decreases tumor growth and metastases in intracranial xenografts models of medulloblastoma.

Representative bioluminescence imaging of nude mice intraventricular xenografts treated with (**A**) vehicle control (10% DMSO, n = 11) or (**B**) foretinib (60 mg/kg, n = 11), orally once daily, 6 days a week, for 2 weeks. Foretinib decreases medulloblastoma growth as denoted by a smaller change in total photon flux (**C**) and the total number of metastases (**D**). Data represent group means ± SEM (**P < 0.01). (**E**) Representative H&E analysis of brain and spinal cord samples in the control group and the foretinib treated group. Arrows denote metastatic deposits in a representative animal from the control group while arrowheads denote metastases, smaller in number and size, of a representative animal from the foretinib treated group. Scale bar: 1000 μm.

2.3.8 Foretinib is Effective Against the Primary and the Metastatic Compartments in a Transgenic Model of Metastatic SHH Medulloblastoma

To further validate our findings we tested the efficacy of foretinib in a recently published metastatic mouse model of SHH medulloblastoma[175]. The authors used the Sleeping Beauty (SB) transposon system where random insertion events through the genome lead to activation of oncogenes and disruption of tumor suppressor genes. Mobilizing the SB transposon in the cerebellar progenitor cells of Ptch+/- mice induced a very aggressive form of medulloblastoma with high incidence of leptomeningeal dissemination by 10 weeks of age[175]. We asked whether early and continuous treatment with foretinib could prevent the formation of metastases and improve survival in this mouse model. Osmotic pumps loaded with 6 mg/kg of foretinib or vehicle (10% cremophor) were implanted in 4 to 5 weeks old mice and delivered the drug for 28 days, at a rate of 0.25 µl/hour. Strikingly, foretinib treated animals showed a significant increase in survival (**Figure 2.20A**) and displayed medulloblastomas in the cerebellum with a less invasive phenotype when compared to controls (**Figures 2.20B and 2.20C**). Moreover, treatment with foretinib reduced the incidence of metastases by 36% (**Figure 2.20D**). Mice tolerated intrathecal administration of foretinib although 4 animals presented with intratumoral haemorrhage in the cerebellum (2 animals in the vehicle control group and 2 animals in the foretinib treated group) most likely related to the tumor vasculature and not to the treatment with foretinib.

Taken together, these results demonstrate that foretinib is effective both against the primary and the metastatic compartments in medulloblastoma, by reducing primary tumor invasion and preventing leptomeningeal dissemination in an aggressive mouse model of metastatic SHH medulloblastoma.

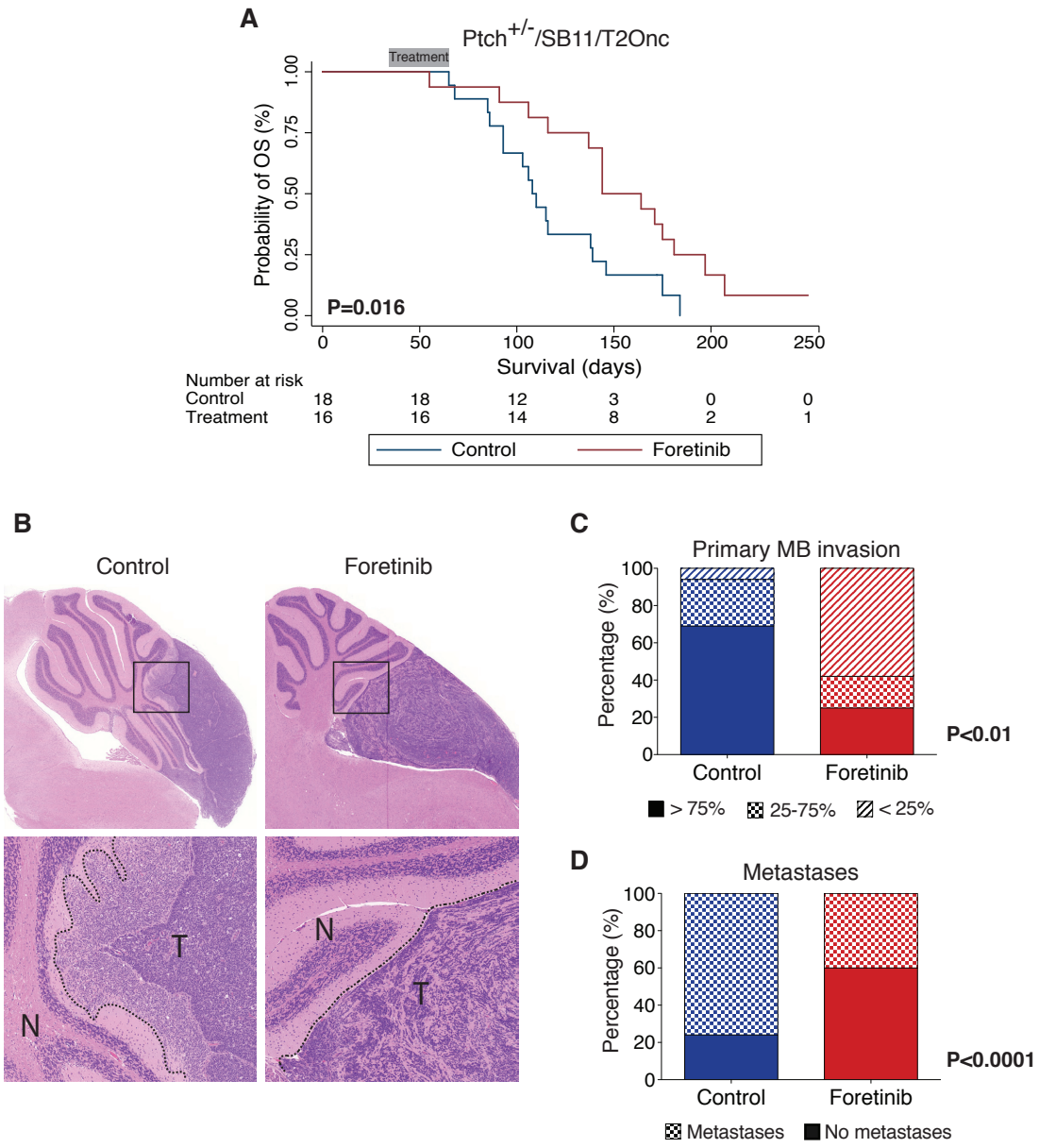

Figure 2.20: Foretinib prevents metastases formation and increases survival in a transgenic mouse model of metastatic SHH medulloblastoma.

(**A**) Kaplan-Meier survival curves demonstrate that *Ptch*$^{+/-}$ mice with *Sleeping Beauty* transposition (*Ptch*$^{+/-}$/SB11/T2Onc) have an increased survival after treatment with 6 mg/kg of foretinib by osmotic pump infusion (rate of 0.25 µl/hour for 28 days; n = 16) when compared to the vehicle control group (n = 18). The grey bar indicates the duration of treatment. (**B and C**) Primary medulloblastomas treated with foretinib display a less invasive phenotype as denoted by (**B**) the dashed line separating the tumor (T) and the normal (N) cerebellum in H&E sections, and by (**C**) the quantification of the percent tumor invasion ($P < 0.01$). (**D**) Foretinib decreases the incidence of metastases in an aggressive model of metastatic medulloblastoma. Data represent group means ± SEM ($P < 0.0001$).

2.4 Discussion

We show here that activation of cMET signaling is a hallmark feature of SHH medulloblastomas and correlates with poor outcome in pediatric patients. Targeting the cMET receptor with foretinib, an FDA approved kinase inhibitor that crosses the blood-brain barrier, significantly reduces primary medulloblastoma growth and invasion, diminishes the incidence of metastases and increases survival in disseminated mouse models of SHH medulloblastoma. Our study identifies for the first time a subgroup-specific targeted drug with promising efficacy against both medulloblastoma primary tumors and metastases.

We demonstrate that cMET is highly expressed in SHH medulloblastomas although the mechanisms leading to cMET up-regulation in this subgroup remain unclear. A recent publication reported a high number of CNAs in SHH medulloblastomas [23] but the analysis of the same large cohort of samples (n=1,239) fail to show any focal gains or amplifications of *cMET*. Furthermore, of 332 medulloblastomas recently sequenced, there were no recurrent mutations or amplifications of the *cMET* gene[192,199-201]. These results suggest that the high expression of cMET is not driven by CNAs but may relate to the specific signaling events or cell of origin of the SHH subgroup. Interestingly, our previous finding that SPINT2, an inhibitor of cMET, is silenced by promoter methylation[34] and the recent publication that cMET is among the most significantly hypermethylated genes in Group 4 tumors[202], suggest that cMET regulation in medulloblastomas may be driven by epigenetic factors.

Examination of molecular pathways characterizing SHH tumors with high and low cMET expression revealed distinct patterns of alteration. While low cMET SHH medulloblastomas were associated with deregulation of biological processes involved in neurogenesis and neurotransmission, high cMET SHH medulloblastomas were characterized by alterations in a number of cancer-related networks, namely cell migration, cell cycle, DNA repair and transcription. The activation of distinct biological pathways in high cMET SHH medulloblastomas supports the existence of a different cell of origin for these tumors, in keeping with a recent study that has shown that a specific population of Nestin-expressing neuronal progenitors in the cerebellum can give rise to SHH-driven medulloblastomas[203].

We identify a gene signature of cMET activators, including cMET and GAB1, unique to SHH-driven tumors. Our results are supported by a previous publication where immunoreactivity for GAB1 was reported to be a surrogate marker for SHH medulloblastomas[25]. Furthermore, we demonstrate that the cMET pathway activation status can segregate patients with SHH medulloblastomas into distinct prognostic outcomes. In

pediatric patients with SHH tumors, activation of cMET is correlated with an increased rate of relapse and a shorter progression-free survival. Notably, this association is not seen in adult SHH patients confirming the previously reported clinical and molecular distinction between adult and pediatric SHH medulloblastomas[22]. Furthermore, p-cMET status does not correlate with the presence of metastases or TP53 mutations, two known markers of poor prognosis across medulloblastoma subgroups[204] and within the SHH subgroup[205], respectively. We show that a simple immunohistochemical analysis of activated cMET provides a high quality clinical trial biomarker for identification of patients who could benefit from targeted therapy using cMET inhibitors.

Foretinib, an FDA approved drug, had a dramatic therapeutic effect in SHH medulloblastoma, both *in vitro* and *in vivo*. Furthermore, our pharmacokinetic studies demonstrate for the first time that foretinib penetrates the blood-brain barrier and is well tolerated and distributed through intrathecal administration. As expected by the high affinity of foretinib to the cMET receptor, its overall antitumor effect is predominantly exerted through blockade of the cMET pathway although we have also shown that foretinib targets PDGFRß with lower affinity. Foretinib reduces primary medulloblastoma growth and invasion, and has also a potent activity against medulloblastoma metastases. Administration of foretinib to an aggressive metastatic mouse model of SHH medulloblastoma increases survival by 45% and diminishes the incidence of metastases by 36%. Interestingly, we show that foretinib also targets AKT, a downstream effector of both cMET and PDGFRß signaling, and recently identified as a key contributor to leptomeningeal dissemination in medulloblastoma[175,176]. Therefore, the anti-metastatic properties of foretinib may be related to its unique ability to target three key drivers in medulloblastoma dissemination, namely cMET, PDGFRß and PI3K.

Given the high expression of cMET in SHH-driven medulloblastomas, the therapeutic regimen that may offer maximum benefit in this subset of patients is the combination of foretinib with an antagonist of SHH signaling. A significant antitumor effect was reported in a patient with metastatic medulloblastoma after inhibition of smoothened (SMO), a critical component of SHH pathway, although the response was transient due to the emergence of acquired resistance[162]. Thus, we anticipate that combining foretinib with a SMO inhibitor may have a synergistic and an anti-resistance effect treating cMET-dependent SHH medulloblastomas.

In summary, we show that the FDA approved drug foretinib is effective treatment in preclinical murine models of metastatic SHH medulloblastoma. Given the dismal outcome

and lack of options for these patients, our results provide strong rationale for repurposing foretinib as a targeted agent in SHH-driven medulloblastoma.

Chapter 3
The Connectivity Map Identifies Novel Small Molecules to Target Group 3 Medulloblastoma[v]

3.1 Introduction

As described previously, medulloblastoma consists of at least four distinct molecular subgroups: WNT, SHH, Group 3 and Group 4[13,16]. These subgroups are characterized by divergent genetic aberrations, cytogenetic features, and distinct phenotypes including patient demographics and clinical outcome. Tumors with WNT pathway activation have the most favorable prognosis whereas Group 3 medulloblastomas have the worst outcome. Group 3 tumors are restricted to pediatric patients, exhibit overexpression or amplification of *MYC*, and are frequently metastatic at the time of diagnosis[18,20]. These tumors are particularly resistant to conventional therapies with radiation and chemotherapy, even at maximal tolerated doses, highlighting the need for novel and more effective therapeutic options[191,206].

We used the Connectivity Map (C-MAP), a bioinformatic tool based on gene expression, to discover small molecules with high likelihood of efficacy against Group 3 medulloblastomas. The C-MAP contains gene expression signatures of various cultured cancer cell lines treated with a library of small molecule compounds already approved by the Food and Drug Administration (FDA)[207,208]. This platform links drugs, genes and diseases by measuring similarity or dissimilarity in gene expression. Using a pattern-matching algorithm, the program is able to identify drugs predicted to revert the oncogenic gene signature of a given cancer to a nonmalignant or drug-sensitive gene expression profile. Previous studies have successfully used this approach to identify compounds with the ability to modulate various biological pathways or diseases[209-212].

In this study we identified subgroup-specific signatures with genes differentially expressed between each medulloblastoma subgroup and normal cerebellum. We then selected

[v] The gene expression analysis in medulloblastoma samples and cell lines, and the C-MAP analysis were performed by Sameer Agnihotri and Stephen Mack. Assistance with cell viability assays using M441 and hf5281 stem cells was obtained from Michelle Kushida, Renee Head and Xin Wang. Assistance with Western blot experiments using Group 3 medulloblastoma cell lines was obtained from Brian Golbourn, Samantha Olsen, Melissa Bryant and Mathiew Bebenek. The remainder of experiments described in this chapter were performed by the candidate.

the top up- and down-regulated genes to query the C-MAP database and obtain a list of compounds with likelihood to reverse the direction of gene expression in medulloblastoma. Piperlongumine (PL), a natural product isolated from the fruit of the Piper longum and previously known to have cytotoxic properties in cancer[213], was the top candidate for non-WNT tumors. Alsterpaullone (ALP), a CDK inhibitor, was identified as a potential therapeutic agent for Group 3 medulloblastomas. In subsequent validation experiments we sought to validate the predictions of the *in silico* drug screen. We showed that ALP is highly effective and selective in treating Group 3 medulloblastoma cell lines and mouse xenografts. Furthermore, ALP reverses Group 3 medulloblastomas gene signature and downregulates many cell cycle-related genes, including *MYC*.

3.2 Materials and Methods

3.2.1 Connectivity Map Analysis

The subgroup-specific gene expression profiles of primary medulloblastomas were obtained from previously published datasets[16]. A list of genes differentially expressed between each medulloblastoma subgroup and normal cerebellum was obtained and the top 200 up- and downregulated genes were selected to query the C-MAP database. Compounds with a negative enrichment score, which implies the ability to reverse the direction of expression of the gene signature of interest, and a p-value inferior to 0.05 were recorded as potential therapeutic agents for medulloblastoma[207,208].

3.2.2 Medulloblastoma Cell Lines

The medulloblastoma cell lines (D425 and D458) were kindly provided by Dr. Annie Huang, Hospital for Sick Children, Toronto, Canada. D458-GFP/Luciferase cells were generated as described previously[193]. The primary medulloblastoma stem cell line (M441) and the fetal normal human brain stem cell line (hf5281) were generously provided by Dr. Peter Dirks, Hospital for Sick Children, Toronto, Canada. M441 cells were derived from a surgical specimen from a child with a Group 3 medulloblastoma of the cerebellum and obtained as previously described[214,215].

3.2.3 Cell Proliferation Assays

D425 and D458 cells were grown as suspension cultures and seeded in 96-well microplates at 10,000 cells per well. M441 and hf5281 were grown as adherent cultures and seeded in 96-well microplates at 4,000 and 5,000 cells per well, respectively. Cells were treated for 48h with different concentrations of PL (INDOFINE Chemical Company), ALP (A. G. Scientific), rottlerin (RTL; A. G. Scientific) and flunarizine (FZ; Sigma) or DMSO (control). Cell viability was determined by MTS and the absorbance measured at 490 nm (CellTiter 96 Aqueous One Solution Reagent; Promega). Three independent experiments were performed with 16 repeats per treatment condition.

3.2.4 Medulloblastoma Mouse Xenografts

All mouse studies were approved by the Institutional Animal Care and Use Committee of the University of Toronto and the Hospital for Sick Children, in Toronto, and performed in accordance to their policies and regulations.

Medulloblastoma intracranial xenografts were established in 5-6 weeks old athymic nude mice (D425 and D458 cell lines) and in NOD scid gamma mice (M441 cell line) (both from Charles River Laboratories). Medulloblastoma cells (250,000 D425 and D458 cells; 100,000 M441 cells) were implanted in the right cerebellum of mice. Six days after cell inoculation, animals were randomized into treatment cohorts, which included subcutaneous injections with vehicle control (10% DMSO), PL (50 mg/kg, daily for 2 weeks), ALP (30 mg/kg, daily for 2 weeks), RTL (20 mg/kg, every other day for 2 weeks) or FZ (50 mg/Kg, daily for 2 weeks).

In animals bearing D458-GFP/Luciferase xenografts, bioluminescence imaging was performed at 6 days after intracranial injection. Mice with a detectable signal were included in the study and tumor growth was monitored at one-week intervals using the IVIS Spectrum Optical In-vivo Imaging System (Caliper Life Sciences).

Animals with signs of sickness or weight loss greater than 20% were euthanized and the brains harvested and fixed in 10% formalin.

3.2.5 Immunoblotting

Cell lysates were prepared by adding RIPA buffer (Sigma) containing protease inhibitors (F. Hoffman-La Roche AG), 0.2 M sodium orthovanadate, 0.2 M sodium pyrophosphate and 0.2 M sodium fluoride. The Pierce BCA Protein Assay Kit (Thermo Scientific) was used to determine protein concentration. Proteins were separated on 7.5% or 10% SDS-PAGE gels and transferred to PVDF membranes using a semidry transfer apparatus (Bio-Rad). The following antibodies were used: PARP (1:1,000; Cell Signaling), AKT (1:1,000; Cell Signaling), phospho-AKT (1:2,000; Ser473, Cell Signaling), α-tubulin (1:1,000; Cell Signaling), anti-mouse IgG conjugated to horseradish peroxidase (1:5,000; Amersham Biosciences) and anti-rabbit IgG conjugated to horseradish peroxidase (1:5,000; Cell Signaling).

3.2.6 RNA Extraction and Gene Expression Analysis

D425 and D458 medulloblastoma cells were treated with 5 μM of PL, 5 μM of ALP or DMSO (control) for 48h. RNA isolation was performed using the RNeasy Mini Kit (Qiagen) and gene expression data were generated using the Human PrimeView Arrays.

GSEA was performed using gene sets from the NCI, GO, KEGG, PFAM and Biocarta pathway databases. Significant gene sets were identified (FDR < 0.05; P < 0.01) and visualized in Cytoscape and Enrichment Map software.

A list of genes up- and down-regulated by ALP in D425 and D458 medulloblastoma cells was generated. The top 200 genes were selected to query the C-MAP database and to determine if ALP and PL were able to reverse the gene expression profile of Group 3 medulloblastoma cells ($P < 0.05$).

3.2.7 Statistical Analysis

The Kaplan-Meier estimate and a log-rank test were used to generate survival curves. Experiments were performed in triplicate and results were expressed as mean ± SEM. Statistical analysis was performed using GraphPad Prism 5 Software. A P-value inferior to 0.05 was considered as significant.

3.3 Results

3.3.1 The C-MAP Identifies Novel Candidate Drugs to Treat Medulloblastoma

To identify novel drugs with potential antitumor effect in medulloblastoma we queried the C-MAP database using the previously published gene expression signatures of the four molecular subgroups of medulloblastoma[16]. The top 20 drugs that were able to reverse the gene expression profile of each medulloblastoma subgroup are listed in **Table 3.1**. Piperlongumine, a natural product derived from the plant species *Piper longum*, was the compound with the highest negative enrichment score for non-WNT medulloblastomas. The compounds identified as potential novel therapies for WNT medulloblastomas are distinct from the ones identified for non-WNT tumors. On the other hand, the drugs listed for Group 3 and Group 4 tumors are very similar.

We then asked which compounds were specific for Group 3 medulloblastomas. On top of the list, a CDK inhibitor (alsterpaullone), a protein kinase C (PKC) inhibitor (rottlerin) and two calcium channel inhibitors (denatonium benzoate and flunarizine) showed significant negative enrichment (**Table 3.2**).

Table 3.1: Top 20 drugs with predicted efficacy by the Connectivity Map analysis (P<0.05), for each medulloblastoma subgroup.

WNT			SHH			Group 3			Group 4		
Rank	**C-MAP name**	**Enrichment**	**Rank**	**C-MAP name**	**Enrichment**	**Rank**	**C-MAP name**	**Enrichment**	**Rank**	**C-MAP name**	**Enrichment**
9	monobenzone	-0.855	**66**	piperlongumine	-0.919	**1**	phenoxybenzamine	-0.957	**12**	piperlongumine	-0.971
24	chrysin	-0.841	**20**	trazodone	-0.916	**28**	piperlongumine	-0.95	**1**	phenoxybenzamine	-0.93
5	hexamethonium bromide	-0.806	**4**	luteolin	-0.915	**93**	1,4-chrysenequinone	-0.892	**13**	etacrynic acid	-0.902
13	simvastatin	-0.805	**5**	phenoxybenzamine	-0.909	**101**	DL-thiorphan	-0.885	**92**	1,4-chrysenequinone	-0.896
14	pimozide	-0.805	**8**	apigenin	-0.899	**11**	monobenzone	-0.841	**28**	chrysin	-0.865
8	astemizole	-0.796	**10**	Prestwick-1084	-0.897	**13**	carbachol	-0.833	**51**	0297417-0002B	-0.825
10	antimycin A	-0.787	**117**	DL-thiorphan	-0.869	**47**	doxorubicin	-0.833	**14**	apigenin	-0.815
43	reserpine	-0.786	**18**	bepridil	-0.856	**14**	puromycin	-0.828	**63**	Prestwick-559	-0.811
46	etacrynic acid	-0.783	**54**	chrysin	-0.834	**51**	etacrynic acid	-0.828	**16**	tyloxapol	-0.81
19	methylprednisolone	-0.774	**56**	ronidazole	-0.833	**16**	imipenem	-0.815	**64**	doxorubicin	-0.809
20	chlorphenesin	-0.772	**23**	thiostrepton	-0.831	**63**	chrysin	-0.807	**17**	imipenem	-0.808
11	pyrimethamine	-0.763	**25**	puromycin	-0.83	**18**	luteolin	-0.801	**70**	ronidazole	-0.803
12	halcinonide	-0.746	**29**	repaglinide	-0.809	**19**	trifluridine	-0.797	**21**	Prestwick-1084	-0.801
25	aminophylline	-0.745	**79**	0297417-0002B	-0.803	**21**	GW-8510	-0.796	**34**	sulconazole	-0.771
61	esculetin	-0.745	**31**	GW-8510	-0.797	**72**	0297417-0002B	-0.793	**6**	levonorgestrel	-0.759
26	3-nitropropionic acid	-0.743	**33**	monobenzone	-0.795	**2**	resveratrol	-0.785	**111**	milrinone	-0.759
29	etoposide	-0.724	**87**	etacrynic acid	-0.789	**7**	levonorgestrel	-0.779	**38**	protriptyline	-0.754
3	methotrexate	-0.723	**39**	thioguanosine	-0.78	**90**	alsterpaullone	-0.777	**41**	GW-8510	-0.75
30	semustine	-0.722	**40**	cyproterone	-0.78	**30**	metyrapone	-0.771	**43**	metyrapone	-0.747
31	parthenolide	-0.72	**43**	sulconazole	-0.766	**9**	medrysone	-0.77	**44**	sulfametoxydiazine	-0.746
33	lomustine	-0.708									

NOTE: The compounds were ranked based on negative enrichment score.

Table 3.1: Top 15 drugs specific for Group 3 medulloblastomas, as predicted by the Connectivity Map analysis (P<0.05).

Rank	C-MAP name	Enrichment	Drug category
96	alsterpaullone	-0.765	CDK inhibitor
130	rottlerin	-0.725	PKC inhibitor
69	denatonium benzoate	-0.701	calcium channel inhibitor
104	flunarizine	-0.664	calcium channel inhibitor
107	bupropion	-0.661	dopamine receptor antagonist
117	pyridoxine	-0.651	pyridoxal kinase agonist
31	flunisolide	-0.644	phospholipase A2 inhibitor
125	etamsylate	-0.643	prostaglandin inhibitor
135	prenylamine	-0.635	calcium channel inhibitor
139	practolol	-0.631	beta-adrenergic antagonist
140	betaxolol	-0.629	beta-adrenergic antagonist
144	propylthiouracil	-0.626	thyroid peroxidase inhibitor
136	lorglumide	-0.57	colecystokinin antagonist
138	amiodarone	-0.569	calcium channel inhibitor
113	PNU-0251126	-0.549	not assessed

NOTE: The compounds were ranked based on negative enrichment score.
CDK, cyclin-dependent kinase; PKC, protein kinase C

3.3.2 C-MAP Candidate Drugs Piperlongumine, Alsterpaullone, Rottlerin and Flunarizine Reduce Proliferation of Group 3 Medulloblastoma Cell Lines

To validate the results of our C-MAP analysis we selected piperlongumine (the best candidate for non-WNT medulloblastomas) and the top three drugs predicted to be specific for Group 3 medulloblastomas (alsterpaullone, rottlerin and flunarizine). Denatonium benzoate is known to be the bitterest compound and was excluded from our study.

We examined the effects of each drug on the proliferation of three Group 3 medulloblastoma cell lines (the established cell lines D425 and D458, and the primary medulloblastoma stem cell line M441) and a fetal neural stem cell line (hf5281). Piperlongumine (PL) and rottlerin (RTL) treatment for 48 hours markedly reduced cell proliferation in medulloblastoma cells at 5 μM (**Figures 3.1A and 3.1B**) whereas alsterpaullone (ALP) treatment showed the same efficacy at 1 μM (**Figure 3.1C**). Treatment with flunarizine (FZ) decreased cell proliferation at higher concentrations (50 and 100 μM) (**Figure 3.1D**).

Interestingly, the most sensitive cell line to the Group 3 medulloblastoma candidate drugs was the primary stem cell line derived from a patient with a Group 3 medulloblastoma of the cerebellum (M441). When primary normal cells (hf5281) were incubated with PL, ALP and RTL there was little reduction in cell proliferation, even at the highest concentration tested of 10 μM, thus indicating that these compounds may have selective killing properties to medulloblastoma tumor cells.

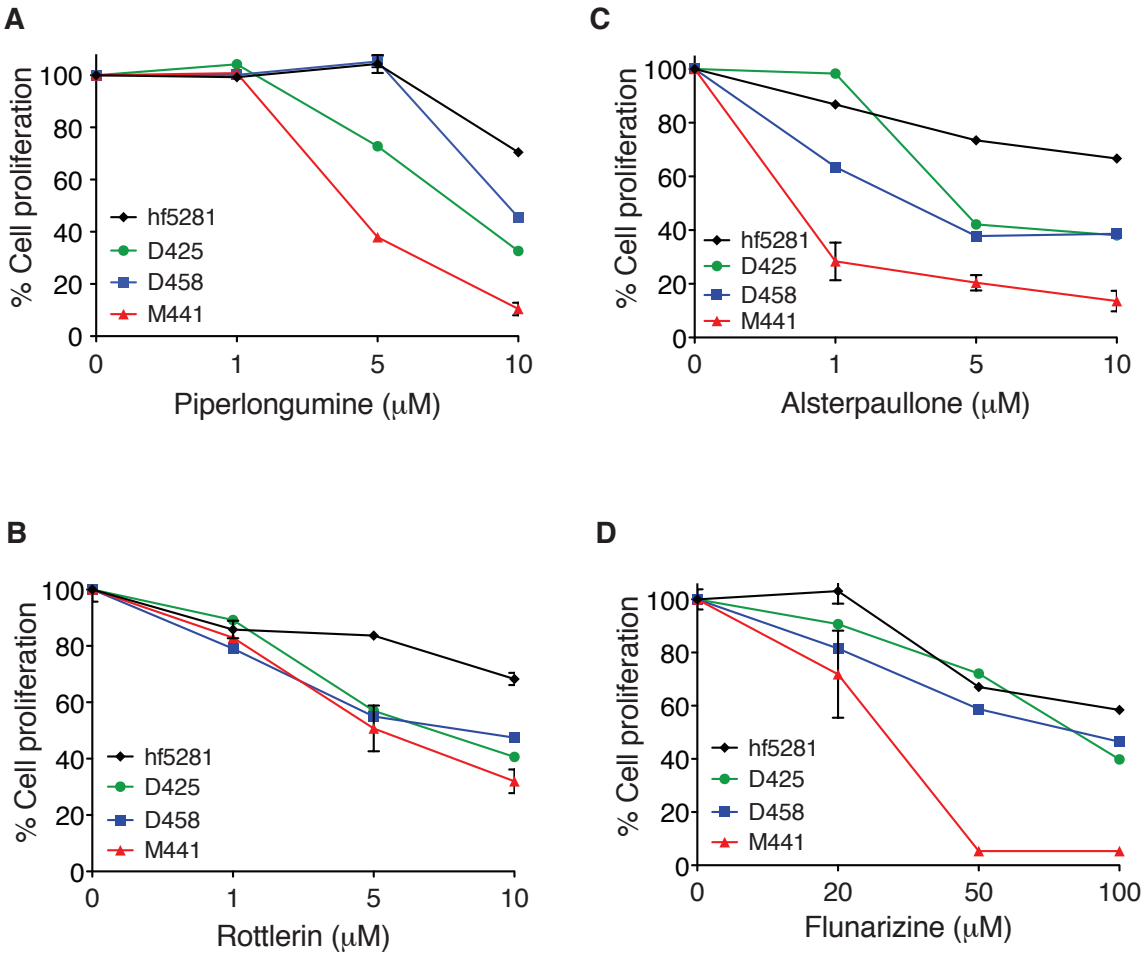

Figure 3.1: Cytotoxic effect of piperlongumine, alsterpaullone, rottlerin and flunarizine in Group 3 medulloblastoma cell lines.

Established medulloblastoma cell lines (D425 and D458), a primary medulloblastoma stem cell line (M441) and a fetal neural stem cell line (hf5281) were treated with various concentrations of (**A**) piperlongumine, (**B**) rottlerin, (**C**) alsterpaullone and (**D**) flunarizine for 48 hours. Cell viability was measured by MTS assay. Data represent mean of triplicates ± SEM.

3.3.3 *In Vivo* Antitumor Effect of Piperlongumine, Alsterpaullone and Rottlerin in Group 3 Medulloblastomas

We next investigated the efficacy of PL, ALP, RTL and FZ in established medulloblastoma xenografts representative of Group 3 medulloblastomas. D458 cells expressing luciferase were implanted in the right cerebellum of nude mice and bioluminescence imaging was performed at 6 days post inoculation. Animals with a detectable signal were treated by subcutaneous injection with PL (50 mg/kg, daily for 2 weeks), ALP (30 mg/kg, daily for 2 weeks), RTL (20 mg/kg, every other day for 2 weeks), FZ (50 mg/Kg, daily for 2 weeks) or vehicle control (10% DMSO). Marked reduction in medulloblastoma growth was observed in mice treated with PL, ALP and RTL when compared to DMSO-treated controls, as confirmed by bioluminescence imaging (**Figures 3.2A and 3.2B**) and by histological examination (H&E stain) of the brains (**Figure 3.3**). A significant increase in survival was also seen in mice treated with PL (**Figure 3.4A**; $P = 0.0011$), ALP (**Figure 3.4B**; $P = 0.0043$) and RTL (**Figure 3.4C**; $P = 0.0262$). As expected by the in vitro effects of FZ in cell proliferation, only seen at very high concentrations, this drug was not able to prolong survival of mice bearing medulloblastoma xenografts (**Figure 3.4D**).

We then tested the two most promising drugs, PL and ALP, in nude mice with D425 cerebellar xenografts and showed that both drugs significantly increase survival (**Figures 3.5A and 3.5B**; $P < 0.05$) and reduce medulloblastoma growth (**Figure 3.5C**).

Collectively, these results confirm that the C-MAP top predicted drugs for Group 3 medulloblastomas are effective in treating orthotopic mouse models of the disease.

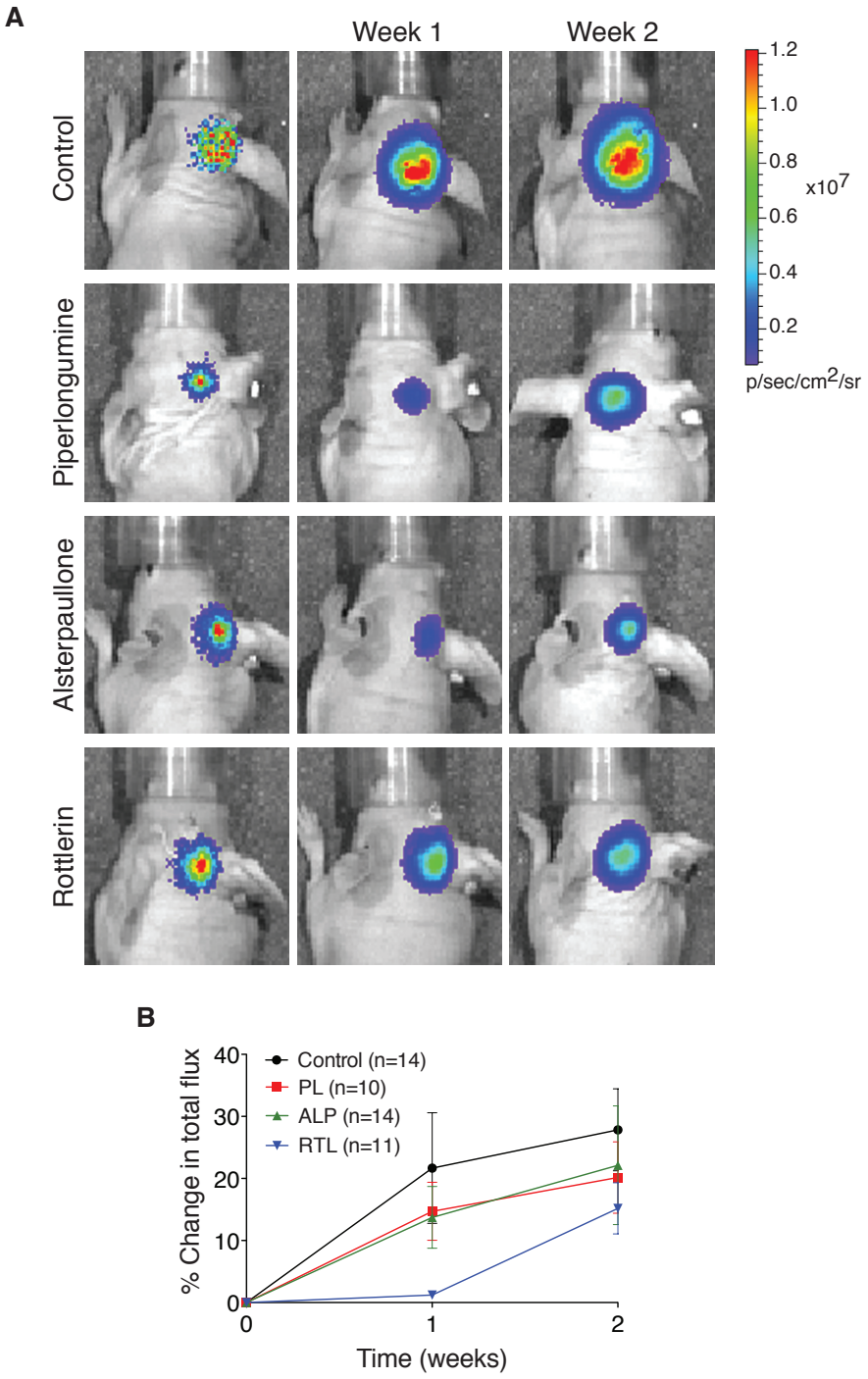

Figure 3.2: Piperlongumine, alsterpaullone, and rottlerin, reduce tumor growth in D458 medulloblastoma xenografts.

(**A**) Representative bioluminescence imaging of D458 cerebellar xenografts treated with vehicle control (10% DMSO, n = 14), piperlongumine (50 mg/kg, s.c., daily for 2 weeks; n = 10), alsterpaullone (30 mg/kg, s.c., daily for 2 weeks; n = 14) and rottlerin (20 mg/kg, s.c., every other day for 2 weeks; n = 11). (**B**) Connectivity Map predicted drugs reduce medulloblastoma growth as denoted by a smaller change in total photon flux. Data represent group means ± SEM.

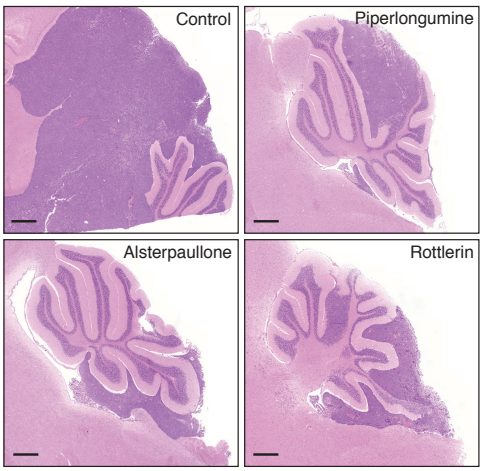

Figure 3.3: Representative H&E staining of D458 medulloblastomas treated with piperlongumine, alsterpaullone and rottlerin.

Representative H&E staining demonstrates that mice bearing D458 tumors treated with piperlongumine, alsterpaullone and rottlerin have smaller medulloblastomas in the cerebellum. Scale bar: 500 µm.

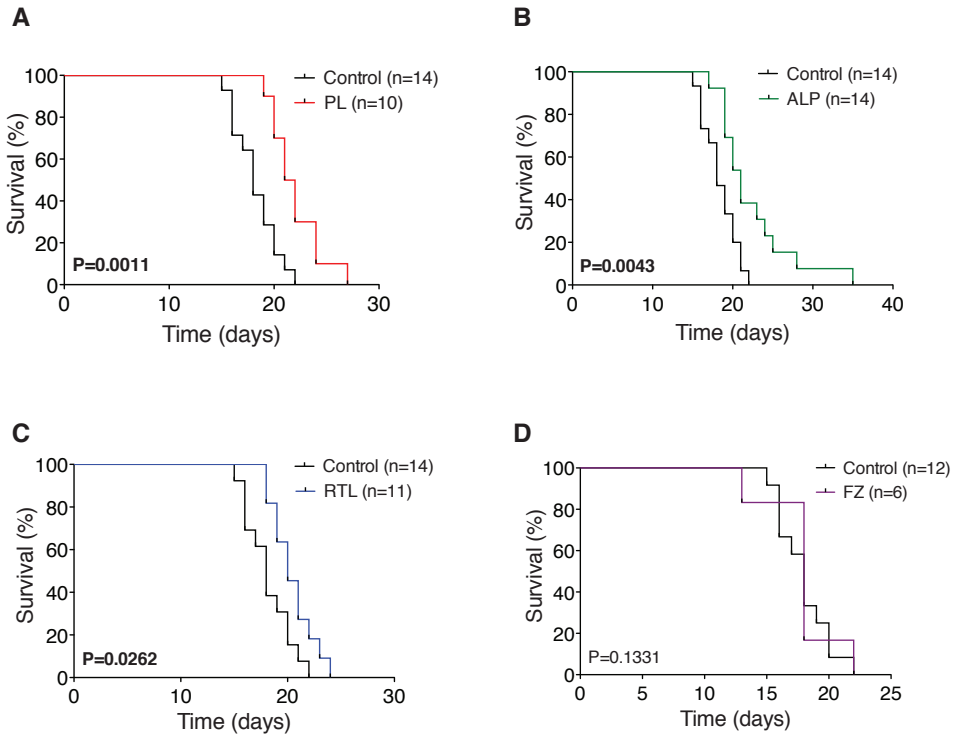

Figure 3.4: Survival of D458 intracranial xenografts treated with piperlongumine, alsterpaullone, rottlerin and flunarizine.

(**A – D**) Kaplan-Meier survival curves demonstrate that mice harboring orthotopic D458 medulloblastoma xenografts have an increased survival after treatment with piperlongumine (PL; P = 0.0011), alsterpaullone (ALP; P = 0.0043) and rottlerin (RTL; P = 0.0262). Survival differences were calculated using a log-rank test.

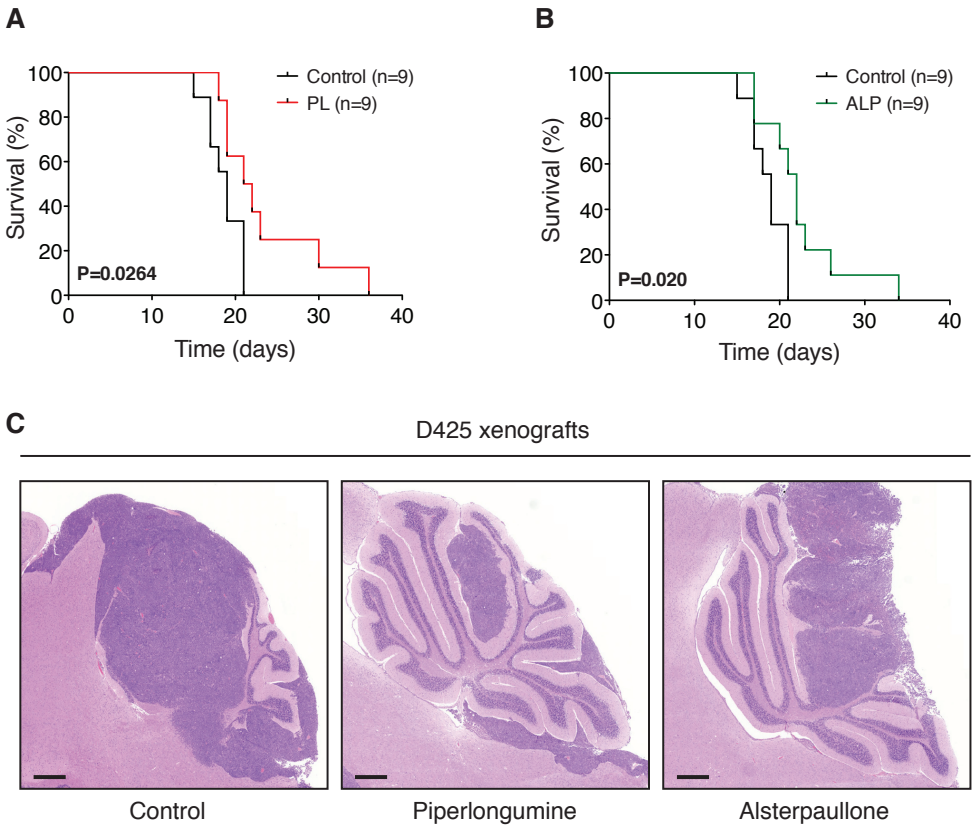

Figure 3.5: Piperlongumine and alsterpaullone increase survival of D425 medulloblastoma xenografts.

Kaplan-Meier estimate displays survival of nude mice with D425 cerebellar xenografts treated with (**A**) piperlongumine (PL) or (**B**) alsterpaullone (ALP). Survival differences were calculated using a log-rank test. (**C**) Representative H&E staining demonstrates reduction in medulloblastoma growth after treatment with PL and ALP, when compared to the control group. Scale bar: 500 μm.

3.3.4 Alsterpaullone Shows *In Vitro* and *In Vivo* Specificity for Group 3 Primary Medulloblastoma Stem Cells

To determine the mechanisms by which PL and ALP exert their antitumor effect, we treated D425, D458 and M441 medulloblastoma cells with both drugs for 48h and assessed apoptosis and AKT pathway inhibition. Western blot analysis showed that ALP induced apoptosis (**Figure 3.6A**) and potently inhibited AKT pathway activation (**Figure 3.6B**) at lower concentrations than PL.

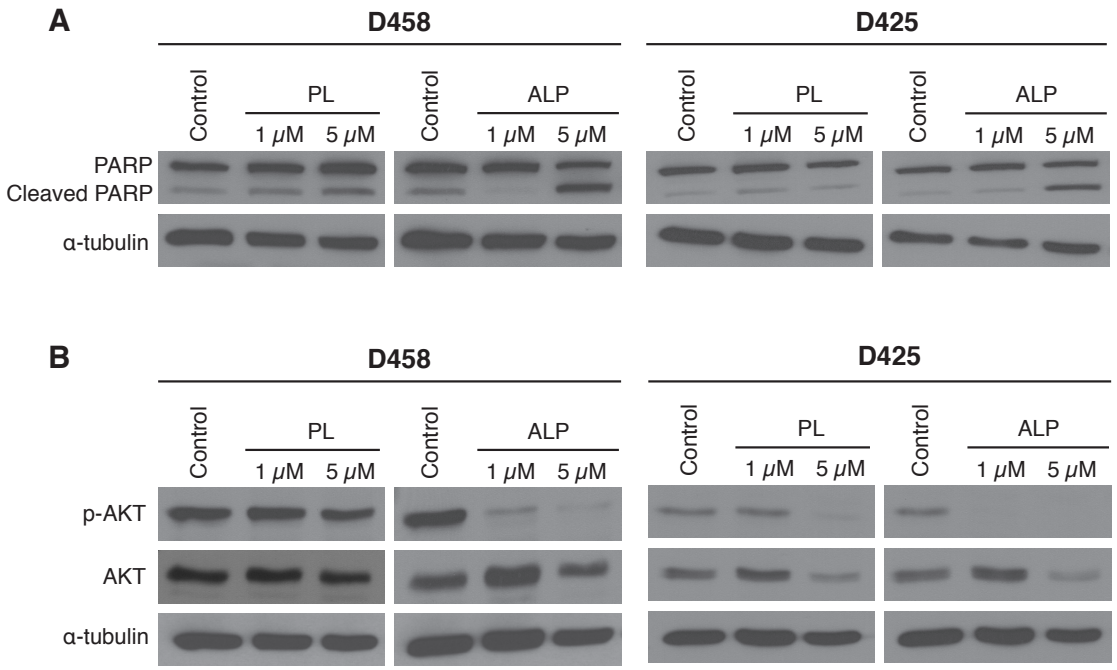

Figure 3.6: Piperlongumine and alsterpaullone induce apoptosis and inhibit AKT pathway activation.
Representative Western blots demonstrating (**A**) induction of apoptosis and (**B**) AKT pathway inhibition after piperlongumine (PL) and alsterpaullone (ALP) treatment for 48h in D458 and D425 medulloblastoma cells.

Interestingly, the patient derived medulloblastoma stem cell line was particularly sensitive to the *in vitro* effect of the Group 3 specific drug, ALP (**Figures 3.7A – 3.7C**). Furthermore, M441 cerebellar xenografts treated with PL did not show a survival advantage when compared to the control group (**Figure 3.8A**) whereas treatment with ALP significantly increased survival and decreased medulloblastoma tumor growth (**Figures 3.8B and 3.8C**).

These results validate the subgroup specific C-MAP predictions and identify ALP as an effective therapy for Group 3 medulloblastoma.

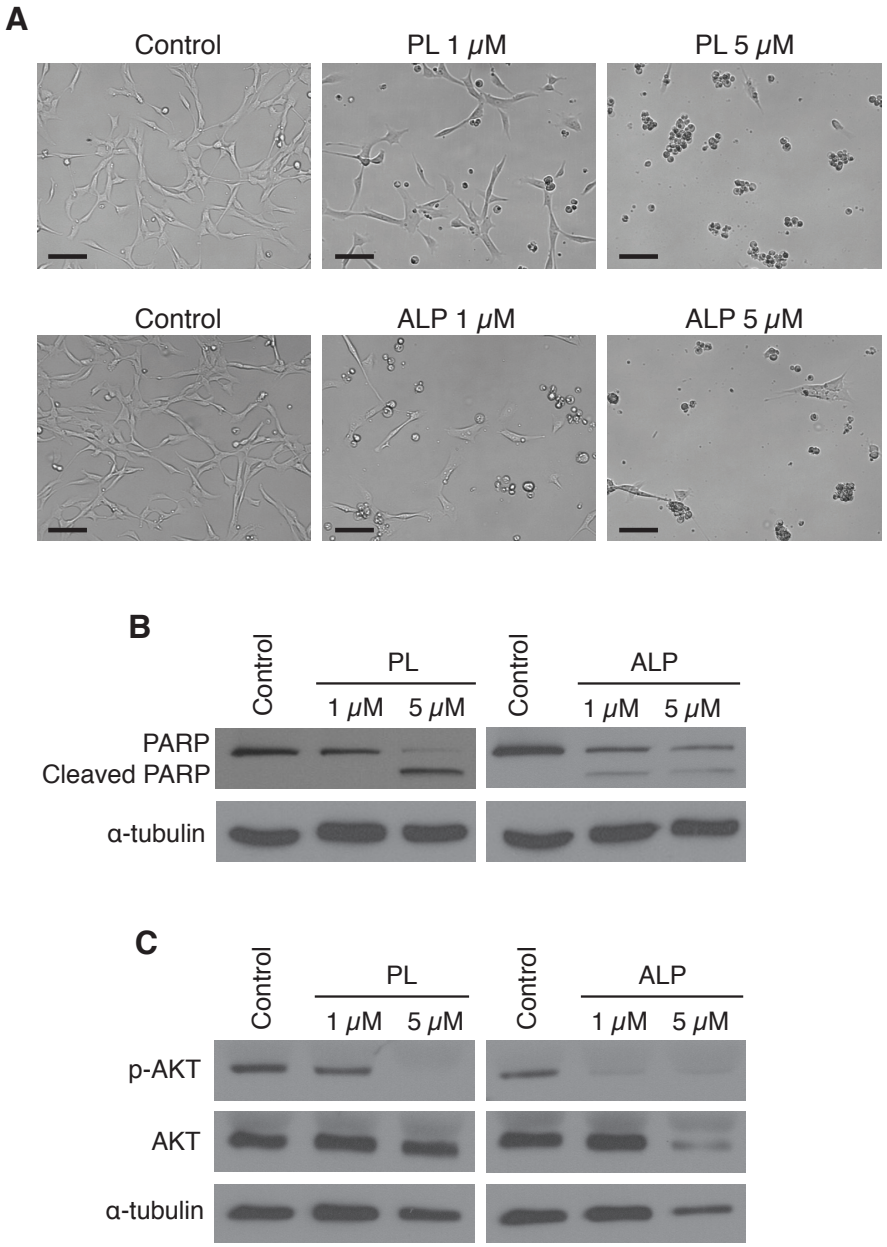

Figure 3.7: *In vitro* efficacy of alsterpaullone targeting medulloblastoma stem cells derived from a patient with a Group 3 medulloblastoma.

(**A**) Primary medulloblastoma stem cells (M441) are more sensitive to the cytotoxic effects of alsterpaullone (ALP) than of piperlongumine (PL). Scale bar: 50 μm. (**B**) Representative Western blots demonstrate induction of apoptosis in M441 cells after PL treatment (at 5 μM) and ALP treatment (at 1 μM). (**C**) ALP potently inhibits AKT pathway activation in Group 3 derived medulloblastoma stem cells.

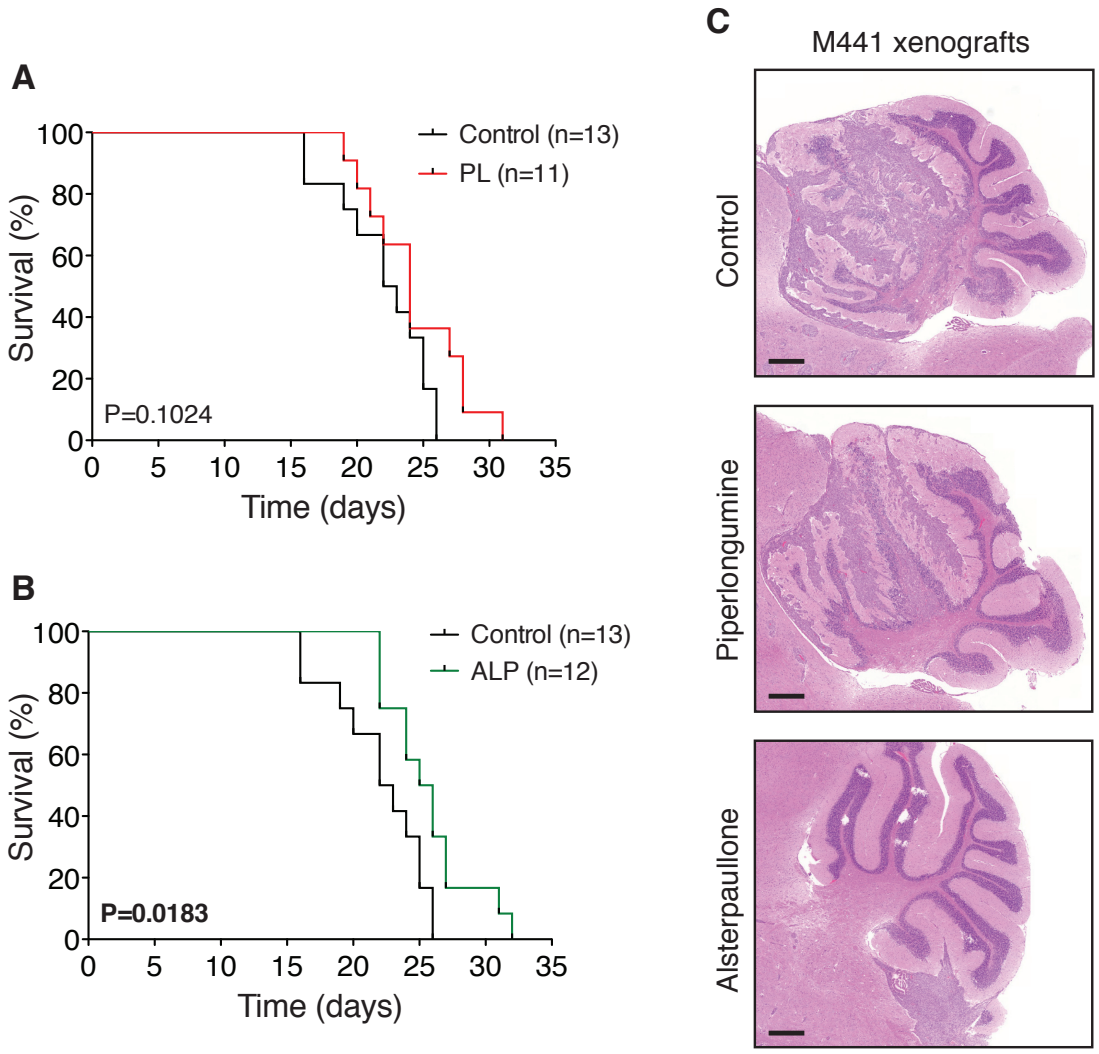

Figure 3.8: *In vivo* efficacy of alsterpaullone treating mice with primary cerebellar xenografts.

(**A and B**) Kaplan-Meier survival curves demonstrate the subgroup-specific efficacy of alsterpaullone (ALP) increasing survival of mice with M441 cerebellar xenografts. Survival differences were calculated using a log-rank test. (**C**) Representative H&E staining of mouse cerebellar xenografts in the control group, the piperlongumine (PL) treated group and the ALP treated group. Scale bar: 500 µm.

3.3.5 Alsterpaullone Inhibits *MYC* and other Cell Cycle Related Genes

To identify downstream transcriptional events induced by ALP, we performed the genomic profiling of Group 3 medulloblastoma cell lines (D425 and D458), after treatment for 48 hours. When compared to DMSO treated medulloblastoma cells, ALP treated cells showed down-regulation of genes involved in cell cycle, including *MYC* (**Figure 3.9A**). GSEA was performed with gene sets compiled from the NCI, GO, KEGG, PFAM and Biocarta pathway databases. To visualize significant gene sets (FDR < 0.05; P < 0.01) as interaction networks Cytoscape and Enrichment Map were used. The top-scoring gene sets down-regulated by ALP were mainly cell cycle-related transcriptional signatures (**Figures 3.9B and 3.9C**). In addition, ALP also inhibits several cancer-related networks (namely mTOR signaling, PTEN signaling, RAS signaling, Aurora kinase signaling, insulin signaling) and other biological processes including RNA processing, transport and splicing, DNA repair, chromatin organization and histone modifications, carbon metabolism and phosphatase activity (**Figure 3.10**). Gene sets up-regulated by ALP involve the inflammatory response (TNF signaling, MHC antigen presentation) and tissue regeneration (wound response and coagulation cascade, tissue morphogenesis, muscle contraction), as well as olfactory signaling, STAT signaling, alkene metabolism, lipid transport and neuropeptide receptor activity (**Figure 3.10**).

Interestingly, when we queried the C-MAP database using the gene expression profiling of D425 and D458 medulloblastoma cells after treatment with ALP and PL, we found that only ALP was able to significantly reverse gene expression as determined by the high positive enrichment score (0.995) and low p-value (P < 0.000001) (**Figures 3.11 and 3.12**).

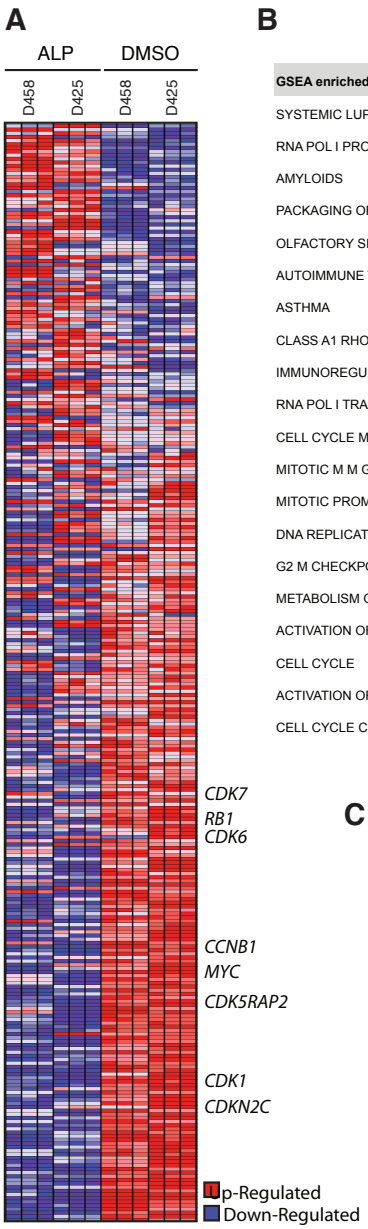

B

GSEA enriched pathway	Direction	Rank	FDR-corrected (q-value)
SYSTEMIC LUPUS ERYTHEMATOSUS	Up-Regulated	1	1.00E-06
RNA POL I PROMOTER OPENING	Up-Regulated	2	1.00E-06
AMYLOIDS	Up-Regulated	3	1.00E-06
PACKAGING OF TELOMERE ENDS	Up-Regulated	4	1.00E-06
OLFACTORY SIGNALING PATHWAY	Up-Regulated	5	4.80E-04
AUTOIMMUNE THYROID DISEASE	Up-Regulated	6	4.00E-04
ASTHMA	Up-Regulated	7	3.43E-04
CLASS A1 RHODOPSIN LIKE RECEPTORS	Up-Regulated	8	0.001080874
IMMUNOREGULATORY INTERACTIONS BETWEEN A LYMPHOID AND A NON LYMPHOID CELL	Up-Regulated	9	0.001415851
RNA POL I TRANSCRIPTION	Up-Regulated	10	0.001674173
CELL CYCLE MITOTIC	Down-Regulated	1	1.00E-06
MITOTIC M M G1 PHASES	Down-Regulated	2	1.00E-06
MITOTIC PROMETAPHASE	Down-Regulated	3	1.00E-06
DNA REPLICATION	Down-Regulated	4	1.00E-06
G2 M CHECKPOINTS	Down-Regulated	5	1.00E-06
METABOLISM OF NON CODING RNA	Down-Regulated	6	1.00E-06
ACTIVATION OF THE PRE REPLICATIVE COMPLEX	Down-Regulated	7	1.00E-06
CELL CYCLE	Down-Regulated	8	1.00E-06
ACTIVATION OF ATR IN RESPONSE TO REPLICATION STRESS	Down-Regulated	9	1.00E-06
CELL CYCLE CHECKPOINTS	Down-Regulated	10	1.00E-06

C

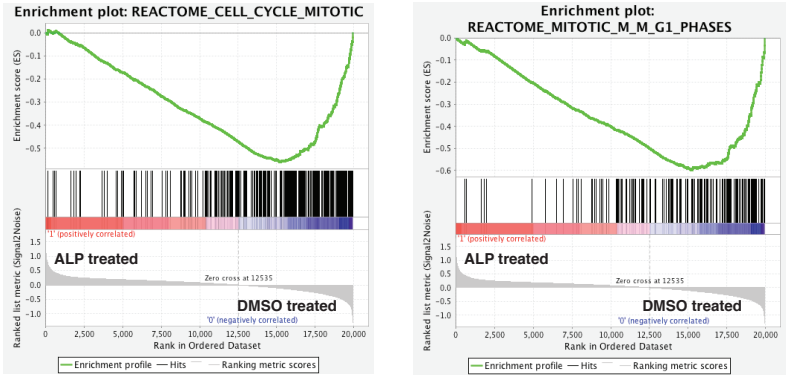

Figure 3.9: Genomic profiling of Group 3 medulloblastoma cell lines treated with alsterpaullone demonstrates down-regulation of cell cycle related genes, including *MYC*.
(**A**) Heatmap illustrating the genes up and down-regulated following treatment with alsterpaullone (ALP) in two Group 3 medulloblastoma cell lines. *MYC* and other genes involved in cell cycle are down-regulated by ALP. (**B**) Table of the top 10 gene sets up-regulated or down-regulated by ALP. (**C**) Enrichment plots showing inhibition of cell cycle related gene sets.

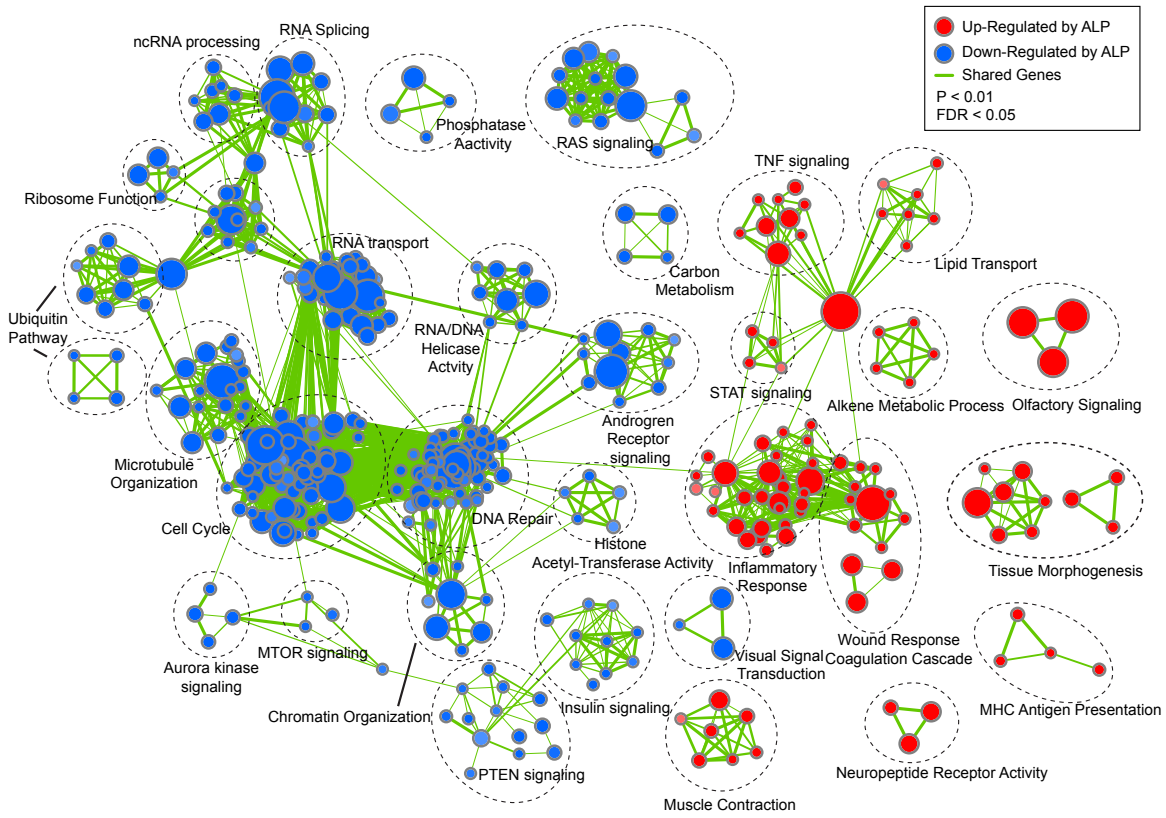

Figure 3. 10: Biological pathways and processes up- and down-regulated by alsterpaullone. Gene Set Enrichment Analysis (GSEA) comparing gene sets up- and down-regulated by alsterpaullone (ALP) in D458 and D425 medulloblastoma cells (FDR < 0.05; P< 0.01). Cytoscape and Enrichment Map were used for visualization of the GSEA results. The enriched gene sets were grouped by their similarity, represented as nodes, and mapped as a network. The size of each node determines the total number of genes within each gene set.

A

cmap name	mean	n	enrichment	p-value	specificity	% non-null
alsterpaullone	0.853	3	0.995	< 0.000001	0.0116	100

rank	batch	cmap name	dose	cell	score	up	down	instance_id
4	1066	alsterpaullone	10 µM	MCF7	.934	.248	-.366	7051
9	1067	alsterpaullone	10 µM	PC3	.904	.208	-.385	7056
31	1073	alsterpaullone	10 µM	PC3	.720	.146	-.327	7078

B

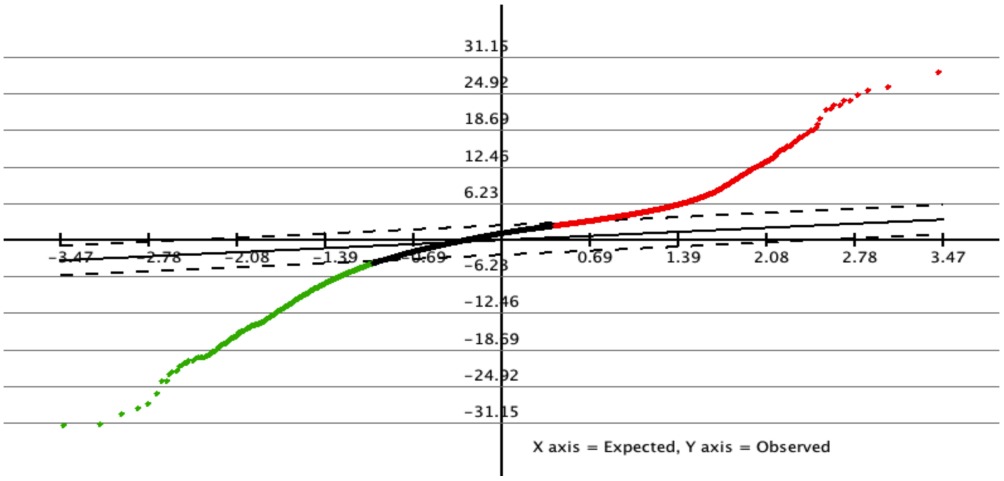

Figure 3.11: Alsterpaullone reverses Group 3 medulloblastoma gene expression signature. Alsterpaullone is highly ranked as a compound with the ability to reverse the gene expression profile of Group 3 medulloblastoma cell lines as shown by (a) the C-MAP analysis and (b) the Significance Analysis of Microarrays (SAM) plot.

A

cmap name	mean	n	enrichment	p-value	specificity	% non-null
piperlongumine	-0.061	2	-0.474	0.59627	0.7342	50

rank	batch	cmap name		dose	cell	score	up	down	instance_id
614	641	piperlongumine		13 µM	HL60	.499	.067	-.095	1764
5943	662	piperlongumine		13 µM	MCF7	-.621	-.128	.130	2757

B

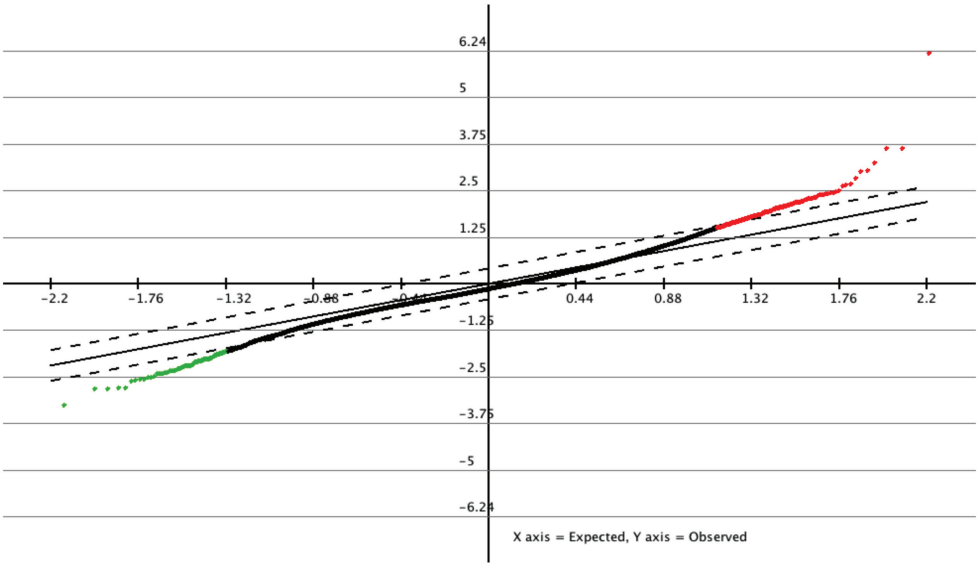

Figure 3.12: The gene expression profile of Group 3 medulloblastomas is not affected by piperlongumine.

(A and B) The gene expression profile of Group 3 medulloblastoma cell lines is not affected by piperlongumine treatment as determined by (a) the C-MAP analysis and (b) the Significance Analysis of Microarrays (SAM) plot.

3.4 Discussion

We have used an *in silico* gene expression-based screening for drug discovery in medulloblastoma. Our approach, called the Connectivity Map (C-MAP), identified the CDK inhibitor ALP as a compound with the ability to reverse the gene expression signature of Group 3 medulloblastomas and, therefore, with potential specific antitumor effect. We validated the C-MAP hypothesis by demonstrating the efficacy of ALP both in *in vitro* and *in vivo* models of Group 3 medulloblastoma. Our study provides evidence for the use of chemical genomics to identify modulators of biological processes that drive the medulloblastoma subgroups.

The C-MAP analysis, using the gene expression signatures of the four molecular subgroups of medulloblastoma, led to interesting observations. The drugs predicted for the WNT subgroup were distinct from the other subgroups. Strikingly, methylprednisolone (a steroid known to have a beneficial effect in brain tumors) and four chemotherapeutic agents currently in use for medulloblastoma treatment (etoposide, methotrexate, semustine and lomustine) were only listed in the WNT subgroup, which has the best response to treatment and the best outcome. On the other hand, PL was the top ranked compound for non-WNT medulloblastomas suggesting the ability of this compound to reverse common biological processes in these tumors. The predictions for Group 3 and Group 4 medulloblastomas included several shared compounds, in agreement with the genetic similarity between the two subgroups. Doxorubicin, a well-known chemotherapeutic agent but not used to treat medulloblastoma, was identified has a drug with potential efficacy for both Group 3 and Group 4 tumors.

The top ranked compound with predicted specificity for Group 3 medulloblastoma was ALP, a potent inhibitor of CDK1/cyclin B and CDK 5. The cell-cycle kinases play an important role in normal development and their deregulation is associated with aberrant division and uncontrolled proliferation in various cancers[216,217]. In cerebellar development, cyclins D1 and D2 play a crucial role in the postnatal expansion of the granule neuron precursors in the EGL. As these cells exit the cell cycle and begin to differentiate, they migrate inwards through the Purkinje cell layer to form the IGL of the adult cerebellum[6,218]. The SHH pathway regulates the GNPs proliferation inducing the expression of the transcription factor GLI1, which up-regulates the expression of cyclin D1 and cyclin D2, via N-MYC[219,220]. Removal of both cyclins D1 and D2 in animal models results in severe cerebellar hypoplasia due to decreased proliferation and increased apoptosis of GNPs[221]. In

Ptch$^{+/-}$ mice, known to develop spontaneous cerebellar medulloblastomas, loss of cyclin D1 (*Ptch*$^{+/-}$*;Ccnd1*$^{-/-}$) significantly reduces the incidence of tumors[222]. On the other hand, loss of CDK inhibitors, *Ink4c* or *Ink4d*, triggers medulloblastoma formation in p53-null mice[223]. A recent study has shown that CDK5 is also required for the normal development of the cerebellum. Cdk5 conditional knockout mice display a smaller cerebellum and a profound disturbance in migration of granule cells[224].

Members of the Cyclin/CDK complex are frequently amplified or up-regulated in human medulloblastoma. Li *et al.* described amplifications of the *CDK4*, *CDK6*, *CCND1* (or cyclin D1) and *CCND2* (or cyclin D2) genes in primary medulloblastomas[225], raising the possibility of using CDK inhibition to suppress medulloblastoma formation. Interestingly, it has been shown in mouse models of lymphoma and hepatoblastoma that MYC sensitizes tumor cells to undergo apoptosis in response to CDK1 inhibition, through a mechanism independent of *p53* status[226]. Due to the limited success in developing small molecule inhibitors of MYC, targeting important cellular processes, such as the cell cycle, may prove to be a suitable therapeutic strategy in MYC-dependent tumors, including Group 3 medulloblastomas.

Previous studies have shown the antitumor effects of ALP through induction of apoptosis in breast cancer and leukemia cells[227-229]. We report for the first time the cytotoxic effects of ALP in medulloblastoma. ALP effectively decreased cell proliferation and induced apoptosis through AKT pathway blockade. In mouse xenografts of Group 3 medulloblastoma, treatment with ALP significantly reduced tumor growth and improved survival. As for the other top candidate for non-WNT tumors, PL, it showed *in vitro* efficacy for higher drug concentrations than ALP and it failed to improve survival of primary medulloblastoma xenografts. These experimental results confirm the C-MAP hypothesis pointing ALP as a Group 3-specific drug. In fact, we demonstrate that ALP down-regulates several cell cycle related genes, including *MYC*, and, unlike PL, treatment with ALP reverses the gene expression profile of Group 3 medulloblastoma cell lines. Our chemical genomics study provides strong rationale for advancing alsterpaullone as a targeted therapy in Group 3 medulloblastoma.

Chapter 4
Concluding Remarks and Future Directions

For a neurosurgeon, the complete resection of a brain tumor is an extremely rewarding experience and we tend to believe that such a successful operation will cure the patient. That is true for many cases but not all, particularly the malignant neoplasms. This simultaneously intriguing and disappointing observation highlights the need to better understand the biology of brain tumors for improving patient management.

I have decided to study medulloblastoma, the commonest malignant pediatric brain tumor, and a cause of severe neurological disabilities in children, secondary to therapy. An ever-increasing amount of genomic data on medulloblastoma is being generated in laboratories around the world using high-throughput technologies. Converting the data contained in the gene signatures of medulloblastoma into therapeutic approaches remains challenging but it is critically needed to improve the survival and quality of life of children with medulloblastoma.

The main goal of my research project was to use genomic data for drug discovery in medulloblastoma. I started with a simple approach using a therapeutic target known to be relevant in medulloblastoma. Our studies identified cMET as a hallmark of SHH medulloblastomas and demonstrated a significant correlation of high cMET expression with increased tumor relapse and poor survival. Therefore, cMET can be used as a clinical biomarker to identify patients who may benefit from anti-cMET therapies. Foretinib, an FDA approved inhibitor of cMET with the ability to cross the blood-brain barrier, was highly effective in preclinical models of SHH medulloblastoma. Strikingly, foretinib reduced the number of metastasis and increased survival in an aggressive transgenic mouse model of metastatic SHH medulloblastoma.

The results from this study provide strong evidence to advance foretinib into clinical trials for SHH medulloblastomas. However, there are interesting questions to be followed in the future. First, the mechanisms of cMET up-regulation remain unclear, since the genomic analysis performed in large cohorts of medulloblastoma samples failed to demonstrate recurrent mutations or amplifications of the *cMET* gene. Previous findings that the cMET inhibitor, *SPINT2*, is silenced by promoter methylation in primary medulloblastomas suggest a role for epigenetics in cMET regulation. Second, the high expression of cMET in SHH-

driven medulloblastomas raises the important question whether a combined therapy with foretinib and a SMO inhibitor would offer a survival benefit and overcome drug resistance.

Group 3 medulloblastomas are *MYC*-driven tumors associated with a very poor prognosis. Since MYC direct targeting hasn't been successfully achieved, an alternative approach is to identify compounds that inhibit important cellular processes. We have used the C-MAP, a gene expression-based computational drug screen, to identify small molecules with predicted ability to reverse the gene expression signature of Group 3 medulloblastomas. Our study identified 15 compounds with high likelihood of efficacy against this subgroup of medulloblastoma. The top-ranked drug was ALP, a CDK inhibitor. Subsequent validation of these findings confirmed that ALP is highly effective and specific both in *in vitro* and *in vivo* models of Group 3 medulloblastomas. Interestingly, the chemical genomic profiling of ALP confirms inhibition of MYC-associated transcriptional activity and reveals enrichment of cell cycle signatures.

The clinical aggressiveness of Group 3 medulloblastomas anticipates that the design of novel therapeutic regimens will need to include a combination of drugs. An open question from our study is whether ALP, as a cell cycle modulator, could sensitize medulloblastoma cells to standard chemotherapy and radiation. The combination of ALP with chromatin modifiers such as the histone deacetylase inhibitors (HDAC), represents another important therapeutic avenue for future studies, since the deregulation of chromatin-associated genes has been recently identified in Group 3 medulloblastomas[192,199-201,230].

In summary, the results from my research led to the following original conclusions, which can be immediately translated into the clinic:

1. cMET is a molecular biomarker of the SHH subgroup of medulloblastomas and can identify a subset of patients who may benefit from cMET targeted therapies. cMET and p-cMET can be easily detected by immunohistochemistry in any pathology lab.
2. Foretinib is a potent cMET inhibitor, FDA approved, that crosses the blood-brain barrier. Our preclinical studies indicate that this drug is a good candidate to be included in clinical trials as targeted therapy in SHH medulloblastoma.
3. We describe a methodology using mass spectrometry to sistematically identify and quantify small molecule inhibitors in the central nervous system, a key approach in neuro-oncology.

4. The preclinical studies with Alsterpaullone indicate this drug is a good candidate for Group 3 medulloblastomas and suggest it can be readily advanced into clinical trials, either alone or in combination with conventional therapies.

***

I will conclude with some brief more personal remarks.

The three years spent in Toronto set the stage for a greater challenge: to create a Brain Tumor Research Centre in Portugal. The first steps were successfully taken with the establishment of a Brain Tumor Bank at the Biobank of Instituto de Medicina Molecular (Biobanco-IMM). In just over two years we have collected more than 300 brain tumor samples with matched blood, plasma and detailed clinical information. While most samples come from patients treated at the Department of Neurosurgery at Hospital de Santa Maria, we have gradually been collecting samples from other hospitals in Lisbon and across the country. We can proudly say that we have the largest clinically annotated collection of brain tumors in Portugal comprising over 1,000 biological samples. Furthermore, we have implemented at Biobanco-IMM the primary stem cell culture of brain tumors and metastasis. My vision for this project is to foster brain tumor research and to be part of major discoveries in the field through teamwork and collaboration. In keeping with this goal I have already established national and international collaborations, such as the participation in the medulloblastoma international consortium, MAGIC. Recently, an award from Fundação Millennium bcp allowed the project to spread its wings promoting both neurosurgical care and brain tumor research to help children in Africa, namely in Portuguese speaking countries like Angola and Mozambique. Through a cooperation protocol between IMM, Hospital de Santa Maria and the Ministry of Health of those African countries, we aim to provide education and surgical training to local neurosurgeons and to help them establishing a brain tumor bank.

I am looking forward for the busy and exciting years ahead.

References

1. Crawford, J.R., MacDonald, T.J. & Packer, R.J. Medulloblastoma in childhood: new biological advances. *Lancet Neurol* **6**, 1073-1085 (2007).

2. Kaatsch, P., Rickert, C.H., Kuhl, J., Schuz, J. & Michaelis, J. Population-based epidemiologic data on brain tumors in German children. *Cancer* **92**, 3155-3164 (2001).

3. Alston, R.D.*, et al.* Childhood medulloblastoma in northwest England 1954 to 1997: incidence and survival. *Dev Med Child Neurol* **45**, 308-314 (2003).

4. Giordana, M.T., Schiffer, P., Lanotte, M., Girardi, P. & Chio, A. Epidemiology of adult medulloblastoma. *Int J Cancer* **80**, 689-692 (1999).

5. Armstrong, G.T.*, et al.* Long-term outcomes among adult survivors of childhood central nervous system malignancies in the Childhood Cancer Survivor Study. *J Natl Cancer Inst* **101**, 946-958 (2009).

6. Roussel, M.F. & Hatten, M.E. Cerebellum development and medulloblastoma. *Curr Top Dev Biol* **94**, 235-282 (2011).

7. Hatten, M.E. & Roussel, M.F. Development and cancer of the cerebellum. *Trends Neurosci* **34**, 134-142 (2011).

8. Louis, D.N.*, et al.* The 2007 WHO classification of tumours of the central nervous system. *Acta Neuropathol* **114**, 97-109 (2007).

9. Gilbertson, R.J. & Ellison, D.W. The origins of medulloblastoma subtypes. *Annu Rev Pathol* **3**, 341-365 (2008).

10. Taylor, M.D.*, et al.* Familial posterior fossa brain tumors of infancy secondary to germline mutation of the hSNF5 gene. *Am J Hum Genet* **66**, 1403-1406 (2000).

11. Taylor, M.D.*, et al.* Mutations in SUFU predispose to medulloblastoma. *Nat Genet* **31**, 306-310 (2002).

12. Taylor, M.D., Mainprize, T.G. & Rutka, J.T. Molecular insight into medulloblastoma and central nervous system primitive neuroectodermal tumor biology from hereditary syndromes: a review. *Neurosurgery* **47**, 888-901 (2000).

13. Taylor, M.D.*, et al.* Molecular subgroups of medulloblastoma: the current consensus. *Acta Neuropathol* **123**, 465-472 (2012).

14. Northcott, P.A., Korshunov, A., Pfister, S.M. & Taylor, M.D. The clinical implications of medulloblastoma subgroups. *Nat Rev Neurol* **8**, 340-351 (2012).

15. Remke, M.*, et al.* Adult medulloblastoma comprises three major molecular variants. *J Clin Oncol* **29**, 2717-2723 (2011).

16. Northcott, P.A., *et al.* Medulloblastoma comprises four distinct molecular variants. *J Clin Oncol* **29**, 1408-1414 (2011).

17. Clifford, S.C., *et al.* Wnt/Wingless pathway activation and chromosome 6 loss characterize a distinct molecular sub-group of medulloblastomas associated with a favorable prognosis. *Cell Cycle* **5**, 2666-2670 (2006).

18. Northcott, P.A., *et al.* Medulloblastomics: the end of the beginning. *Nat Rev Cancer* **12**, 818-834 (2012).

19. Pfaff, E., *et al.* TP53 mutation is frequently associated with CTNNB1 mutation or MYCN amplification and is compatible with long-term survival in medulloblastoma. *J Clin Oncol* **28**, 5188-5196 (2010).

20. Kool, M., *et al.* Molecular subgroups of medulloblastoma: an international meta-analysis of transcriptome, genetic aberrations, and clinical data of WNT, SHH, Group 3, and Group 4 medulloblastomas. *Acta Neuropathol* **123**, 473-484 (2012).

21. Gibson, P., *et al.* Subtypes of medulloblastoma have distinct developmental origins. *Nature* **468**, 1095-1099 (2010).

22. Northcott, P.A., *et al.* Pediatric and adult sonic hedgehog medulloblastomas are clinically and molecularly distinct. *Acta Neuropathol* **122**, 231-240 (2011).

23. Northcott, P.A., *et al.* Subgroup-specific structural variation across 1,000 medulloblastoma genomes. *Nature* **488**, 49-56 (2012).

24. Thompson, M.C., *et al.* Genomics identifies medulloblastoma subgroups that are enriched for specific genetic alterations. *J Clin Oncol* **24**, 1924-1931 (2006).

25. Ellison, D.W., *et al.* Medulloblastoma: clinicopathological correlates of SHH, WNT, and non-SHH/WNT molecular subgroups. *Acta Neuropathol* **121**, 381-396 (2011).

26. Al-Halabi, H., *et al.* Preponderance of sonic hedgehog pathway activation characterizes adult medulloblastoma. *Acta Neuropathol* **121**, 229-239 (2011).

27. Schuller, U., *et al.* Acquisition of granule neuron precursor identity is a critical determinant of progenitor cell competence to form Shh-induced medulloblastoma. *Cancer Cell* **14**, 123-134 (2008).

28. Grammel, D., *et al.* Sonic hedgehog-associated medulloblastoma arising from the cochlear nuclei of the brainstem. *Acta Neuropathol* **123**, 601-614 (2012).

29. Yang, Z.J., *et al.* Medulloblastoma can be initiated by deletion of Patched in lineage-restricted progenitors or stem cells. *Cancer Cell* **14**, 135-145 (2008).

30. Guan, Y., *et al.* Amplification of PVT1 contributes to the pathophysiology of ovarian and breast cancer. *Clin Cancer Res* **13**, 5745-5755 (2007).

31. Pei, Y., *et al.* An animal model of MYC-driven medulloblastoma. *Cancer Cell* **21**, 155-167 (2012).

32. Kawauchi, D.*, et al.* A mouse model of the most aggressive subgroup of human medulloblastoma. *Cancer Cell* **21**, 168-180 (2012).

33. Remke, M.*, et al.* FSTL5 is a marker of poor prognosis in non-WNT/non-SHH medulloblastoma. *J Clin Oncol* **29**, 3852-3861 (2011).

34. Kongkham, P.N.*, et al.* An epigenetic genome-wide screen identifies SPINT2 as a novel tumor suppressor gene in pediatric medulloblastoma. *Cancer Res* **68**, 9945-9953 (2008).

35. Birchmeier, C. & Gherardi, E. Developmental roles of HGF/SF and its receptor, the c-Met tyrosine kinase. *Trends Cell Biol* **8**, 404-410 (1998).

36. Huh, C.G.*, et al.* Hepatocyte growth factor/c-met signaling pathway is required for efficient liver regeneration and repair. *Proc Natl Acad Sci U S A* **101**, 4477-4482 (2004).

37. Chmielowiec, J.*, et al.* c-Met is essential for wound healing in the skin. *J Cell Biol* **177**, 151-162 (2007).

38. Trusolino, L., Bertotti, A. & Comoglio, P.M. MET signalling: principles and functions in development, organ regeneration and cancer. *Nat Rev Mol Cell Biol* **11**, 834-848 (2010).

39. Miyazawa, K.*, et al.* Molecular cloning and sequence analysis of the cDNA for a human serine protease reponsible for activation of hepatocyte growth factor. Structural similarity of the protease precursor to blood coagulation factor XII. *J Biol Chem* **268**, 10024-10028 (1993).

40. Kawaguchi, T.*, et al.* Purification and cloning of hepatocyte growth factor activator inhibitor type 2, a Kunitz-type serine protease inhibitor. *J Biol Chem* **272**, 27558-27564 (1997).

41. Shimomura, T.*, et al.* Hepatocyte growth factor activator inhibitor, a novel Kunitz-type serine protease inhibitor. *J Biol Chem* **272**, 6370-6376 (1997).

42. Birchmeier, C., Birchmeier, W., Gherardi, E. & Vande Woude, G.F. Met, metastasis, motility and more. *Nat Rev Mol Cell Biol* **4**, 915-925 (2003).

43. Zhang, Y.W., Wang, L.M., Jove, R. & Vande Woude, G.F. Requirement of Stat3 signaling for HGF/SF-Met mediated tumorigenesis. *Oncogene* **21**, 217-226 (2002).

44. Guo, A.*, et al.* Signaling networks assembled by oncogenic EGFR and c-Met. *Proc Natl Acad Sci U S A* **105**, 692-697 (2008).

45. Bertotti, A., Comoglio, P.M. & Trusolino, L. Beta4 integrin activates a Shp2-Src signaling pathway that sustains HGF-induced anchorage-independent growth. *J Cell Biol* **175**, 993-1003 (2006).

46. Orian-Rousseau, V., Chen, L., Sleeman, J.P., Herrlich, P. & Ponta, H. CD44 is required for two consecutive steps in HGF/c-Met signaling. *Genes Dev* **16**, 3074-3086 (2002).

47. Lai, A.Z., Abella, J.V. & Park, M. Crosstalk in Met receptor oncogenesis. *Trends Cell Biol* **19**, 542-551 (2009).

48. Kermorgant, S. & Parker, P.J. c-Met signalling: spatio-temporal decisions. *Cell Cycle* **4**, 352-355 (2005).

49. Kermorgant, S. & Parker, P.J. Receptor trafficking controls weak signal delivery: a strategy used by c-Met for STAT3 nuclear accumulation. *J Cell Biol* **182**, 855-863 (2008).

50. Hammond, D.E., Urbe, S., Vande Woude, G.F. & Clague, M.J. Down-regulation of MET, the receptor for hepatocyte growth factor. *Oncogene* **20**, 2761-2770 (2001).

51. Rong, S., Segal, S., Anver, M., Resau, J.H. & Vande Woude, G.F. Invasiveness and metastasis of NIH 3T3 cells induced by Met-hepatocyte growth factor/scatter factor autocrine stimulation. *Proc Natl Acad Sci U S A* **91**, 4731-4735 (1994).

52. Takayama, H.*, et al.* Diverse tumorigenesis associated with aberrant development in mice overexpressing hepatocyte growth factor/scatter factor. *Proc Natl Acad Sci U S A* **94**, 701-706 (1997).

53. Abounader, R.*, et al.* In vivo targeting of SF/HGF and c-met expression via U1snRNA/ribozymes inhibits glioma growth and angiogenesis and promotes apoptosis. *FASEB J* **16**, 108-110 (2002).

54. Benvenuti, S. & Comoglio, P.M. The MET receptor tyrosine kinase in invasion and metastasis. *J Cell Physiol* **213**, 316-325 (2007).

55. Boccaccio, C. & Comoglio, P.M. Invasive growth: a MET-driven genetic programme for cancer and stem cells. *Nat Rev Cancer* **6**, 637-645 (2006).

56. Kammula, U.S.*, et al.* Molecular co-expression of the c-Met oncogene and hepatocyte growth factor in primary colon cancer predicts tumor stage and clinical outcome. *Cancer Lett* **248**, 219-228 (2007).

57. Abounader, R. & Laterra, J. Scatter factor/hepatocyte growth factor in brain tumor growth and angiogenesis. *Neuro Oncol* **7**, 436-451 (2005).

58. Wojtukiewicz, M.Z., Sierko, E., Klement, P. & Rak, J. The hemostatic system and angiogenesis in malignancy. *Neoplasia* **3**, 371-384 (2001).

59. Boccaccio, C.*, et al.* The MET oncogene drives a genetic programme linking cancer to haemostasis. *Nature* **434**, 396-400 (2005).

60. Boccaccio, C. & Comoglio, P.M. A functional role for hemostasis in early cancer development. *Cancer Res* **65**, 8579-8582 (2005).

61. Bussolino, F.*, et al.* Hepatocyte growth factor is a potent angiogenic factor which stimulates endothelial cell motility and growth. *J Cell Biol* **119**, 629-641 (1992).

62. Zhang, Y.W., Su, Y., Volpert, O.V. & Vande Woude, G.F. Hepatocyte growth factor/scatter factor mediates angiogenesis through positive VEGF and negative thrombospondin 1 regulation. *Proc Natl Acad Sci U S A* **100**, 12718-12723 (2003).

63. Stein, U.*, et al.* MACC1, a newly identified key regulator of HGF-MET signaling, predicts colon cancer metastasis. *Nat Med* **15**, 59-67 (2009).

64. Arlt, F. & Stein, U. Colon cancer metastasis: MACC1 and Met as metastatic pacemakers. *Int J Biochem Cell Biol* **41**, 2356-2359 (2009).

65. Marino, S. Medulloblastoma: developmental mechanisms out of control. *Trends Mol Med* **11**, 17-22 (2005).

66. Bladt, F., Riethmacher, D., Isenmann, S., Aguzzi, A. & Birchmeier, C. Essential role for the c-met receptor in the migration of myogenic precursor cells into the limb bud. *Nature* **376**, 768-771 (1995).

67. Uehara, Y.*, et al.* Placental defect and embryonic lethality in mice lacking hepatocyte growth factor/scatter factor. *Nature* **373**, 702-705 (1995).

68. Mitchell, K.J.*, et al.* Functional analysis of secreted and transmembrane proteins critical to mouse development. *Nat Genet* **28**, 241-249 (2001).

69. Achim, C.L.*, et al.* Expression of HGF and cMet in the developing and adult brain. *Brain Res Dev Brain Res* **102**, 299-303 (1997).

70. Jung, W.*, et al.* Expression and functional interaction of hepatocyte growth factor-scatter factor and its receptor c-met in mammalian brain. *J Cell Biol* **126**, 485-494 (1994).

71. Ieraci, A., Forni, P.E. & Ponzetto, C. Viable hypomorphic signaling mutant of the Met receptor reveals a role for hepatocyte growth factor in postnatal cerebellar development. *Proc Natl Acad Sci U S A* **99**, 15200-15205 (2002).

72. Maina, F. & Klein, R. Hepatocyte growth factor, a versatile signal for developing neurons. *Nat Neurosci* **2**, 213-217 (1999).

73. Honda, S.*, et al.* Localization and functional coupling of HGF and c-Met/HGF receptor in rat brain: implication as neurotrophic factor. *Brain Res Mol Brain Res* **32**, 197-210 (1995).

74. Zhang, L., Himi, T., Morita, I. & Murota, S. Hepatocyte growth factor protects cultured rat cerebellar granule neurons from apoptosis via the phosphatidylinositol-3 kinase/Akt pathway. *J Neurosci Res* **59**, 489-496 (2000).

75. Hossain, M.A., Russell, J.C., Gomez, R. & Laterra, J. Neuroprotection by scatter factor/hepatocyte growth factor and FGF-1 in cerebellar granule neurons is phosphatidylinositol 3-kinase/akt-dependent and MAPK/CREB-independent. *J Neurochem* **81**, 365-378 (2002).

76. Tong, C.Y., *et al.* Detection of oncogene amplifications in medulloblastomas by comparative genomic hybridization and array-based comparative genomic hybridization. *J Neurosurg* **100**, 187-193 (2004).

77. Li, Y., *et al.* The scatter factor/hepatocyte growth factor: c-met pathway in human embryonal central nervous system tumor malignancy. *Cancer Res* **65**, 9355-9362 (2005).

78. Li, Y., Fan, X., Goodwin, C.R., Laterra, J. & Xia, S. Hepatocyte growth factor enhances death receptor-induced apoptosis by up-regulating DR5. *BMC Cancer* **8**, 325 (2008).

79. Suliman, A., Lam, A., Datta, R. & Srivastava, R.K. Intracellular mechanisms of TRAIL: apoptosis through mitochondrial-dependent and -independent pathways. *Oncogene* **20**, 2122-2133 (2001).

80. Li, Y., *et al.* Functional and molecular interactions between the HGF/c-Met pathway and c-Myc in large-cell medulloblastoma. *Lab Invest* **88**, 98-111 (2008).

81. Dong, W., Chen, X., Xie, J., Sun, P. & Wu, Y. Epigenetic inactivation and tumor suppressor activity of HAI-2/SPINT2 in gastric cancer. *Int J Cancer* **127**, 1526-1534 (2010).

82. Morris, M.R., *et al.* Tumor suppressor activity and epigenetic inactivation of hepatocyte growth factor activator inhibitor type 2/SPINT2 in papillary and clear cell renal cell carcinoma. *Cancer Res* **65**, 4598-4606 (2005).

83. Parr, C., Watkins, G., Mansel, R.E. & Jiang, W.G. The hepatocyte growth factor regulatory factors in human breast cancer. *Clin Cancer Res* **10**, 202-211 (2004).

84. Binning, M.J., *et al.* Hepatocyte growth factor and sonic Hedgehog expression in cerebellar neural progenitor cells costimulate medulloblastoma initiation and growth. *Cancer Res* **68**, 7838-7845 (2008).

85. Kim, K.J., *et al.* Systemic anti-hepatocyte growth factor monoclonal antibody therapy induces the regression of intracranial glioma xenografts. *Clin Cancer Res* **12**, 1292-1298 (2006).

86. Provencal, M., *et al.* c-Met activation in medulloblastoma induces tissue factor expression and activity: effects on cell migration. *Carcinogenesis* **30**, 1089-1096 (2009).

87. Provencal, M., *et al.* Tissue factor mediates the HGF/Met-induced anti-apoptotic pathway in DAOY medulloblastoma cells. *J Neurooncol* **97**, 365-372 (2010).

88. Falanga, A., *et al.* The effect of very-low-dose warfarin on markers of hypercoagulation in metastatic breast cancer: results from a randomized trial. *Thromb Haemost* **79**, 23-27 (1998).

89. Kongkham, P.N., Onvani, S., Smith, C.A. & Rutka, J.T. Inhibition of the MET Receptor Tyrosine Kinase as a Novel Therapeutic Strategy in Medulloblastoma. *Transl Oncol* **3**, 336-343 (2010).

90. Guessous, F.*, et al.* An orally bioavailable c-Met kinase inhibitor potently inhibits brain tumor malignancy and growth. *Anticancer Agents Med Chem* **10**, 28-35 (2010).

91. Coon, V.*, et al.* Molecular therapy targeting Sonic hedgehog and hepatocyte growth factor signaling in a mouse model of medulloblastoma. *Mol Cancer Ther* **9**, 2627-2636 (2010).

92. Stommel, J.M.*, et al.* Coactivation of receptor tyrosine kinases affects the response of tumor cells to targeted therapies. *Science* **318**, 287-290 (2007).

93. Montesano, R.*, et al.* Differential effects of hepatocyte growth factor isoforms on epithelial and endothelial tubulogenesis. *Cell Growth Differ* **9**, 355-365 (1998).

94. Otsuka, T.*, et al.* Disassociation of met-mediated biological responses in vivo: the natural hepatocyte growth factor/scatter factor splice variant NK2 antagonizes growth but facilitates metastasis. *Mol Cell Biol* **20**, 2055-2065 (2000).

95. Kuba, K.*, et al.* HGF/NK4, a four-kringle antagonist of hepatocyte growth factor, is an angiogenesis inhibitor that suppresses tumor growth and metastasis in mice. *Cancer Res* **60**, 6737-6743 (2000).

96. Matsumoto, K. & Nakamura, T. NK4 gene therapy targeting HGF-Met and angiogenesis. *Front Biosci* **13**, 1943-1951 (2008).

97. Matsumoto, K., Nakamura, T. & Sakai, K. Hepatocyte growth factor and Met in tumor biology and therapeutic approach with NK4. *Proteomics* **8**, 3360-3370 (2008).

98. Mazzone, M.*, et al.* An uncleavable form of pro-scatter factor suppresses tumor growth and dissemination in mice. *J Clin Invest* **114**, 1418-1432 (2004).

99. Michieli, P.*, et al.* Targeting the tumor and its microenvironment by a dual-function decoy Met receptor. *Cancer Cell* **6**, 61-73 (2004).

100. Burgess, T.*, et al.* Fully human monoclonal antibodies to hepatocyte growth factor with therapeutic potential against hepatocyte growth factor/c-Met-dependent human tumors. *Cancer Res* **66**, 1721-1729 (2006).

101. Jun, H.T.*, et al.* AMG 102, a fully human anti-hepatocyte growth factor/scatter factor neutralizing antibody, enhances the efficacy of temozolomide or docetaxel in U-87 MG cells and xenografts. *Clin Cancer Res* **13**, 6735-6742 (2007).

102. Gordon, M.S.*, et al.* Safety, pharmacokinetics, and pharmacodynamics of AMG 102, a fully human hepatocyte growth factor-neutralizing monoclonal antibody, in a first-in-human study of patients with advanced solid tumors. *Clin Cancer Res* **16**, 699-710 (2010).

103. Li, Y.*, et al.* Interactions between PTEN and the c-Met pathway in glioblastoma and implications for therapy. *Mol Cancer Ther* **8**, 376-385 (2009).

104. Martens, T.*, et al.* A novel one-armed anti-c-Met antibody inhibits glioblastoma growth in vivo. *Clin Cancer Res* **12**, 6144-6152 (2006).

105. Christensen, J.G., *et al.* Cytoreductive antitumor activity of PF-2341066, a novel inhibitor of anaplastic lymphoma kinase and c-Met, in experimental models of anaplastic large-cell lymphoma. *Mol Cancer Ther* **6**, 3314-3322 (2007).

106. Zou, H.Y., *et al.* An orally available small-molecule inhibitor of c-Met, PF-2341066, exhibits cytoreductive antitumor efficacy through antiproliferative and antiangiogenic mechanisms. *Cancer Res* **67**, 4408-4417 (2007).

107. Zillhardt, M., Christensen, J.G. & Lengyel, E. An orally available small-molecule inhibitor of c-Met, PF-2341066, reduces tumor burden and metastasis in a preclinical model of ovarian cancer metastasis. *Neoplasia* **12**, 1-10 (2010).

108. Bagai, R., Fan, W. & Ma, P.C. ARQ-197, an oral small-molecule inhibitor of c-Met for the treatment of solid tumors. *IDrugs* **13**, 404-414 (2010).

109. Munshi, N., *et al.* ARQ 197, a novel and selective inhibitor of the human c-Met receptor tyrosine kinase with antitumor activity. *Mol Cancer Ther* **9**, 1544-1553 (2010).

110. Zhang, Y.W., *et al.* MET kinase inhibitor SGX523 synergizes with epidermal growth factor receptor inhibitor erlotinib in a hepatocyte growth factor-dependent fashion to suppress carcinoma growth. *Cancer Res* **70**, 6880-6890 (2010).

111. Qian, F., *et al.* Inhibition of tumor cell growth, invasion, and metastasis by EXEL-2880 (XL880, GSK1363089), a novel inhibitor of HGF and VEGF receptor tyrosine kinases. *Cancer Res* **69**, 8009-8016 (2009).

112. Mahadevan, D., *et al.* A novel tyrosine kinase switch is a mechanism of imatinib resistance in gastrointestinal stromal tumors. *Oncogene* **26**, 3909-3919 (2007).

113. Welsh, J.W., *et al.* The c-Met receptor tyrosine kinase inhibitor MP470 radiosensitizes glioblastoma cells. *Radiat Oncol* **4**, 69 (2009).

114. Qi, W., *et al.* MP470, a novel receptor tyrosine kinase inhibitor, in combination with Erlotinib inhibits the HER family/PI3K/Akt pathway and tumor growth in prostate cancer. *BMC Cancer* **9**, 142 (2009).

115. Comoglio, P.M., Giordano, S. & Trusolino, L. Drug development of MET inhibitors: targeting oncogene addiction and expedience. *Nat Rev Drug Discov* **7**, 504-516 (2008).

116. Eder, J.P., Vande Woude, G.F., Boerner, S.A. & LoRusso, P.M. Novel therapeutic inhibitors of the c-Met signaling pathway in cancer. *Clin Cancer Res* **15**, 2207-2214 (2009).

117. Rosen, P.J., Sweeney C.J., Park D.J. AMG102, an HGF/SF antagonist, in combination with anti- angiogenesis targeted therapies in adult patients with advanced solid tumors. *J Clin Oncol* **26**(2008).

118. Reardon, D.A., Cloughsey T.F., Raizer J.J. Phase II study of AMG 102, a fully human neutralizing antibody against hepatocyte growth factor/scatter factor, in patients with recurrent glioblastoma multiforme. *J Clin Oncol* **26**(2008).

119. Naran, S., Zhang, X. & Hughes, S.J. Inhibition of HGF/MET as therapy for malignancy. *Expert Opin Ther Targets* **13**, 569-581 (2009).

120. Smolen, G.A.*, et al.* Amplification of MET may identify a subset of cancers with extreme sensitivity to the selective tyrosine kinase inhibitor PHA-665752. *Proc Natl Acad Sci U S A* **103**, 2316-2321 (2006).

121. Mayor, S. MET inhibitors: translating from bench to bedside. *Lancet Oncol* **12**, 14 (2011).

122. Diamond, S.*, et al.* Species-specific metabolism of SGX523 by aldehyde oxidase and the toxicological implications. *Drug Metab Dispos* **38**, 1277-1285 (2010).

123. Liu, X., Newton, R.C. & Scherle, P.A. Developing c-MET pathway inhibitors for cancer therapy: progress and challenges. *Trends Mol Med* **16**, 37-45 (2010).

124. Gottardo, N.G. & Gajjar, A. Current therapy for medulloblastoma. *Curr Treat Options Neurol* **8**, 319-334 (2006).

125. Eberhart, C.G.*, et al.* Histopathologic grading of medulloblastomas: a Pediatric Oncology Group study. *Cancer* **94**, 552-560 (2002).

126. von Hoff, K.*, et al.* Large cell/anaplastic medulloblastoma: outcome according to myc status, histopathological, and clinical risk factors. *Pediatr Blood Cancer* **54**, 369-376 (2010).

127. Packer, R.J.*, et al.* Outcome for children with medulloblastoma treated with radiation and cisplatin, CCNU, and vincristine chemotherapy. *J Neurosurg* **81**, 690-698 (1994).

128. Mulhern, R.K.*, et al.* Neurocognitive consequences of risk-adapted therapy for childhood medulloblastoma. *J Clin Oncol* **23**, 5511-5519 (2005).

129. Massimino, M.*, et al.* Childhood medulloblastoma. *Crit Rev Oncol Hematol* **79**, 65-83 (2011).

130. Packer, R.J.*, et al.* Phase III study of craniospinal radiation therapy followed by adjuvant chemotherapy for newly diagnosed average-risk medulloblastoma. *J Clin Oncol* **24**, 4202-4208 (2006).

131. Oyharcabal-Bourden, V.*, et al.* Standard-risk medulloblastoma treated by adjuvant chemotherapy followed by reduced-dose craniospinal radiation therapy: a French Society of Pediatric Oncology Study. *J Clin Oncol* **23**, 4726-4734 (2005).

132. Gajjar, A.*, et al.* Risk-adapted craniospinal radiotherapy followed by high-dose chemotherapy and stem-cell rescue in children with newly diagnosed medulloblastoma (St Jude Medulloblastoma-96): long-term results from a prospective, multicentre trial. *Lancet Oncol* **7**, 813-820 (2006).

133. Merchant, T.E.*, et al.* Multi-institution prospective trial of reduced-dose craniospinal irradiation (23.4 Gy) followed by conformal posterior fossa (36 Gy) and primary site irradiation (55.8 Gy) and dose-intensive chemotherapy for average-risk medulloblastoma. *Int J Radiat Oncol Biol Phys* **70**, 782-787 (2008).

134. Lannering, B., *et al.* Hyperfractionated versus conventional radiotherapy followed by chemotherapy in standard-risk medulloblastoma: results from the randomized multicenter HIT-SIOP PNET 4 trial. *J Clin Oncol* **30**, 3187-3193 (2012).

135. Zeltzer, P.M., *et al.* Metastasis stage, adjuvant treatment, and residual tumor are prognostic factors for medulloblastoma in children: conclusions from the Children's Cancer Group 921 randomized phase III study. *J Clin Oncol* **17**, 832-845 (1999).

136. Kortmann, R.D., *et al.* Postoperative neoadjuvant chemotherapy before radiotherapy as compared to immediate radiotherapy followed by maintenance chemotherapy in the treatment of medulloblastoma in childhood: results of the German prospective randomized trial HIT '91. *Int J Radiat Oncol Biol Phys* **46**, 269-279 (2000).

137. Taylor, R.E., *et al.* Outcome for patients with metastatic (M2-3) medulloblastoma treated with SIOP/UKCCSG PNET-3 chemotherapy. *Eur J Cancer* **41**, 727-734 (2005).

138. Gandola, L., *et al.* Hyperfractionated accelerated radiotherapy in the Milan strategy for metastatic medulloblastoma. *J Clin Oncol* **27**, 566-571 (2009).

139. Strother, D., *et al.* Feasibility of four consecutive high-dose chemotherapy cycles with stem-cell rescue for patients with newly diagnosed medulloblastoma or supratentorial primitive neuroectodermal tumor after craniospinal radiotherapy: results of a collaborative study. *J Clin Oncol* **19**, 2696-2704 (2001).

140. Chi, S.N., *et al.* Feasibility and response to induction chemotherapy intensified with high-dose methotrexate for young children with newly diagnosed high-risk disseminated medulloblastoma. *J Clin Oncol* **22**, 4881-4887 (2004).

141. Finlay, J.L., *et al.* Pilot study of high-dose thiotepa and etoposide with autologous bone marrow rescue in children and young adults with recurrent CNS tumors. The Children's Cancer Group. *J Clin Oncol* **14**, 2495-2503 (1996).

142. Mahoney, D.H., Jr., *et al.* High-dose melphalan and cyclophosphamide with autologous bone marrow rescue for recurrent/progressive malignant brain tumors in children: a pilot pediatric oncology group study. *J Clin Oncol* **14**, 382-388 (1996).

143. Dunkel, I.J., *et al.* High-dose carboplatin, thiotepa, and etoposide with autologous stem-cell rescue for patients with recurrent medulloblastoma. Children's Cancer Group. *J Clin Oncol* **16**, 222-228 (1998).

144. Dunkel, I.J., *et al.* High-dose carboplatin, thiotepa, and etoposide with autologous stem cell rescue for patients with previously irradiated recurrent medulloblastoma. *Neuro Oncol* **12**, 297-303 (2010).

145. Ridola, V., *et al.* High-dose chemotherapy with autologous stem cell rescue followed by posterior fossa irradiation for local medulloblastoma recurrence or progression after conventional chemotherapy. *Cancer* **110**, 156-163 (2007).

146. Nicholson, H.S., *et al.* Phase 2 study of temozolomide in children and adolescents with recurrent central nervous system tumors: a report from the Children's Oncology Group. *Cancer* **110**, 1542-1550 (2007).

147. Ruggiero, A.*, et al.* Phase I study of temozolomide combined with oral etoposide in children with recurrent or progressive medulloblastoma. *Eur J Cancer* **46**, 2943-2949 (2010).

148. Needle, M.N.*, et al.* Phase II study of daily oral etoposide in children with recurrent brain tumors and other solid tumors. *Med Pediatr Oncol* **29**, 28-32 (1997).

149. Silvani, A.*, et al.* Adult medulloblastoma: multiagent chemotherapy with cisplatinum and etoposide: a single institutional experience. *J Neurooncol* **106**, 595-600 (2012).

150. Turner, C.D.*, et al.* Phase II study of irinotecan (CPT-11) in children with high-risk malignant brain tumors: the Duke experience. *Neuro Oncol* **4**, 102-108 (2002).

151. Bomgaars, L.R.*, et al.* Phase II trial of irinotecan in children with refractory solid tumors: a Children's Oncology Group Study. *J Clin Oncol* **25**, 4622-4627 (2007).

152. Levy, A.S.*, et al.* Phase 1 and pharmacokinetic study of concurrent carboplatin and irinotecan in subjects aged 1 to 21 years with refractory solid tumors. *Cancer* **115**, 207-216 (2009).

153. Grill, J.*, et al.* Phase II study of irinotecan in combination with temozolomide (TEMIRI) in children with recurrent or refractory medulloblastoma: a joint ITCC and SIOPE brain tumor study. *Neuro Oncol* (2013).

154. Ris, M.D., Packer, R., Goldwein, J., Jones-Wallace, D. & Boyett, J.M. Intellectual outcome after reduced-dose radiation therapy plus adjuvant chemotherapy for medulloblastoma: a Children's Cancer Group study. *J Clin Oncol* **19**, 3470-3476 (2001).

155. Jakacki, R.I.*, et al.* Outcome of children with metastatic medulloblastoma treated with carboplatin during craniospinal radiotherapy: a Children's Oncology Group Phase I/II study. *J Clin Oncol* **30**, 2648-2653 (2012).

156. Gajjar, A. & Pizer, B. Role of high-dose chemotherapy for recurrent medulloblastoma and other CNS primitive neuroectodermal tumors. *Pediatr Blood Cancer* **54**, 649-651 (2010).

157. Ajeawung, N.F., Wang, H.Y. & Kamnasaran, D. Progress from clinical trials and emerging non-conventional therapies for the treatment of Medulloblastomas. *Cancer Lett* **330**, 130-140 (2013).

158. Walter, A.W.*, et al.* Survival and neurodevelopmental outcome of young children with medulloblastoma at St Jude Children's Research Hospital. *J Clin Oncol* **17**, 3720-3728 (1999).

159. Padovani, L.*, et al.* Reirradiation and concomitant metronomic temozolomide: an efficient combination for local control in medulloblastoma disease? *J Pediatr Hematol Oncol* **33**, 600-604 (2011).

160. Aguilera, D.*, et al.* Response to bevacizumab, irinotecan, and temozolomide in children with relapsed medulloblastoma: a multi-institutional experience. *Childs Nerv Syst* **29**, 589-596 (2013).

161. Rudin, C.M. Vismodegib. *Clin Cancer Res* **18**, 3218-3222 (2012).

162. Rudin, C.M.*, et al.* Treatment of medulloblastoma with hedgehog pathway inhibitor GDC-0449. *N Engl J Med* **361**, 1173-1178 (2009).

163. Low, J.A. & de Sauvage, F.J. Clinical experience with Hedgehog pathway inhibitors. *J Clin Oncol* **28**, 5321-5326 (2010).

164. Yauch, R.L.*, et al.* Smoothened mutation confers resistance to a Hedgehog pathway inhibitor in medulloblastoma. *Science* **326**, 572-574 (2009).

165. Buonamici, S.*, et al.* Interfering with resistance to smoothened antagonists by inhibition of the PI3K pathway in medulloblastoma. *Sci Transl Med* **2**, 51ra70 (2010).

166. Kimura, H., Ng, J.M. & Curran, T. Transient inhibition of the Hedgehog pathway in young mice causes permanent defects in bone structure. *Cancer Cell* **13**, 249-260 (2008).

167. Ajeawung, N.F., Wang, H.Y., Gould, P. & Kamnasaran, D. Advances in molecular targets for the treatment of medulloblastomas. *Clin Invest Med* **35**, E246 (2012).

168. Hallahan, A.R.*, et al.* The SmoA1 mouse model reveals that notch signaling is critical for the growth and survival of sonic hedgehog-induced medulloblastomas. *Cancer Res* **64**, 7794-7800 (2004).

169. Fouladi, M.*, et al.* Phase I trial of MK-0752 in children with refractory CNS malignancies: a pediatric brain tumor consortium study. *J Clin Oncol* **29**, 3529-3534 (2011).

170. Krop, I.*, et al.* Phase I pharmacologic and pharmacodynamic study of the gamma secretase (Notch) inhibitor MK-0752 in adult patients with advanced solid tumors. *J Clin Oncol* **30**, 2307-2313 (2012).

171. Gajjar, A.*, et al.* Clinical, histopathologic, and molecular markers of prognosis: toward a new disease risk stratification system for medulloblastoma. *J Clin Oncol* **22**, 984-993 (2004).

172. Gilbertson, R.J.*, et al.* ERBB receptor signaling promotes ependymoma cell proliferation and represents a potential novel therapeutic target for this disease. *Clin Cancer Res* **8**, 3054-3064 (2002).

173. Fouladi, M.*, et al.* Phase I trial of lapatinib in children with refractory CNS malignancies: a Pediatric Brain Tumor Consortium study. *J Clin Oncol* **28**, 4221-4227 (2010).

174. Fouladi, M.*, et al.* A molecular biology and phase II trial of lapatinib in children with refractory CNS malignancies: a pediatric brain tumor consortium study. *J Neurooncol* (2013).

175. Wu, X.*, et al.* Clonal selection drives genetic divergence of metastatic medulloblastoma. *Nature* **482**, 529-533 (2012).

176. Mumert, M., *et al.* Functional genomics identifies drivers of medulloblastoma dissemination. *Cancer Res* **72**, 4944-4953 (2012).

177. Gherardi, E., Birchmeier, W., Birchmeier, C. & Vande Woude, G. Targeting MET in cancer: rationale and progress. *Nat Rev Cancer* **12**, 89-103 (2012).

178. Onvani, S., *et al.* Molecular genetic analysis of the hepatocyte growth factor/MET signaling pathway in pediatric medulloblastoma. *Genes Chromosomes Cancer* **51**, 675-688 (2012).

179. Guessous, F., *et al.* Cooperation between c-Met and focal adhesion kinase family members in medulloblastoma and implications for therapy. *Mol Cancer Ther* **11**, 288-297 (2012).

180. Zillhardt, M., *et al.* Foretinib (GSK1363089), an orally available multikinase inhibitor of c-Met and VEGFR-2, blocks proliferation, induces anoikis, and impairs ovarian cancer metastasis. *Clin Cancer Res* **17**, 4042-4051 (2011).

181. You, W.K., *et al.* VEGF and c-Met blockade amplify angiogenesis inhibition in pancreatic islet cancer. *Cancer Res* **71**, 4758-4768 (2011).

182. Huynh, H., Ong, R. & Soo, K.C. Foretinib demonstrates anti-tumor activity and improves overall survival in preclinical models of hepatocellular carcinoma. *Angiogenesis* **15**, 59-70 (2012).

183. Eder, J.P., *et al.* A phase I study of foretinib, a multi-targeted inhibitor of c-Met and vascular endothelial growth factor receptor 2. *Clin Cancer Res* **16**, 3507-3516 (2010).

184. Choueiri, T.K., *et al.* Phase II and biomarker study of the dual MET/VEGFR2 inhibitor foretinib in patients with papillary renal cell carcinoma. *J Clin Oncol* **31**, 181-186 (2013).

185. MacDonald, T.J., *et al.* Expression profiling of medulloblastoma: PDGFRA and the RAS/MAPK pathway as therapeutic targets for metastatic disease. *Nat Genet* **29**, 143-152 (2001).

186. Gilbertson, R.J. & Clifford, S.C. PDGFRB is overexpressed in metastatic medulloblastoma. *Nat Genet* **35**, 197-198 (2003).

187. Abouantoun, T.J., Castellino, R.C. & MacDonald, T.J. Sunitinib induces PTEN expression and inhibits PDGFR signaling and migration of medulloblastoma cells. *J Neurooncol* **101**, 215-226 (2011).

188. Ammoun, S. & Hanemann, C.O. Emerging therapeutic targets in schwannomas and other merlin-deficient tumors. *Nat Rev Neurol* **7**, 392-399 (2011).

189. Kool, M., *et al.* Integrated genomics identifies five medulloblastoma subtypes with distinct genetic profiles, pathway signatures and clinicopathological features. *PLoS One* **3**, e3088 (2008).

190. Fattet, S.*, et al.* Beta-catenin status in paediatric medulloblastomas: correlation of immunohistochemical expression with mutational status, genetic profiles, and clinical characteristics. *J Pathol* **218**, 86-94 (2009).

191. Cho, Y.J.*, et al.* Integrative genomic analysis of medulloblastoma identifies a molecular subgroup that drives poor clinical outcome. *J Clin Oncol* **29**, 1424-1430 (2011).

192. Robinson, G.*, et al.* Novel mutations target distinct subgroups of medulloblastoma. *Nature* **488**, 43-48 (2012).

193. Diaz, R.J., Golbourn, B., Shekarforoush, M., Smith, C.A. & Rutka, J.T. Aurora kinase B/C inhibition impairs malignant glioma growth in vivo. *J Neurooncol* **108**, 349-360 (2012).

194. Valster, A.*, et al.* Cell migration and invasion assays. *Methods* **37**, 208-215 (2005).

195. Agnihotri, S.*, et al.* Alkylpurine-DNA-N-glycosylase confers resistance to temozolomide in xenograft models of glioblastoma multiforme and is associated with poor survival in patients. *J Clin Invest* **122**, 253-266 (2012).

196. Triscott, J.*, et al.* Personalizing the treatment of pediatric medulloblastoma: Polo-like kinase PLK1 as a molecular target in high-risk children. *Cancer Res* (2013).

197. Reagan-Shaw, S., Nihal, M. & Ahmad, N. Dose translation from animal to human studies revisited. *FASEB J* **22**, 659-661 (2008).

198. Beauchesne, P. Intrathecal chemotherapy for treatment of leptomeningeal dissemination of metastatic tumours. *Lancet Oncol* **11**, 871-879 (2010).

199. Parsons, D.W.*, et al.* The genetic landscape of the childhood cancer medulloblastoma. *Science* **331**, 435-439 (2011).

200. Jones, D.T.*, et al.* Dissecting the genomic complexity underlying medulloblastoma. *Nature* **488**, 100-105 (2012).

201. Pugh, T.J.*, et al.* Medulloblastoma exome sequencing uncovers subtype-specific somatic mutations. *Nature* **488**, 106-110 (2012).

202. Schwalbe, E.C.*, et al.* DNA methylation profiling of medulloblastoma allows robust subclassification and improved outcome prediction using formalin-fixed biopsies. *Acta Neuropathol* **125**, 359-371 (2013).

203. Li, P.*, et al.* A population of Nestin-expressing progenitors in the cerebellum exhibits increased tumorigenicity. *Nat Neurosci* **16**, 1737-1744 (2013).

204. Ellison, D.W.*, et al.* Definition of disease-risk stratification groups in childhood medulloblastoma using combined clinical, pathologic, and molecular variables. *J Clin Oncol* **29**, 1400-1407 (2011).

205. Zhukova, N.*, et al.* Subgroup-specific prognostic implications of TP53 mutation in medulloblastoma. *J Clin Oncol* **31**, 2927-2935 (2013).

206. Ryan, S.L., *et al.* MYC family amplification and clinical risk-factors interact to predict an extremely poor prognosis in childhood medulloblastoma. *Acta Neuropathol* **123**, 501-513 (2012).

207. Lamb, J. The Connectivity Map: a new tool for biomedical research. *Nat Rev Cancer* **7**, 54-60 (2007).

208. Lamb, J., *et al.* The Connectivity Map: using gene-expression signatures to connect small molecules, genes, and disease. *Science* **313**, 1929-1935 (2006).

209. Hieronymus, H., *et al.* Gene expression signature-based chemical genomic prediction identifies a novel class of HSP90 pathway modulators. *Cancer Cell* **10**, 321-330 (2006).

210. De Preter, K., *et al.* Meta-mining of neuroblastoma and neuroblast gene expression profiles reveals candidate therapeutic compounds. *Clin Cancer Res* **15**, 3690-3696 (2009).

211. Zimmer, M., *et al.* The connectivity map links iron regulatory protein-1-mediated inhibition of hypoxia-inducible factor-2a translation to the anti-inflammatory 15-deoxy-delta12,14-prostaglandin J2. *Cancer Res* **70**, 3071-3079 (2010).

212. Wang, G., *et al.* Expression-based in silico screening of candidate therapeutic compounds for lung adenocarcinoma. *PLoS One* **6**, e14573 (2011).

213. Raj, L., *et al.* Selective killing of cancer cells by a small molecule targeting the stress response to ROS. *Nature* **475**, 231-234 (2011).

214. Singh, S.K., *et al.* Identification of a cancer stem cell in human brain tumors. *Cancer Res* **63**, 5821-5828 (2003).

215. Singh, S.K., *et al.* Identification of human brain tumour initiating cells. *Nature* **432**, 396-401 (2004).

216. Malumbres, M. & Barbacid, M. Cell cycle, CDKs and cancer: a changing paradigm. *Nat Rev Cancer* **9**, 153-166 (2009).

217. Lapenna, S. & Giordano, A. Cell cycle kinases as therapeutic targets for cancer. *Nat Rev Drug Discov* **8**, 547-566 (2009).

218. Kenney, A.M. & Rowitch, D.H. Sonic hedgehog promotes G(1) cyclin expression and sustained cell cycle progression in mammalian neuronal precursors. *Mol Cell Biol* **20**, 9055-9067 (2000).

219. Knoepfler, P.S., Cheng, P.F. & Eisenman, R.N. N-myc is essential during neurogenesis for the rapid expansion of progenitor cell populations and the inhibition of neuronal differentiation. *Genes Dev* **16**, 2699-2712 (2002).

220. Kenney, A.M., Cole, M.D. & Rowitch, D.H. Nmyc upregulation by sonic hedgehog signaling promotes proliferation in developing cerebellar granule neuron precursors. *Development* **130**, 15-28 (2003).

221. Ciemerych, M.A., *et al.* Development of mice expressing a single D-type cyclin. *Genes Dev* **16**, 3277-3289 (2002).

222. Pogoriler, J., Millen, K., Utset, M. & Du, W. Loss of cyclin D1 impairs cerebellar development and suppresses medulloblastoma formation. *Development* **133**, 3929-3937 (2006).

223. Zindy, F., *et al.* Hemangiosarcomas, medulloblastomas, and other tumors in Ink4c/p53-null mice. *Cancer Res* **63**, 5420-5427 (2003).

224. Kumazawa, A., *et al.* Cyclin-dependent kinase 5 is required for normal cerebellar development. *Mol Cell Neurosci* **52**, 97-105 (2013).

225. Li, M., *et al.* Multiple CDK/CYCLIND genes are amplified in medulloblastoma and supratentorial primitive neuroectodermal brain tumor. *Cancer Genet* **205**, 220-231 (2012).

226. Goga, A., Yang, D., Tward, A.D., Morgan, D.O. & Bishop, J.M. Inhibition of CDK1 as a potential therapy for tumors over-expressing MYC. *Nat Med* **13**, 820-827 (2007).

227. Lahusen, T., De Siervi, A., Kunick, C. & Senderowicz, A.M. Alsterpaullone, a novel cyclin-dependent kinase inhibitor, induces apoptosis by activation of caspase-9 due to perturbation in mitochondrial membrane potential. *Mol Carcinog* **36**, 183-194 (2003).

228. Soni, D.V. & Jacobberger, J.W. Inhibition of cdk1 by alsterpaullone and thioflavopiridol correlates with increased transit time from mid G2 through prophase. *Cell Cycle* **3**, 349-357 (2004).

229. Cui, C., Wang, Y., Zhao, M. & Peng, S. Alsterpaullone, a Cyclin-Dependent Kinase Inhibitor, Mediated Toxicity in HeLa Cells through Apoptosis-Inducing Effect. *J Anal Methods Chem* **2013**, 602091 (2013).

230. Faria, C.M., Rutka, J.T., Smith, C. & Kongkham, P. Epigenetic mechanisms regulating neural development and pediatric brain tumor formation. *J Neurosurg Pediatr* **8**, 119-132 (2011).

Publications

Book Chapters

Claudia C. Faria, Roberto J. Diaz and James T. Rutka (2014). Novel Therapies and Next Generation Clinical Trials in Medulloblastoma, Medulloblastoma Book, Dr. Dimitris Kombogiorgas (Ed.), Nova Science Publishers, ISBN: 978-1-63117-190-1 (in press).

Claudia C. Faria, Yuzo Terakawa and James T. Rutka (2014). Neurogenetic Basis of Pediatric Neurosurgical Conditions, Principles and Practice of Pediatric Neurosurgery, 3rd ed, Leland Albright, Ian F. Pollack, P. David Adelson (Editors), Thieme Medical Publishers (in press).

Claudia C. Faria, Christian A. Smith and James T. Rutka (2013). New Molecular Targets and Treatments for Pediatric Brain Tumors, Evolution of the Molecular Biology of Brain Tumors and the Therapeutic Implications, Dr. Terry Lichtor (Ed.), ISBN: 978-953-51-0989-1, InTech, doi: 10.5772/53300.

Claudia Faria, Christian Smith and James Rutka (2011). The Role of HGF/c-Met Pathway Signaling in Human Medulloblastoma, Molecular Targets of CNS Tumors, Dr. Miklos Garami (Ed.), ISBN: 978-953-307-736-9, InTech, doi: 10.5772/23296.

Papers in Indexed Journals

Claudia C. Faria, Adrian M. Dubuc, Marc Remke, Brian J. Golbourn, Roberto J. Diaz, Sameer Agnihotri, Amanda Luck, Nesrin Sabha, Samantha Olsen, Xiaochong Wu, Livia Garzia, Vijay Ramaswamy, Stephen C. Mack, Xin Wang, Michael Leadley, Denis Reynaud, Leonardo Ermini, Martin Post, Paul A. Northcott, Stefan M. Pfister, Sidney E. Croul, Marcel Kool, Andrey Korshunov, Christian A. Smith, Michael D. Taylor and James T. Rutka. Foretinib is Effective Therapy for Metastatic Sonic Hedgehog Medulloblastoma. (under revision in *Cancer Research*)

Claudia C. Faria, Sameer Agnihotri, Stephen Mack, Brian Golbourn, Samantha Olsen, Melissa Bryant, Mathiew Bebenek, Michelle Kushida, Renee Head, Xin Wang, Ian Clark, Peter Dirks, Christian A. Smith, Michael D. Taylor, James T. Rutka. The connectivity map identifies alsterpaullone as a novel small molecule to target Group 3 medulloblastoma. (submited to *Acta Neuropathologica*)

Vijay Ramaswamy, Marc Remke, David Shih, Xin Wang, Paul A. Northcott, **Claudia C. Faria**, Charles Raybaud, Uri Tabori, Cynthia Hawkins, James Rutka, Michael D. Taylor, MD and Eric Bouffet. (2014). Duration of the Pre-Diagnostic Interval in Medulloblastoma is Subgroup Dependent. *Pediatric blood & cancer*. doi:10.1002/pbc.25002 (Epub ahead of print).

Shih DJ, Northcott PA, Remke M, Korshunov A, Ramaswamy V, Kool M, Luu B, Yao Y, Wang X, Dubuc AM, Garzia L, Peacock J, Mack SC, Wu X, Rolider A, Morrissy AS, Cavalli FM, Jones DT, Zitterbart K, **Faria CC**, Schüller U, Kren L, Kumabe T, Tominaga T, Shin Ra Y, Garami M, Hauser P, Chan JA, Robinson S, Bognár L, Klekner A, Saad AG, Liau LM, Albrecht S, Fontebasso A, Cinalli G, De Antonellis P, Zollo M, Cooper MK, Thompson RC, Bailey S, Lindsey JC, Di Rocco C, Massimi L, Michiels EM, Scherer SW, Phillips JJ, Gupta N, Fan X, Muraszko KM, Vibhakar R, Eberhart CG, Fouladi M, Lach B, Jung S, Wechsler-Reya RJ, Fèvre-Montange M, Jouvet A, Jabado N, Pollack IF, Weiss WA, Lee JY, Cho BK, Kim SK, Wang KC, Leonard JR, Rubin JB, de Torres C, Lavarino C, Mora J, Cho YJ, Tabori U, Olson JM, Gajjar A, Packer RJ, Rutkowski S, Pomeroy SL, French PJ, Kloosterhof NK,

Kros JM, Van Meir EG, Clifford SC, Bourdeaut F, Delattre O, Doz FF, Hawkins CE, Malkin D, Grajkowska WA, Perek-Polnik M, Bouffet E, Rutka JT, Pfister SM, Taylor MD. (2014). Cytogenetic Prognostication Within Medulloblastoma Subgroups. *Journal of clinical oncology: official journal of the American Society of Clinical Oncology*, 32(9), 886-96. doi:10.1200/JCO.2013.50.9539.

Vijay Ramaswamy, Marc Remke, Eric Bouffet, **Claudia C Faria**, Sebastien Perreault, Yoon-Jae Cho, David J Shih, Betty Luu, Adrian M Dubuc, Paul A Northcott, Ulrich Schüller, Sridharan Gururangan, Roger McLendon, Darell Bigner, Maryam Fouladi, Keith L Ligon, Scott L Pomeroy, Sandra Dunn, Joanna Triscott, Nada Jabado, Adam Fontebasso, David T W Jones, Marcel Kool, Matthias A Karajannis, Sharon L Gardner, David Zagzag, Sofia Nunes, José Pimentel, Jaume Mora, Eric Lipp, Andrew W Walter, Marina Ryzhova, Olga Zheludkova, Ella Kumirova, Jad Alshami, Sidney E Croul, James T Rutka, Cynthia Hawkins, Uri Tabori, Kari-Elise T Codispoti, Roger J Packer, Stefan M Pfister, Andrey Korshunov, Michael D Taylor. (2013). Recurrence patterns across medulloblastoma subgroups: an integrated clinical and molecular analysis. *Lancet Oncol*, 14(12), 1200-7. doi: 10.1016/S1470-2045(13)70449-2.

Marc Remke, Vijay Ramaswamy, John Peacock, David J. H. Shih, Christian Koelsche, Paul A. Northcott, Nadia Hill, Florence M. G. Cavalli, Marcel Kool, Xin Wang, Stephen C. Mack, Mark Barszczyk, A. Sorana Morrissy, Xiaochong Wu, Sameer Agnihotri, Betty Luu, David T. W. Jones, Livia Garzia, Adrian M. Dubuc, Nataliya Zhukova, Robert Vanner, Johan M. Kros, Pim J. French, Erwin G. Van Meir, Rajeev Vibhakar, Karel Zitterbart, Jennifer A. Chan, László Bognár, Almos Klekner, Boleslaw Lach, Shin Jung, Ali G. Saad, Linda M. Liau, Steffen Albrecht, Massimo Zollo, Michael K. Cooper, Reid C. Thompson, Oliver O. Delattre, Franck Bourdeaut, François F. Doz, Miklós Garami, Peter Hauser, Carlos G. Carlotti, Timothy E. Van Meter, Luca Massimi, Daniel Fults, Scott L. Pomeroy, Toshiro Kumabe, Young Shin Ra, Jeffrey R. Leonard, Samer K. Elbabaa, Jaume Mora, Joshua B. Rubin, Yoon-Jae Cho, Roger E. McLendon, Darell D. Bigner, Charles G. Eberhart, Maryam Fouladi, Robert J. Wechsler-Reya, **Claudia C. Faria**, Sidney E. Croul, Annie Huang, Eric Bouffet, Cynthia E. Hawkins, Peter B. Dirks, William A. Weiss, Ulrich Schüller, Ian F. Pollack, Stefan Rutkowski, David Meyronet, Anne Jouvet, Michelle Fèvre-Montange, Nada Jabado, Marta Perek-Polnik, Wieslawa A. Grajkowska, Seung-Ki Kim, James T. Rutka, David Malkin, Uri Tabori, Stefan M. Pfister, Andrey Korshunov, Andreas von Deimling, Michael D. Taylor.

(2013). TERT promoter mutations are highly recurrent in SHH subgroup medulloblastoma. *Acta neuropathologica*, *126*(6), 917–929. doi:10.1007/s00401-013-1198-2.

Northcott PA, Shih DJ, Peacock J, Garzia L, Sorana Morrissy A, Zichner T, Stütz AM, Korshunov A, Reimand J, Schumacher SE, Beroukhim R, Ellison DW, Marshall CR, Lionel AC, Mack S, Dubuc A, Yao Y, Ramaswamy V, Luu B, Rolider A, Cavalli FM, Wang X, Remke M, Wu X, Chiu RY, Chu A, Chuah E, Corbett RD, Hoad GR, Jackman SD, Li Y, Lo A, Mungall KL, Ming Nip K, Qian JQ, Raymond AG, Thiessen N, Varhol RJ, Birol I, Moore RA, Mungall AJ, Holt R, Kawauchi D, Roussel MF, Kool M, Jones DT, Witt H, Fernandez-L A, Kenney AM, Wechsler-Reya RJ, Dirks P, Aviv T, Grajkowska WA, Perek-Polnik M, Haberler CC, Delattre O, Reynaud SS, Doz FF, Pernet-Fattet SS, Cho BK, Kim SK, Wang KC, Scheurlen W, Eberhart CG, Fèvre-Montange M, Jouvet A, Pollack IF, Fan X, Muraszko KM, Yancey Gillespie G, Di Rocco C, Massimi L, Michiels EM, Kloosterhof NK, French PJ, Kros JM, Olson JM, Ellenbogen RG, Zitterbart K, Kren L, Thompson RC, Cooper MK, Lach B, McLendon RE, Bigner DD, Fontebasso A, Albrecht S, Jabado N, Lindsey JC, Bailey S, Gupta N, Weiss WA, Bognár L, Klekner A, Van Meter TE, Kumabe T, Tominaga T, Elbabaa SK, Leonard JR, Rubin JB, Liau LM, Van Meir EG, Fouladi M, Nakamura H, Cinalli G, Garami M, Hauser P, Saad AG, Iolascon A, Jung S, Carlotti CG, Vibhakar R, Shin Ra Y, Robinson S, Zollo M, **Faria CC**, Chan JA, Levy ML, Sorensen PH, Meyerson M, Pomeroy SL, Cho YJ, Bader GD, Tabori U, Hawkins CE, Bouffet E, Scherer SW, Rutka JT, Malkin D, Clifford SC, Jones SJ, Korbel JO, Pfister SM, Marra MA, Taylor MD. (2012). Subgroup-specific structural variation across 1,000 medulloblastoma genomes. *Nature*, *488*(7409), 49–56. doi:10.1038/nature11327.

Faria, C. M. C., Rutka, J. T., Smith, C., & Kongkham, P. (2011). Epigenetic mechanisms regulating neural development and pediatric brain tumor formation. *Journal of neurosurgery Pediatrics*, *8*(2), 119–132. doi:10.3171/2011.5.PEDS1140.